University of Cape Town

Doctoral Thesis

Precision Determination of QCD Fundamental Parameters from Sum Rules

Author:
Sebastian W. Bodenstein

Supervisor:
Em. Prof. C.A. Dominguez
Co-Supervisor:
Dr. W.A. Horowitz

A thesis submitted in fulfilment of the requirements
for the degree of Doctor of Philosophy

in the

Department of Physics

May 2014

Abstract

This thesis consists of three themes. First, we develop a new QCD sum rule approach to determining the charm- and bottom-quark masses. We find a $\overline{\text{MS}}$-scheme charm-quark mass of $\bar{m}_c(3\,\text{GeV}) = 985(8)\,\text{GeV}$ and a bottom-quark mass of $\bar{m}_b(10\,\text{GeV}) = 3624(9)\,\text{MeV}$. These currently represent the most precisely determined charm- and bottom-quark masses by a sum rule approach. In the case of the bottom-quark mass, our result represents the most precise determination obtained by any approach. We also improve the convergence of a previous determination of the strange-quark mass, and obtain $\bar{m}_s(2\,\text{GeV}) = 94(8)\,\text{MeV}$.

The second theme is the lowest-order hadronic contribution to the muon anomalous magnetic moment, $a_\mu^{\text{had,LO}}$. We first show how to obtain the entire heavy-quark contribution to $a_\mu^{\text{had,LO}}$ using perturbative QCD. We then construct a complete set of $e^+e^- \to \text{hadrons}$ data for the low-energy region $\sqrt{s} < 1.8\,\text{GeV}$. A technique is introduced to reduce the contribution of this data to $a_\mu^{\text{had,LO}}$ in favour of theoretical input in the form of the OPE. It is found that this approach significantly reduces the current $3.6\,\sigma$ discrepancy between the muon anomalous magnetic moment obtained via experiment and theory.

The third theme is the hadronic contribution to the running of the electromagnetic coupling, $\Delta\alpha_{\text{had}}(M_Z)$, which is important for the Higgs mass obtained by Standard Model fits to electroweak precision data. We develop a sum rule technique that enables us to determine the heavy-quark contributions directly from perturbative QCD, which reduces the uncertainty in current determinations of $\Delta\alpha_{\text{had}}(M_Z)$ by around 33%. Finally, we show how lattice calculations for $a_\mu^{\text{had,LO}}$ can immediately be used to obtain $\Delta\alpha_{\text{had}}(M_Z)$, giving the first purely (non-model) theoretical determination of $\Delta\alpha_{\text{had}}(M_Z)$.

Acknowledgements

First and foremost, I would like to thank Em. Prof. C.A. Dominguez. He has supported me beyond what I could have expected or even hoped for, and the success of my PhD program can be largely credited to him.

Dr. Will Horowitz has always had his door open for me for long chats about careers, physics, and the future in general. He is both a friend and mentor.

My collaborators from the University of Mainz, Prof. Dr. Karl Schilcher and apl. Prof. Dr. Hubert Spiesberger, for their great ideas and generosity in sharing them. This, coupled with their unfailing patience, made them the ideal collaborators. Their hospitality when they hosted me was also exceptional.

The National Institute for Theoretical Physics and the University of Cape Town for funding my studies, and the Humboldt Foundation for providing funding for yearly research visits to Germany.

The Department of Physics at UCT for all of the support and opportunities they have given me during the years. It has been much appreciated!

Tali Cassidy, for all her support and forbearance.

And finally, my parents, whose love and value of education must have rubbed off on me at some point.

Contents

List of Figures

List of Tables

Publications

The work in this thesis is based on the following publications:

S. Bodenstein, J. Bordes, C. Dominguez, J. Penarrocha, and K. Schilcher, "Charm-quark mass from weighted finite energy QCD sum rules," *Physical Review D* **82** (2010) 114013, arXiv:1009.4325 [hep-ph].

S. Bodenstein, J. Bordes, C. Dominguez, J. Penarrocha, and K. Schilcher, "QCD sum rule determination of the charm-quark mass," *Physical Review D* **83** (2011) 074014, arXiv:1102.3835 [hep-ph].

S. Bodenstein, C. Dominguez, and K. Schilcher, "Hadronic contribution to the muon $g-2$: A Theoretical determination," *Physical Review D* **85** (2012) 014029, arXiv:1106.0427 [hep-ph].

S. Bodenstein, C. Dominguez, K. Schilcher, and H. Spiesberger, "Hadronic contribution to the QED running coupling $\alpha_s(M_Z^2)$," *Physical Review D* **86** (2012) 093013, arXiv:1209.4802 [hep-ph].

S. Bodenstein, J. Bordes, C. Dominguez, J. Penarrocha, and K. Schilcher, "Bottom-quark mass from finite energy QCD sum rules," *Physical Review D* **85** (2012) 034003, arXiv:1111.5742 [hep-ph].

S. Bodenstein, C. Dominguez, S. Eidelman, H. Spiesberger, and K. Schilcher, "Confronting electron-positron annihilation into hadrons with QCD: An Operator product expansion analysis," *Journal of High Energy Physics* **1201** (2012) 039, arXiv:1110.2026 [hep-ph].

S. Bodenstein, C. A. Dominguez, and K. Schilcher, "Strange quark mass from sum rules with improved perturbative QCD convergence," *Journal of High Energy Physics* **1307** (2013) 138, arXiv:1305.3796 [hep-ph].

S. Bodenstein, "Precise determinations of the charm and bottom quark masses," *Modern Physics Letters A* **28** no. 26, (2013) 1360020

S. Bodenstein, "The hadronic contribution to the muon magnetic anomalous moment," *Modern Physics Letters A* **28** no. 26, (2013) 1360021.

S. Bodenstein, C. Dominguez, K. Schilcher, and H. Spiesberger, "Hadronic Contribution to the muon $g-2$ factor," *Physical Review D* **88** (2013) 014005, `arXiv:1302.1735 [hep-ph]`.

Defualt Values of Inputs

Speed of light in vacuum:	c	$=$	1
Reduced Planck's constant:	$\hbar$	$=$	1
Strong coupling at the scale of the M_Z:	$\alpha_s(M_Z)$	$=$	$0.1184(7)$
Fine structure constant:	α_{em}	$=$	$7.2973525698(24) \times 10^{-3}$
Gluon condensate:	$\langle \frac{\alpha_s}{\pi} G^2 \rangle$	$=$	$0.015(15)\,\text{GeV}^4$
Light-quark condensate:	$\langle \bar{q}q \rangle$	$=$	$(-267 \pm 5)^3\,\text{MeV}^3$
Strange-quark condensate:	$\langle \bar{s}s \rangle$	$=$	$0.8(3)\langle \bar{q}q \rangle$
Mass of the τ lepton:	m_τ	$=$	$1.77682(16)\,\text{GeV}$
$\overline{\text{MS}}$ strange-quark mass:	$\bar{m}_s(2\,\text{GeV})$	$=$	$95(5)\,\text{MeV}$
$\overline{\text{MS}}$ up-quark mass:	$\bar{m}_u(2\,\text{GeV})$	$=$	$2.3^{+0.7}_{-0.5}\,\text{MeV}$
$\overline{\text{MS}}$ down-quark mass:	$\bar{m}_d(2\,\text{GeV})$	$=$	$4.8^{+0.5}_{-0.3}\,\text{MeV}$

Abbreviations

OPE	**O**perator **P**roduct **E**xpansion
QCD	**Q**uantum **C**hromodynamics
LQCD	**L**attice **Q**uantum **C**hromodynamics
pQCD	**P**erturbative **Q**uantum **C**hromodynamics
CIPT	**C**ontour **I**mproved **P**ertubtion **T**heory
FOPT	**F**ixed **O**rder **P**ertubtion **T**heory

Chapter 1

Introduction

1.1 QCD Sum Rules

Quantum chromodynamical sum rules (QCD sum rules) are a method to relate hadronic observables to quantities analytically calculable in QCD. The method was introduced in 1979 by the SVZ group [2], it continues to be a powerful tool in analyzing a large class of

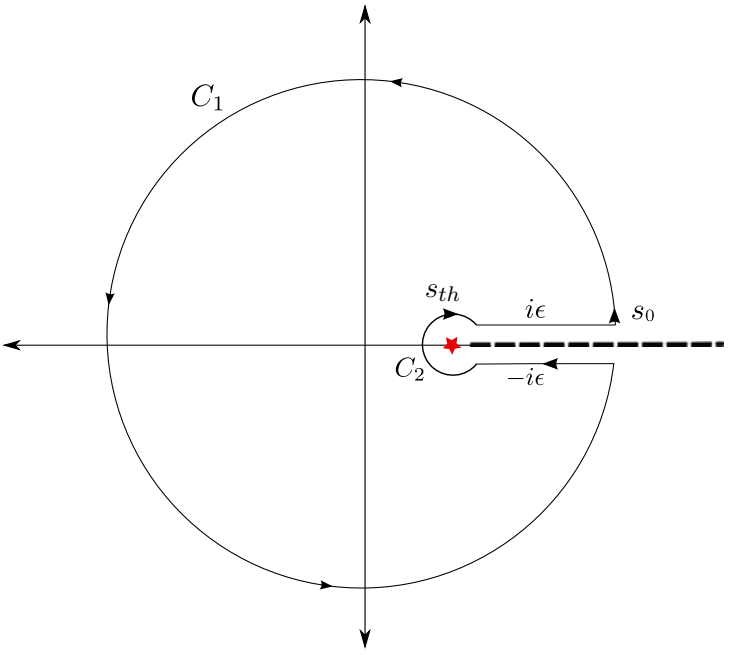

FIGURE 1.1: The integration contour. The threshold for charm-quark production is at s_{th}.

phenomena in strong-interaction physics (for reviews of the method, with applications, see for example [3–7]).

The idea of QCD sum rules is to first calculate correlation functions of currents at large (but not infinite) momentum transfers, where asymptotic freedom allows for pertubation theory to be used and non-perturbative effects added as power corrections in an operator product expansion [8–11]. The sum rules are then obtained by relating the correlation functions to measured spectral densities via dispersion relations, which follow from the analyticity and unitarity of the correlation functions.

For definiteness, consider the correlator of two vector currents

$$(q_\mu q_\nu - q^2 g_{\mu\nu})\Pi(q^2) = i \int dx\, e^{iqx} \langle 0| T[j_\mu(x) j_\nu^\dagger(0)] |0\rangle \,, \tag{1.1}$$

where $j^\mu = \bar{f}\gamma^\mu f$, and f is some quark flavour $f \in \{u, d, s, c, b, t\}$. We will find it useful working with the Mandelstam variable $s \equiv q^2$.
The first important property of the correlator $\Pi(s)$ is its analytic structure :

Theorem 1.1. *The function $\Pi(s)$ is analytic in the entire complex s-plane, except for a branch-cut along the positive real axis.*

The above theorem is a general property of local quantum field theories, independent of perturbation theory (for proofs, see [12–15]).[1].
The second important property of the correlator $\Pi(s)$ is the Optical Theorem,

$$R_f(s) \equiv \frac{\sigma(e^+e^- \to \text{hadrons}(f\bar{f}))}{\sigma(e^+e^- \to \mu^+\mu^-)} = 12\pi \text{Im}\Pi(s), \tag{1.2}$$

where $\sigma(e^+e^- \to \mu^+\mu^-) = 4\pi\alpha_{\text{em}}/3s$ and Q_f is the charge of the f-flavoured quark. This theorem follows directly from unitarity [17].
Now consider a Laurent polynomial $p(s)$,

$$p(s) \equiv \sum_{n=-i}^{k} a_n s^n. \tag{1.3}$$

[1]These analyticity properties formed the basis of S-Matrix theory before the adevent of QCD [16]. It is a highly non-trivial fact that the analyticity properties first postulated in S-Matrix theory are rigorously true also in QCD. This was shown in [13–15] and the references therein.

We immediately have from the Residue Theorem that

$$\oint \Pi(s)p(s)\,\mathrm{d}s = 2\pi i \cdot \mathrm{Res}[\Pi(s)\,p(s), s=0]. \tag{1.4}$$

In the limit $\epsilon \to 0$, and using Schwarz's Symmetry Principle, we obtain

$$\begin{aligned}\oint \Pi(s)p(s)\,\mathrm{d}s = &\int_{|s|=s_0} \Pi(s)\,p(s)\,\mathrm{d}s + 2i\int_{s_{th}}^{s_0} p(s)\,\mathrm{Im}\Pi(s)\,\mathrm{d}s \\ &+ \int_{C_2} \Pi(s)\,p(s)\,\mathrm{d}s.\end{aligned} \tag{1.5}$$

Assuming the vanishing of the integral about C_2 as $\epsilon \to 0$ and using the Optical Theorem, we obtain

$$\frac{1}{6\pi}\int_{s_{th}}^{s_0} p(s)\,R_f(s)\,\mathrm{d}s = i\int_{|s|=s_0} \Pi(s)\,p(s)\,\mathrm{d}s + 2\pi\,\mathrm{Res}[\Pi(s)\,p(s), s=0]. \tag{1.6}$$

The above result is exact. However, we cannot in general (analytically) compute $\Pi(s)$ from QCD. As mentioned, we can however approximate $\Pi(s)$ using a combination of pQCD and an OPE for values of s that are sufficiently far from the quark-pair production threshold, s_{th}. We can then set[2] $\Pi(s) \approx \Pi_{\mathrm{OPE}}(s)$ and finally obtain

$$\frac{1}{6\pi}\int_{s_{th}}^{s_0} p(s)\,R_f(s)\,\mathrm{d}s = i\int_{|s|=s_0} \Pi_{\mathrm{OPE}}(s)\,p(s)\,\mathrm{d}s + 2\pi\,\mathrm{Res}[\Pi_{\mathrm{OPE}}(s)\,p(s), s=0] \tag{1.7}$$

The above sum rule allows us to relate an experimentally measurable quantity on the LHS to a quantity on the RHS computable in QCD. This will be our key result that will be used throughout the thesis.

The idea behind the OPE expansion of the correlator, $\Pi_{\mathrm{OPE}}(s)$, will now be discussed in some more detail. We have a product of currents $j_\mu(x)j_\nu^\dagger(0)$ in (1.1). Formally, the OPE is an expansion of this product in the short-distance (or high-energy) limit $x \to 0$ as a series of operators defined at a single point. Inserting this into (1.1), we have a series

$$\Pi_{\mathrm{OPE}}(s) = \sum_{n=0}^{\infty} C_{2n}(q^2,\mu^2)\langle 0|\hat{O}_{2n}(\mu^2)|0\rangle \tag{1.8}$$

where the operators $\hat{O}_{2n}$ are dimension $d = 2n$ gauge-invariant Lorentz scalars. The coefficients C_{2n} are known as *Wilson coefficients*, and can be calculated in pQCD, whilst the operators $\hat{O}_{2n}$ encode the non-perturbative information and (by definition) are not

[2] The replacement $\Pi(s) \approx \Pi_{\mathrm{OPE}}(s)$ is an assumption often referred to as *local quark-hadron duality*.

calculable in pQCD. They must be determined either phenomenologically or via a non-perturbative method, such as lattice QCD (LQCD).

The operators $\hat{O}_{2n}$ must be constructed from either quark or gluon fields. The first term in the expansion (1.8) is simply $C_0(q^2, \mu^2) \cdot \hat{1} \equiv \Pi_{\text{pQCD}}$. The lowest-order (in the strong coupling) contribution to this is shown in Fig. 1.2. As there are no dimension $d = 2$ operators that can be constructed out of quark and gluon fields, it is traditionally assumed that $\langle 0|\hat{O}_2(\mu^2)|0\rangle$ vanishes (other than for mass insertions). This assumption will be checked in §3. We can construct a dimension $d = 4$ operator out of gluon fields, $\langle \frac{\alpha_s}{\pi} G^{\mu\nu} G_{\mu\nu} \rangle$. This is known as the *gluon condensate*, and it is a *renormalization group invariant*, as the scale dependence μ of the gluon fields cancels with that of the coupling. In the case of the light-quark fields, one can construct dimension $d = 4$ operators of the form $m_q \langle \bar{q} q \rangle$ for $i = \{u, d, s\}$, shown in Fig. 1.3. This is again a renormalization group invariant. The number of possible operators grows quickly for dimension $d = 6$ and above. We will discuss determinations of the numerical values of these condensates in the next section.

There is a useful physical interpretation of the condensates in terms of Feynman diagrams. Consider a diagram with a large external momentum flow, which goes along a quark loop. Although this would seem to be the exemplar of a process where asymptotic freedom allows us to use perturbation theory, there can be internal gluon lines which receive little momentum transfer. This leads to a large strong coupling, inappropriate for perturbation theory. The OPE factors out the large-momentum part (and calculates it perturbatively), whilst parameterizing the low-momentum gluon contributions in terms of the gluon condensate. This is illustrated in Fig. 1.2, where the loop represents the large-momentum piece (the Wilson coefficient), whilst the dots represent an average over the low-momentum gluon contributions (given by the gluon condensate).

1.1.1 Structure of this Thesis

This thesis will be broken into three pieces:

Chapter 1: A calculation of the bottom, charm and strange-quark masses.

Chapter 2: An analysis of the lowest-order hadronic contribution to the muon anomalous magnetic moment.

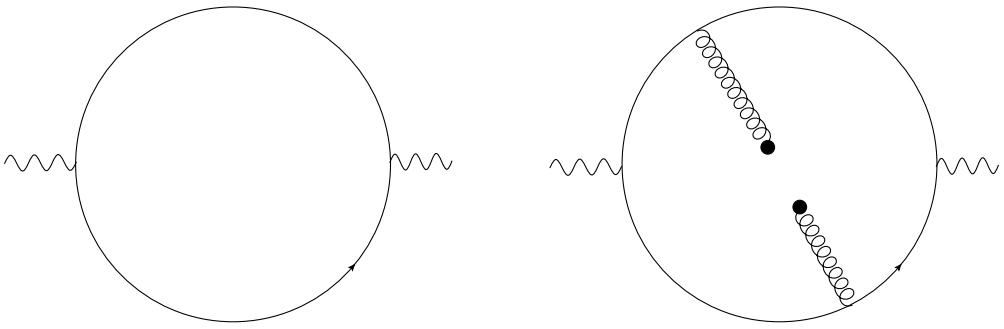

FIGURE 1.2: The lowest-order contribution to $\Pi_{\rm pQCD}$ (*left figure*) and the gluon condensate (*right figure*).

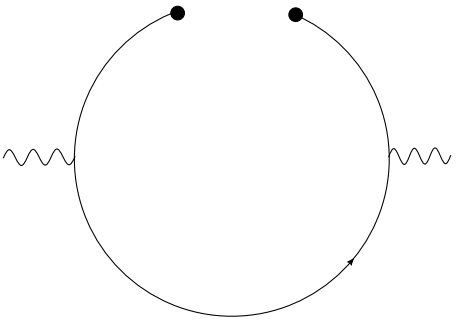

FIGURE 1.3: The quark-mass condensate.

Chapter 3: A theoretically driven determination of the hadronic contribution to the running of the electromagnetic coupling.

Each of these will make critical use of the sum rule approach outlined above.

Chapter 2

Quark Mass Determinations

There are currently believed to be six quark flavours, whose PDG-averaged masses in the $\overline{\text{MS}}$-scheme are [1]

$$\begin{aligned}
\overline{m}_u(\overline{m}_u) &= 2.3^{+0.7}_{-0.5}\,\text{MeV}\ (\sim 26\%\,\text{error}),\\
\overline{m}_d(\overline{m}_d) &= 4.8^{+0.5}_{-0.3}\,\text{MeV}\ (\sim 8\%\,\text{error}),\\
\overline{m}_s(\overline{m}_s) &= 95(5)\,\text{MeV}\ (5\%\,\text{error}),\\
\overline{m}_c(\overline{m}_c) &= 1275(25)\,\text{MeV}\ (2\%\,\text{error}),\\
\overline{m}_b(\overline{m}_b) &= 4180(30)\,\text{MeV}\ (0.7\%\,\text{error}),\\
\overline{m}_t(\overline{m}_t) &= 173070(890)\,\text{MeV}\ (0.5\%\,\text{error}).
\end{aligned}$$

There is a clear trend with regards to the relative errors: the larger the mass, the more precisely known it is. One general reason for this trend is confinement. As quarks are confined, their masses can only be determined indirectly by inferring them from various hadronic observables. The smaller the mass, the smaller are the contributions of these masses on hadronic observables, making the mass contributions harder to isolate.
The exception to this argument is the top quark, which does not hadronize: its lifetime is $\sim 0.5 \times 10^{-24}\,\text{s}$, which is shorter than the expected time to form top-flavoured hadrons [18]. The top mass determination will clearly require very different techniques from those of the other quarks. We will not cover these techniques in this thesis.

There are two classes of methods that provide competitive precision for (non-top) quark mass determinations. On the numerical side, we have LQCD, and on the analytical side

are QCD Sum Rules. The latter approach makes use of a sum rule like (1.7). As $\Pi_{\rm OPE}$ will in general depend on the quark masses, one can determine the quark masses by demanding that the sum rule is satisfied.

In this section, we will introduce a new sum rule technique to increase the precision of the charm and bottom quark masses. We will also reanalyse a previous sum rule determination of the strange quark mass, and introduce a technique to improve the convergence of the pQCD series.

2.1 The Bottom and Charm Quark Masses

2.1.1 Introduction

The earliest attempts at determining the bottom (m_b) and charm (m_c) quark masses were via models. One example from 1980 [19] involves fitting a linear-plus-Coulomb potential model

$$V(r) = -\frac{\kappa}{r} + \frac{r}{a^2}, \tag{2.1}$$

to observed hadron-spectra. The model, along with the observed $J/\psi - \psi(2s)$ and $\Upsilon(2s) - \Upsilon(1S)$ splitting, leads to charm and bottom masses

$$m_c \sim 1.65\,\text{GeV} \tag{2.2}$$

$$m_b \sim 5.17\,\text{GeV} \tag{2.3}$$

Yet such determinations had multiple shortcomings. Chief among them is that in the Standard Model, the quark masses are free parameters in the (n_f flavour) QCD Lagrangian,

$$\mathcal{L}_{\rm QCD} = \sum_{k=1}^{n_f} \overline{q}_k (i\gamma^\mu D_\mu - m_k) q_k - \frac{1}{4} G_{\mu\nu} G^{\mu\nu}, \tag{2.4}$$

where the k^{th} quark mass parameter is m_k. There exists no way of relating the model masses (2.2) to the mass parameters in the QCD Lagrangian, which are (like any other parameter in the Standard Model Lagrangian) renormalized quantities that are both scale- and scheme-dependent.

The sum rule approach using (1.7) does not suffer from this problem, as (1.7) relates hadronic observables directly to $\Pi_{\rm OPE}$ which is derivable directly from $\mathcal{L}_{\rm QCD}$.

The most common sum rule approach used to determine both the charm and bottom quark masses make use of so-called Hilbert-moment sum rules (see for example [20]). This is equivalent to the choice $p(s) = 1/s^{n+1}$ (where n is an integer and $n > 0$), and taking the limit $s_0 \to \infty$. Then the integral around the contour $|s| = s_0$ goes to 0,[1] and so (1.7) becomes

$$\int_{s_{th}}^{\infty} \frac{R_f(s)}{s^{n+1}}\,\mathrm{d}s = \frac{12\pi^2}{n!}\left[\frac{d}{ds}\right]^n \Pi_{\mathrm{OPE}}(s)\Big|_{s=0} \tag{2.5}$$

Now n can in principle be arbitrarily chosen. However, there turn out to be two competing constraints. First on the experimental side: we know $R_f(s)$ very well close to the pair-production threshold (it is dominated by the well-known Υ resonances in the bottom case, and J/ψ and $\psi(2s)$ for the charm). As we move away from the threshold, the experimental uncertainties on $R_f(s)$ start increasing. Thus the larger the choice of n, the more suppression we have of the poorly known region beyond the narrow resonances. However, the cost is that the perturbative series for $\left[\frac{d}{ds}\right]^n \Pi_{\mathrm{OPE}}(s)\Big|_{s=0}$ converges poorly for large n, whilst the (badly known) non-perturbative terms start contributing greatly also for large n.[2] The commonly used approach to choosing n is thus to find the value of n that minimizes the total uncertainty.

Another approach in the literature is to choose $p(s)$ without any inverse powers of s (for example [22–24]), whereby (1.7) becomes

$$\int_{s_{th}}^{s_0} p(s)\,R_f(s)\,\mathrm{d}s = 6\pi i \int_{|s|=s_0} \Pi_{\mathrm{OPE}}(s)\,p(s)\,\mathrm{d}s \tag{2.6}$$

In this approach, $p(s)$ is taken to be a linear combination of powers of s, chosen to enhance the contribution of the narrow resonances. A similar constraint applies in this case: the more powers of s are included, the better control one has over the data, yet the greater the contribution of non-perturbative terms and the poorer the pQCD convergence.

Rather than consider these special cases of (1.7), we realized that the greatest precision could be achieved by keeping things general, and considering linear combinations of arbitrary powers of s. The philosophy is then to define a set of uncertainty metrics, and

[1] This is because the vector correlator has asymptotic behaviour $\lim_{s\to\infty}\Pi(s) \propto \log(s)$. But $\oint_{|s|=s_0} s^{-2}\log(s) \propto 1/s_0$, which vanishes as $s_0 \to \infty$. For higher inverse powers of s, it will also obviously vanish.

[2] The problem of the convergence and large non-perturbative contributions for large n can be overcome by choosing a more suitable mass definition (in this case some threshold mass). See [21] for such an approach. The precision from this approach is still not competitive however.

engineer $p(s)$ to minimize the total uncertainty. This approach was first used by us for the charm quark and bottom quarks [25–27], obtaining

$$\bar{m}_c(3\,\text{GeV}) = 987(9)\,\text{MeV} \tag{2.7}$$

$$\bar{m}_b(10\,\text{GeV}) = 3623(9)\,\text{MeV}. \tag{2.8}$$

The above value of $\bar{m}_c(3\,\text{GeV})$ is the most precise result for charm mass using any sum rule method (though there is a more precise LQCD value [28]). In the case of the bottom quark mass, this is the most precise value obtained by any method. For comparison, the latest LQCD results are [28]

$$\bar{m}_c(3\,\text{GeV}) = 986(6)\,\text{MeV}, \tag{2.9}$$

$$\bar{m}_b(10\,\text{GeV}) = 3617(25)\,\text{MeV}. \tag{2.10}$$

The agreement between our results and those of LQCD are particularly impressive.

We will proceed as follows: we will first give a detailed discussion of the existing information on $\Pi_{\text{OPE}}(s)$, which is used for both charm and bottom quark masse determinations. As the experimental situation is different for the charm and mass, we will consider these seperately.

2.1.2 The Correlator $\Pi_{\text{OPE}}(s)$

The correlator $\Pi_{\text{OPE}}(s)$ can be decomposed as

$$\Pi_{\text{OPE}}(s) = \Pi_{\text{pQCD}}(s) + \Pi_{\text{NP}}(s) + \Pi_{\text{qed}}(s), \tag{2.11}$$

where $\Pi_{\text{pQCD}}(s)$ is the dominant pQCD contribution, $\Pi_{\text{NP}}(s)$ are non-perturbative contributions and $\Pi_{\text{qed}}(s)$ are QED contributions. We will need all of these in both the high-energy (to perform the contour integral in (1.7)) and low-energy limits (to evaluate the residue in (1.7)).

First consider $\Pi_{\text{pQCD}}(s)$. The Laurent-expansion of $\Pi_{\text{pQCD}}(s)$ about $s = -\infty$ is customarily cast in the form

$$\Pi_{\text{pQCD}}(s) = Q_f^2 \sum_{n=0} \left(\frac{\alpha_s(\mu^2)}{\pi}\right)^n \Pi^{(n)}(s), \tag{2.12}$$

$$\Pi^{(n)}(s) = \sum_{i=0} \left(\frac{\bar{m}_Q^2}{s}\right)^i \Pi_i^{(n)}. \tag{2.13}$$

Here $\bar{m}_Q \equiv \bar{m}_Q(\mu)$ is the $\overline{\text{MS}}$-scheme quark mass at the renormalization scale μ. We take the $\mathcal{O}(\alpha_s^2(\bar{m}_b^2)^6)$ result from Ref. [29]. At $\mathcal{O}(\alpha_s^3)$ we have $\Pi_0^{(3)}$ and $\Pi_1^{(3)}$ from Ref. [30], and the logarithmic terms for $\Pi_2^{(3)}$ from Ref. [31]. The constant term in $\Pi_2^{(3)}$ is not known exactly, but has been been estimated using Padé approximants [32]. At $\mathcal{O}(\alpha_s^4)$ we have the exact logarithmic terms for $\Pi_0^{(4)}$ and $\Pi_1^{(4)}$ [33, 34], whilst the constant terms are not yet known. Given that these constant terms will contribute when we use kernels containing terms s^{-1} and s^0 respectively, we will for the sake of consistency not include any $\mathcal{O}(\alpha_s^4)$ terms and perform our entire analysis at $\mathcal{O}(\alpha_s^3)$. The first few terms are

$$\Pi_{\text{pQCD}}(s) = \frac{3Q_f^2}{16\pi^2}\left(\frac{20}{9} - \frac{4}{3}\log\left[-\frac{s}{\bar{m}_Q^2}\right] + \frac{8\bar{m}_Q^2}{s} + \mathcal{O}(\bar{m}_Q^4)\right) + \mathcal{O}(\alpha_s) \tag{2.14}$$

We want to use (2.12) to perform the contour integral in (1.7). Now (2.12) is only formally guaranteed to converge above $\sqrt{s} = 4m_f$, due to non-planar diagrams having cuts starting here. We will therefore always choose s_0 to be above this.

We can also Taylor expand $\Pi_{\text{pQCD}}(s)$ about $s = 0$, which is customarily put in the form

$$\Pi_{\text{pQCD}}(s) = \frac{3Q_f^2}{16\pi^2} \sum_{n\geq 0} \bar{C}_n z^n, \tag{2.15}$$

where $z \equiv s/(4\bar{m}_Q^2)$. The coefficients $\bar{C}_n$ can be expanded in powers of $\alpha_s(\mu)$

$$\begin{aligned}\bar{C}_n =& \bar{C}_n^{(0)} + \frac{\alpha_s(\mu)}{\pi}(\bar{C}_n^{(10)} + \bar{C}_n^{(11)} l_m) \\ &+ \left(\frac{\alpha_s(\mu)}{\pi}\right)^2 (\bar{C}_n^{(20)} + \bar{C}_n^{(21)} l_m + \bar{C}_n^{(22)} l_m^2) \qquad (2.16) \\ &+ \left(\frac{\alpha_s(\mu)}{\pi}\right)^3 (\bar{C}_n^{(30)} + \bar{C}_n^{(31)} l_m + \bar{C}_n^{(32)} l_m^2 + \bar{C}_n^{(33)} l_m^3) + \ldots \qquad (2.17)\end{aligned}$$

where $l_m \equiv \ln(\mu^2/\bar{m}_Q^2)$. Up to $\mathcal{O}(\alpha_s^2)$, the coefficients up to $n = 30$ of $\bar{C}_n$ are known [35–37]. At $\mathcal{O}(\alpha_s^3)$, we have $\bar{C}_0$ and $\bar{C}_1$ from [35, 38], $\bar{C}_2$ from [36, 37], and $\bar{C}_3$ from [39].

The results for $\bar{C}_0$ and $\bar{C}_1$ are only given at a choice of $\mu = \bar{m}$ in the references, yet we require the full scale-dependence. Thus we give these two coefficients with arbitrary scale in §A.4. In the bottom-quark case, there is also a subleading contribution of order $\mathcal{O}(\alpha_s^2(\bar{m}_c/\bar{m}_b)^2)$ that will affect the coefficient $\bar{C}_n^{(20)}$ that must be included [40]. The kernel $p(s)$ will be chosen so that no coefficients $\bar{C}_3$ and above contribute to our sum rule (1.7).

We will use the Particle Data Group value for the (five-flavour) strong coupling, $\alpha_s(M_Z) = 0.1184(7)$ [41]. We will require the four-flavour coupling when determining the charm mass. We will use the Mathematica package RunDec [42] to perform the decoupling when crossing flavour thresholds.[3]

The leading-order contribution to $\Pi_{\text{NP}}(s)$ comes from the gluon condensate. This contribution has been determined in Ref. [44]. We give the full result in §A.5. The value of the gluon condensate is badly known, as can be seen in Table 2.1, which shows the most recent determinations. We will use a conservative value of

$$\langle \frac{\alpha_s}{\pi} G^2 \rangle = 0.015 \pm 0.015 \,\text{GeV}^4 \tag{2.18}$$

throughout the thesis. This value is chosen to be consistent with almost all determinations. Using this value, the gluon condensate contribution is negligible for the bottom quark mass, and contributes roughly 1 MeV to the charm quark mass. The rest of the terms in the OPE are not known at all. The usual procedure is to assume that these will contribute less than the leading-order correction, and thus be neglected.

The QED term $\Pi_{\text{qed}}(s)$ can be obtained directly from the QCD correlator. One simply takes the $\mathcal{O}(\alpha_s)$ term in $\Pi_{\text{pQCD}}(s)$, and replaces the internal gluon with a photon. This amounts to the replacement $\alpha_s \to Q_f^2 \alpha_{\text{em}}$ and dividing through by the colour factor $C_f = 4/3$. In the high-energy limit,

$$\Pi_{\text{qed}}(s) = \frac{\alpha_{\text{em}}}{\pi} \frac{3Q_f^4}{16\pi^2} \left[\frac{55}{12} - 4 \log\left(-\frac{s}{\mu^2} \right) - \zeta(3) + \mathcal{O}(\bar{m}^2) \right]. \tag{2.19}$$

[3] A note regarding this: We are using the $\overline{\text{MS}}$ renormalization scheme, in which the QCD β-function is independent of the quark masses. Now we know from the Appelquist-Carazzone theorem [43] that the heavy quarks must decouple from the light quarks, but due to the lack of dependence of the β-function on the quark masses, it is not obvious how this decoupling is to be implemented. The solution is to create different decoupling regions, in which we create an effective field theory containing the $\overline{\text{MS}}$ running mass $\bar{m}_f^{(n_f)}$ which behaves as though there were only $n_f - 1$ light quarks. Matching this effective theory to the full theory allows us to connect the $n_f - 1$ and n_f flavour strong coupling.

$\langle\frac{\alpha_s}{\pi}G^2\rangle\,(\mathrm{GeV}^4)$	Method	Date	Reference
0.048 ± 0.030	Bottomonium superconvergent sum rules	1999	[45]
0.03 ± 0.02	LQCD	2002	[46]
0.009 ± 0.007	Charmonium sum rules	2003	[47]
$0.005^{+0.001}_{-0.004}$	Charmonium sum rules	2004	[48]
0.04 ± 0.01	LQCD	2005	[49]
0.001 ± 0.0012	Global Fit ALEPH τ-decay	2005	[50]
0.01 ± 0.01	FESR ALEPH τ-decay	2007	[51]
-0.022 ± 0.004	Global fit ALEPH τ-decay (A-V Channel)	2008	[52]
0.022 ± 0.003	Charmonium sum rules	2012	[53]
0.015 ± 0.015	Estimate used in this thesis		

TABLE 2.1: The most recent determinations of the gluon condensate. The last value is a conservative estimate of $\langle\frac{\alpha_s}{\pi}G^2\rangle$ that will be used throughout this thesis. It is chosen to be consistent with almost all of the above determinations.

In the low-energy limit, the QED contribution is

$$\Pi_{\mathrm{qed}}(s) = \frac{1}{C_f}\frac{3Q_f^4}{16\pi^2}\frac{\alpha_{\mathrm{em}}}{\pi}\sum_{n\geq 0}(\bar{C}_n^{(10)} + \bar{C}_n^{(11)} l_m) z^n. \tag{2.20}$$

2.1.3 The Charm Quark Mass

This section will be based on the work in our publications [24, 26, 27].

2.1.3.1 Data Input

To evaluate the left-hand side of (1.7), we need to use experimental input. The lowest-lying charmonium states are the J/ψ and $\psi(2s)$. Their contribution to (1.7) using the narrow-width approximation is

$$R_c^{\mathrm{res}} = \sum_i \frac{9\pi M_i \Gamma_i}{\alpha_{\mathrm{em}}^2(s)}\delta(s - M_i^2), \tag{2.21}$$

where $i \in \{J/\psi, \psi(2s)\}$. We take the masses and widths from the Particle Data Group [1]. For the leptonic widths, we have $\Gamma_{J/\psi} = 5.55(14)\,\mathrm{keV}$ and $\Gamma_{\psi(2s)} = 2.35(4)\,\mathrm{keV}$, whilst the masses are $M_{J/\psi} = 3.096916(11)\,\mathrm{GeV}$ and $M_{\psi(2s)} = 3.68609(4)\,\mathrm{GeV}$. The

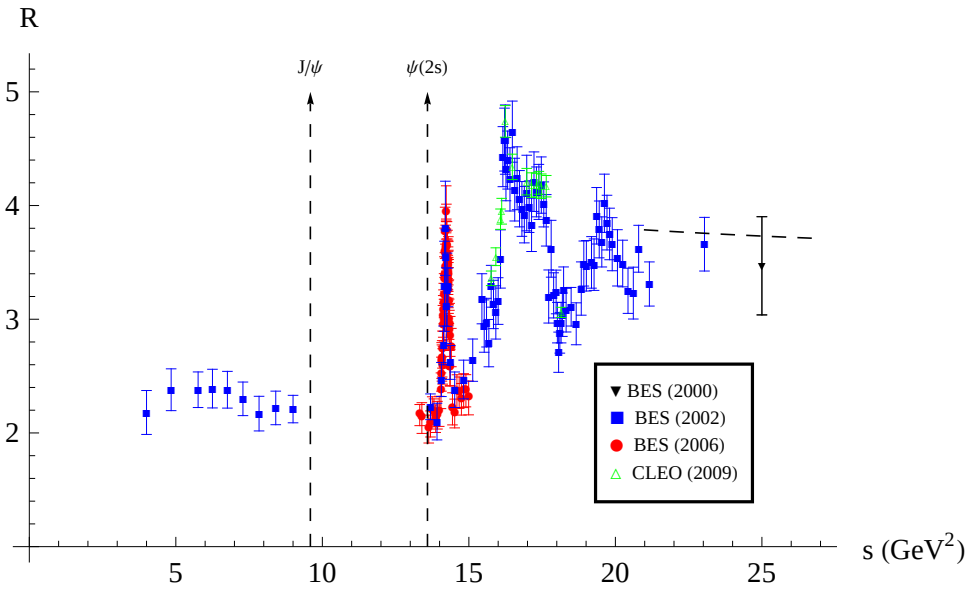

FIGURE 2.1: The data is from BES 2000 [54], BES 2002 [55], BES 2006 [56] and CLEO 2009 [57]. The error bars give the systematic and statistical uncertainties added in quadrature. The dashed line is the prediction of perturbative QCD.

effective electromagnetic couplings are $\alpha_{\rm em}(M_{J/\psi}) = 1/134.112$ and $\alpha_{\rm em}(M_{\psi(2s)}) = 1/133.955$, which we have taken from [58].

Just above the J/ψ and $\psi(2s)$ lies a *continuum resonance region*, where pQCD is not yet valid and where we cannot use the finite-width approximation. We thus require experimental measurements of $R_c(s)$ in this region. Measurements only exist though for $R_{\rm tot}(s)$, which includes the contributions from the light quarks, secondary charm-production originating from gluon splitting, and from singlet type diagrams, where the external vector current couples to two different fermion loops.[4] Examples of these processes are given in Fig. 2.2. These contributions we will denote by "background", and must be subtracted from $R_{\rm tot}$ to obtain R_c.

The experimental situation for $R_{\rm tot}(s)$ is as follows. The 2002 BES collaboration [55] have a measurement in the range $2\,{\rm GeV} < \sqrt{s} < 5\,{\rm GeV}$. More precise measurements in the $\psi(3770)$ region ($3.650\,{\rm GeV} \leq \sqrt{s} \leq 3.872\,{\rm GeV}$) were obtained by BES in 2006 [56], which we will use in place of the older BES data in this region. There is also an older 2000 BES measurement [54]. We will only use their data point at $\sqrt{s} = 5\,{\rm GeV}$, as this is the only data set that has a point at $\sqrt{s} = 5\,{\rm GeV}$. Finally, we also have data from CLEO [57] in the range $3.97\,{\rm GeV} < \sqrt{s} < 4.26\,{\rm GeV}$. We will use the CLEO data in this

[4] The reason these do not contribute is that their Feynman diagrams have cuts starting from $s = 0$, and hence can't be included in our sum rule (1.7).

range exclusively, due to its lower uncertainties than the BES data in this region. This is illustrated in Fig. 2.1.

Obtaing $R_c(s)$ from $R_{\mathbf{tot}}(s)$

It was found in [58] that the total background is different[5] from the light-quark contribution, R_{uds}, by $\approx 0.01\%$, and thus the non-R_{uds} contributions are entirely negligible. The perturbative prediction for R_{uds} is known up to $\mathcal{O}(\alpha_s^4)$ [30, 33], and is

$$\begin{aligned} R_{uds} = \sum_{f\in\{u,d,s\}} Q_f^2 \Big[& 1 + a_s + (1.9857 - 0.1152 n_f) a_s^2 \\ & + (-6.63694 - 1.20013 n_f - 0.00518 n_f^2) a_s^3 \\ & + (-156.61 + 18.77 n_f - 0.7974 n_f^2 + 0.0215 n_f^2) a_s^4 + \mathcal{O}(a_s^5) \Big] \end{aligned} \tag{2.22}$$

where $a_s \equiv \alpha_s(s)/\pi$. The sum over the light quark flavours is $\sum_{\mathrm{u,d,s}} e_Q^2 = 2$.

There are two ways of proceeding to obtain R_c. The most obvious approach is simply to use $R_c = R_{\mathrm{tot}}(s) - R_{uds}$. The issue with this approach is that the systematic uncertainties for R_c become (proportionally) very large. We will follow a more sophisticated approach introduced by [58]. The idea is to make use of the BES data below the $\psi(2s)$, which is a measurement of R_{uds} (we can neglect the widths of the $\psi(2s)$ and J/ψ). We can then fit the theoretical prediction of R_{uds} to the BES data points below $\sqrt{s} = M_{\psi(2s)}$, assuming energy independence, and then extrapolating this with the theoretical energy dependence into the threshold region. It was found in [58] that this procedure involves multiplying R_{uds} by 1.038 when subtracting from the 2002 BES data, and by 0.991 when subtracting from the 2006 BES data. It assumed that some cancellation of systematic uncertainties takes place with this procedure, increasing the accuracy.
As we are only using a single point from BES 2000 [54], we use the simplest procedure and subtract R_{uds} without any fitting. The CLEO 2009 [57] data is the easiest to handle. As explained in the CLEO paper [57], it amounts simply to removing 2.285 from all of the ISR-corrected R-ratio values in their Table VIII.

We should mention here that we don't have any data in the region $25\,\mathrm{GeV}^2$ to $49\,\mathrm{GeV}^2$, after which there is data up to about $110\,\mathrm{GeV}^2$ from [59], which we won't make use of.

[5] See Table 1 in [58].

2.1.3.2 Data Uncertainties

The treatment of the random uncertainties is standard, and are largely averaged out for the regions in which there are many data points (though not in the region $s \in [22, 25]\text{GeV}^2$, where we have few data points). The systematic uncertainties require a bit more thought. From the fitting (for the BES data), we have obtained a systematic uncertainty for R_{uds}, which is positively correlated with that of the measured R_{tot}. One might thus be tempted to simply subtract the systematic uncertainty of R_{uds} from R_{tot} to obtain the systematic uncertainty of R_c. However, as pointed out in [60], this will underestimate the systematic uncertainty. We proceed by assuming that the systematic uncertainties of the charmed and non-charmed final states are equal, which is equivalent to multiplying the systematic uncertainties of R_{tot} by a factor of $\frac{1}{\sqrt{2}}$ to obtain the corresponding systematic uncertainties of R_c. For the CLEO 2009 [57] data, we take the same systematic uncertainties for $R_c(s)$ as were given for R_{tot}.

We will make the conservative assumption that the systematic uncertainties of the three BES data sets are not independent[6], and hence add them linearly rather than in quadrature. We do assume the CLEO systematic uncertainties are independent from the BES ones. When numerically integrating this data, we will use linear interpolation.

2.1.3.3 Choosing the kernel $p(s)$

We want to design a kernel $p(s)$ that suppresses the poorly-known continuum threshold region in favour of the well-known J/ψ and $\psi(2s)$ resonances, whilst preserving the convergence of pQCD. We will choose $p(s)$ to be linear combinations of powers in the set $\mathcal{S} = \{s^{-2}, s^{-1}, 1\}$. The reason for this is that if we have higher inverse powers of s, then the convergence of the correlator in the $\overline{\text{MS}}$-scheme starts converging badly and non-perturbative contributions become important. If we choose powers of s greater than s^0, then unknown terms at $\mathcal{O}(\alpha_s^3)$ in the high-energy expansion start contributing. In general, the more terms $p(s)$ contains, the worse the convergence. We found that the optimal number is two terms in $p(s)$. Finally, although pQCD is consistent with the last data points in Fig. 2.1, these data have very large uncertainties and they are very sparse. We are thus not really sure if pQCD is valid yet at the end of our data. To make

[6] The BES detectors used in 2000, 2002 and 2006 are presumably the same machines, with only a few modifications. Thus the systematic uncertainties would not be entirely independent.

		Uncertainties (MeV)				
$p(s)$	$\bar{m}_c(3\,\text{GeV})$	ΔExp.	$\Delta\alpha_s$	$\Delta\mu$	ΔNP	ΔTotal
s^{-2}	995	9	3	1	1	10
s^{-3}	977	6	8	9	8	17
$1-s_0/s$	995	8	3	3	2	10
$1-(s_0/s)^2$	987	7	4	1	1	9
$1-(s_0/s)^3$	974	5	10	8	9	17
$s^{-1}(1-s_0/s)$	985	6	4	2	1	8

TABLE 2.2: The results for $\bar{m}_c(3\,\text{GeV})$ using a number of different kernels. The sources of uncertainties are from experiment (ΔEXP), the strong coupling constant ($\Delta\alpha_s$), the variation of the renormalization scale by $\pm1\,\text{GeV}$ about $\mu = 3\,\text{GeV}$ ($\Delta\mu$), and the gluon condensate (ΔNP). We obtain the total uncertainty by adding all the above in quadrature. $\sqrt{s_0} = 4.8\,\text{GeV}$ is used for all these results.

our sum rule less dependent on this, we will use so-called 'pinching' moments that vanish at s_0. Given our constraints, we have three of these, $p(s) = 1 - s_0/s$, $p(s) = 1 - (s_0/s)^2$ and $p(s) = s^{-1}(1 - s_0/s)$.

2.1.3.4 Results

The results for the charm quark mass obtained using our pinching kernels, as well as the Hilbert-moment kernels, are shown in Table 2.2. We see that the most precise kernels are $p(s) = s^{-1}(1 - s_0/s)$ and $p(s) = 1 - (s_0/s)^2$, whose masses are amazingly close. Choosing the mass with the lowest uncertainty, obtained using $p(s) = s^{-1}(1 - s_0/s)$, as our final result, we find

$$\bar{m}_c(3\,\text{GeV}) = 985(8)\,\text{MeV}. \tag{2.23}$$

We compare this result to recent literature determinations in Fig. 2.3. As most results in the literature are given for the scale independent mass, we convert our result. The details of this conversion can be found in §A.1.2.[7] We can note that our result is consistent with all the recent charm mass determinations. Particularly impressive is the remarkable agreement between our method and the latest LQCD result [28], which obtained

$$\bar{m}_c(3\,\text{GeV}) = 986(6)\,\text{MeV}. \tag{2.24}$$

This is a highly non-trivial check on both the LQCD and sum rule approaches.

[7] This conversion is quite sensitive to the value of α_s one uses. Thus two results that are the same at $\mu = 3\,\text{GeV}$ will not necessarily be the same at $\mu = \bar{m}$, which can be seen in Fig. 2.3.

	$\bar{m}_c(3\,\text{GeV})(\text{MeV})$					
$p(s)$	$\bar{m}_c^{(0)}$	$\bar{m}_c^{(1)}$	$\bar{m}_c^{(2)}$	$\bar{m}_c^{(3)}$	$\Delta\mu\,(\text{MeV})$	$\Delta\text{conv}\,(\text{MeV})$
s^{-2}	1129	1021	998	995	1	3
s^{-3}	1175	962	963	977	9	14
$1-s_0/s$	1100	1028	1003	995	3	8
$1-(s_0/s)^2$	1146	1019	991	987	1	4
$1-(s_0/s)^3$	1181	959	960	974	8	14
$s^{-1}(1-s_0/s)$	1160	1017	987	985	2	2

TABLE 2.3: The results for $\bar{m}_c(3\,\text{GeV})$ at different orders of α_s in pQCD. The last two columns are two different estimates of truncation uncertainty. The first ($\Delta\mu$) is obtained by varying the scale by $\pm 1\,\text{GeV}$ about $\mu = 3\,\text{GeV}$, whilst the second (Δconv) is obtained by $\Delta\text{conv} = \bar{m}_c^{(3)} - \bar{m}_c^{(2)}$.

There are two possible sources of uncertainty that should be discussed in more detail.

1. We are not sure whether pQCD is valid at $\sqrt{s_0} = 4.8\,\text{GeV}$. One approach to checking our dependence on this assumption is to vary $\sqrt{s_0}$ below $4.8\,\text{GeV}$, where pQCD (from Fig. 2.1) is clearly not valid, and see how sensitive our result is to this. We show this dependence for our two best kernels in Fig. 2.5 and Fig. 2.6, and find that even varying s_0 in the large range of $15\,\text{GeV}^2 < s < 25\,\text{GeV}^2$, the charm mass obtained with either kernel only varies by $5\,\text{MeV}$. Adding this uncertainty to our result (2.23) would increase its uncertainty by $1\,\text{MeV}$. In comparison, the variation using the kernel $p(s) = 1/s^2$ is shown in Fig. 2.4. Here a variation of $14\,\text{MeV}$ is produced.

2. The convergence of our perturbative series. To estimate the uncertainty from leaving out all terms at $\mathcal{O}(\alpha_s^4)$ and above, we varied the renormalization scale by $1\,\text{GeV}$. This is a fairly arbitrary number, and it may be wondered how good this estimate really is. One check is to use a different approach to estimate the missing terms, which is to find the difference between the $\mathcal{O}(\alpha_s^3)$ and $\mathcal{O}(\alpha_s^2)$ masses, and assume the missing terms don't contribute more than this difference. We show the full convergence information in Table 2.3, and see that for our best kernel $p(s) = s^{-1}(1 - s_0/s)$, the two estimates are exactly the same.

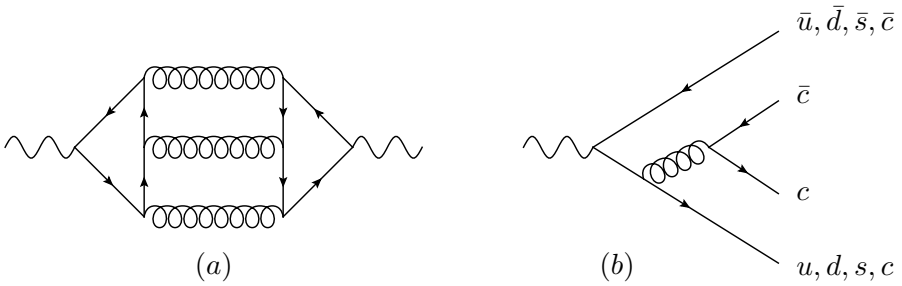

FIGURE 2.2: (a) is an example of a singlet-type diagram. (b) is an example of secondary-charm production.

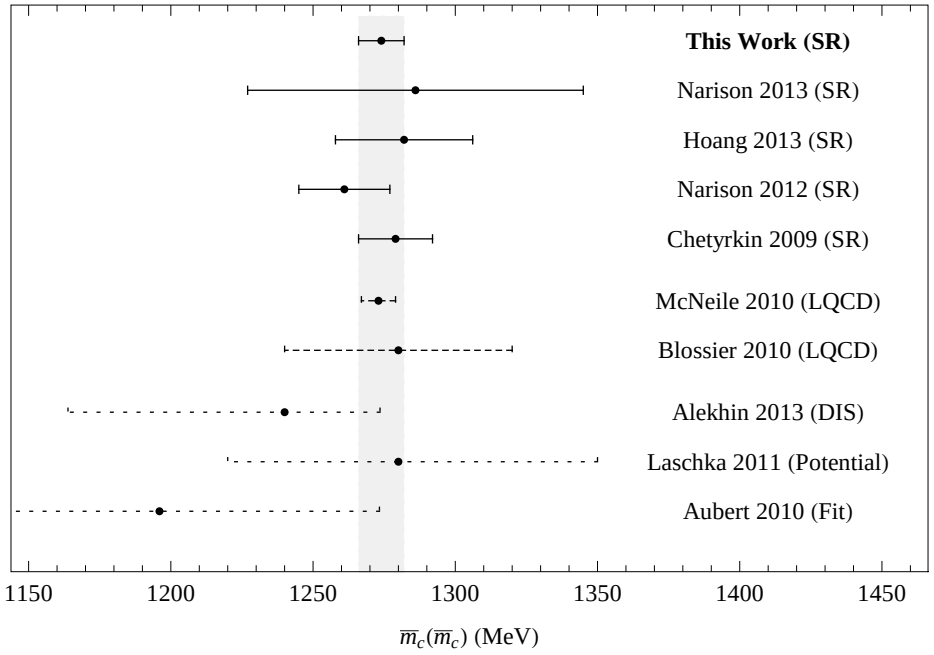

FIGURE 2.3: The value of $\bar{m}_c(\bar{m}_c)$ obtained in Eq. (2.27) compared the most recent determinations in the literature [20, 28, 53, 61–66]. We have separated the results into three general class of method used to determine the charm mass. These are sum rule approach (SR), lattice (LQCD), deep inelastic scattering (DIS), potential approaches (potential) and global fits (fit).

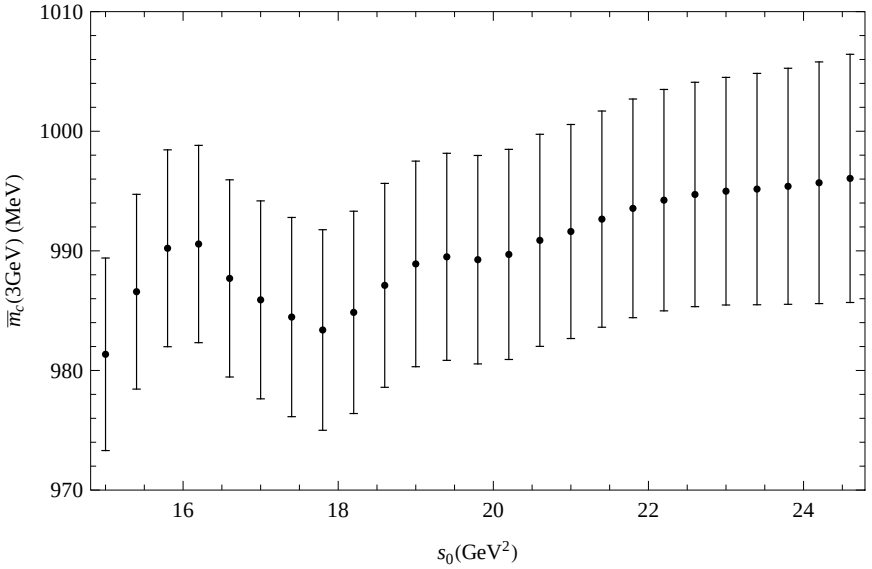

FIGURE 2.4: $\bar{m}_c(3\,\mathrm{GeV})$ as a function of s_0 obtained using $p(s) = 1/s^2$. The total variation of $\bar{m}_c(3\,\mathrm{GeV})$ in the range $15\,\mathrm{GeV}^2 < s < 25\,\mathrm{GeV}^2$ is 13 MeV.

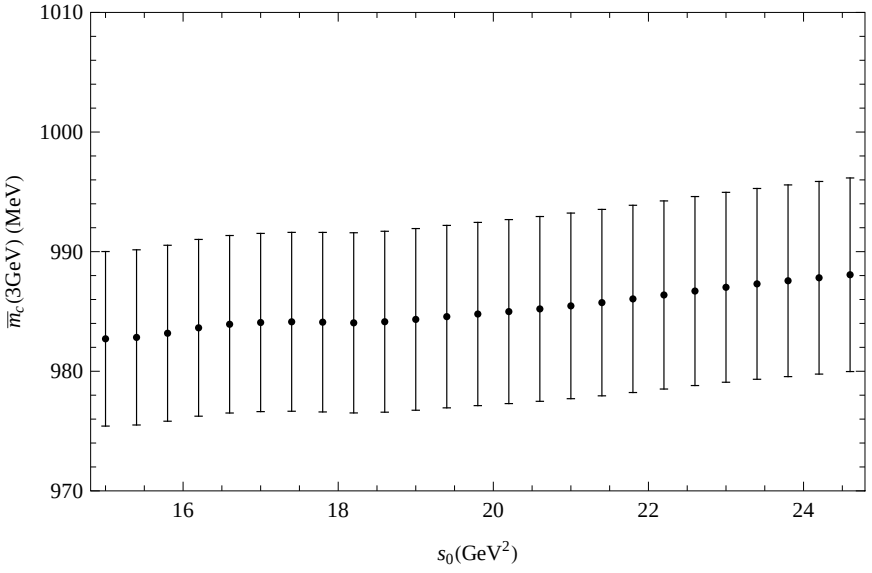

FIGURE 2.5: $\bar{m}_c(3\,\mathrm{GeV})$ as a function of s_0 obtained using $p(s) = 1 - (s_0/s)^2$. The total variation of $\bar{m}_c(3\,\mathrm{GeV})$ in the range $15\,\mathrm{GeV}^2 < s < 25\,\mathrm{GeV}^2$ is 5 MeV.

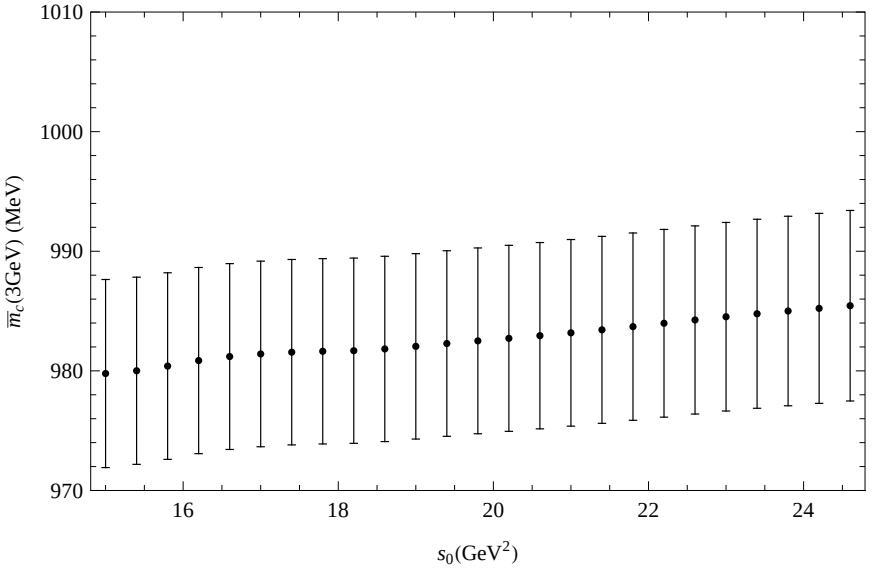

FIGURE 2.6: $\bar{m}_c(3\,\text{GeV})$ as a function of s_0 obtained using $p(s) = s^{-1}(1 - s_0/s)$. The total variation of $\bar{m}_c(3\,\text{GeV})$ in the range $15\,\text{GeV}^2 < s < 25\,\text{GeV}^2$ is 5 MeV.

2.1.4 The Bottom Quark Mass

This section will be heavily based on the analyses of our publications [25, 27].

2.1.4.1 Data Input

To evaluate the left-hand side of (1.7), we need to use experimental input. The lowest-lying bottomonium states are the four narrow Υ-resonances. We calculate their contribution to (1.7) using the narrow-width approximation,

$$R_b^{\text{res}} = \sum_i \frac{9\pi M_i \Gamma_i}{\alpha_{\text{em}}^2(s)} \delta(s - M_i^2), \tag{2.25}$$

where $i \in \{\Upsilon(1S), \Upsilon(2S), \Upsilon(3S), \Upsilon(4S)\}$. We take the masses and widths from the Particle Data Group [1]. The widths are $\Gamma_{\Upsilon(1S)} = 1.340(18)\,\text{keV}$, $\Gamma_{\Upsilon(2S)} = 0.612(11)\,\text{keV}$, $\Gamma_{\Upsilon(3S)} = 0.443(8)\,\text{keV}$ and $\Gamma_{\Upsilon(4S)} = 0.272(29)\,\text{keV}$. Given that the widths of the $\Upsilon(1S), \Upsilon(2S)$ and $\Upsilon(3S)$ were obtained at the same experimental facility, we will (conservatively) assumme that their uncertainties are correlated. The masses are $M_{\Upsilon(1S)} = 9.46030(26)\,\text{GeV}$, $M_{\Upsilon(2S)} = 10.02326(31)\,\text{GeV}$, $M_{\Upsilon(3S)} = 10.3552(5)\,\text{GeV}$ and $M_{\Upsilon(4S)} = 10.5794(12)\,\text{GeV}$. We take the effective electromagnetic couplings from [58].

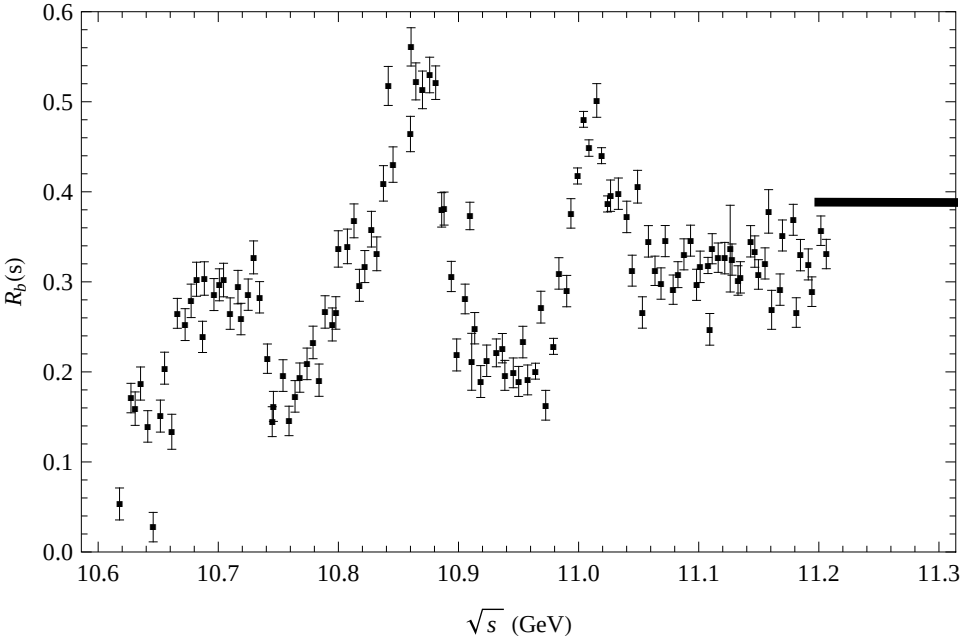

FIGURE 2.7: The corrected *BABAR* data [67] for $R_b(s)$, along with the pQCD prediction (thick black line) obtained using `Rhad` [68].

The *BABAR* Collaboration [67] has performed a direct measurement of R_b in the 'continuum threshold' region between 10.62 GeV and 11.24 GeV. We will take this new measurement to completely supercede the older measurement of this region made by the CLEO Collaboration [69] over 25 years ago. The reason for not averaging the old CLEO data with the current BABAR data is that the CLEO data seem to suffer from inconsistencies. The CLEO experiment [69] found that the values of R_b just below the bottom threshold were roughly 28% larger than the prediction of pQCD. However, a later and more precise CLEO measurement [70] found perfect agreement with pQCD in basically the same energy region. This fact motivated [58] to apply a 28% rescaling of the CLEO data when determining the bottom mass.

It was shown by [20] that this *BABAR* data cannot be used directly in sum rules. First, the radiative tail of the Υ_{4S} resonance must be removed. Second, the initial-state radiation should be removed. Third, the vacuum polarization must be taken into account. We follow the procedure detailed in [20] to correct the *BABAR* data, and these corrected *BABAR* data are shown in Fig. 2.7.

2.1.5 Uncertainties and the kernel $p(s)$

As previously mentioned, we will want to choose some $p(s)$ to minimize the total uncertainties. As we will want to compare our method with the Hilbert-moment method of [20, 71], we will follow their uncertainty metrics. The first set of uncertainties are from the uncertainty in the strong coupling α_s ($\Delta\alpha_s$), the uncertainty in the experimental data (ΔExp), and our incomplete knowledge of pQCD ($\Delta\mu$). The latter was estimated by varying the renormalization scale $\mu = 10\,\text{GeV}$ by $\pm 5\text{GeV}$, and then running the mass calculated at this scale back to $\mu = 10\,\text{GeV}$. The maximum difference is taken as the uncertainty.

A second set of uncertainties were considered in [71]. These arise from the observation that the pQCD prediction for $R_b(s)$ does not agree with the experimentally determined values at the end of the measured data range ($\sqrt{s} = 11.24\,\text{GeV}$), as can be seen in Fig. 2.7. The pQCD prediction is from the software `Rhad` [68].
There exist three possibilities for this:

Option A: The *BABAR* data are correct, but pQCD only starts at higher energies, say at $\sqrt{s} = 13\,\text{GeV}$. Use a linear interpolation between $R_b^{\text{exp}}(11.2\,\text{GeV}) = 0.32$ and $R_b^{\text{pQCD}}(13\,\text{GeV}) = 0.377$, rather than the prediction from `Rhad`.

Option B: The pQCD prediction from `Rhad` is correct, but the *BABAR* data are incorrect, perhaps afflicted by an unreported systematic error. Multiply all the data by a factor of 1.21 to make the data consistent with pQCD.

Option C: The *BABAR* data are correct, and pQCD starts at $\sqrt{s} = 11.24\,\text{GeV}$. However, the pQCD prediction of `RHAD` is incorrect. The exact analytical form for R_b^{pQCD} (rather than just expansions at low- and high-energies) is only known at tree-level and one-loop level. At $\mathcal{O}(\alpha_s^2)$ already, the full anayltic result has to be reconstructed using Padè approximants to patch together information about $\Pi_b(s)$ obtained at $\sqrt{s} = 0$, $\sqrt{s} = 2m_b$ and $\sqrt{s} = -\infty$. Both the Padè method, and the reliance on pQCD results obtained at threshold ($\sqrt{s} = 2m_b$) could introduce unaccounted systematic errors. As a measure of the methods dependence on the reconstructed correlator, we will replace the `RHAD` prediction of R_b^{pQCD} with the high-energy expansion prediction Eq. (2.12), which is closer to the experimental result for $R_b^{\text{exp}}(11.21\,\text{GeV})$.

The first two options were considered by [71], whilst we include the (least plausible) **Option C** for completeness.

The first consideration in choosing $p(s)$ is which s_0 we will need to choose. As mentioned previously, the high energy expansion (2.12) is only guaranteed to converge above $\sqrt{s} = 4\bar{m}_b(\mu) \approx 16\,\text{GeV}$, which is beyond the *BABAR* data. The convergence of this high energy expansion is illustrated in Fig. 2.8 for the tree-level correlator, for which we have the exact pQCD result valid for arbitrary energies [32]. As we only have the first three terms of (2.12) at $\mathcal{O}(\alpha_s^3)$, and use the first seven terms at $\mathcal{O}(\alpha_s^2)$ from [29], we plot this against the exact result, showing that at $s = 16\bar{m}_b^2(\mu) \approx 250\,\text{GeV}^2$ the seven-term high energy expansion is for practical purposes exact. The three-term expansion is not all that good, though this situation is only relevant at $\mathcal{O}(\alpha_s^3)$ whose contribution will be

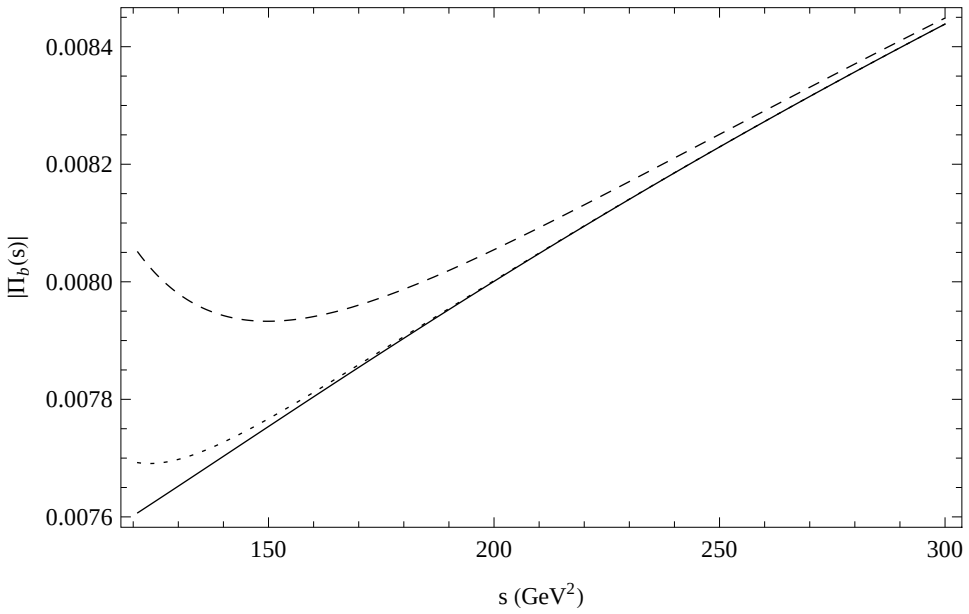

FIGURE 2.8: The magnitude of the tree-level result for $\Pi_b(s)$ given for the exact expression (solid line), the first three terms of the high-energy expansion (dashed line), and the first seven terms of the high-energy expansion (dotted line).

small.[8]

Thus we will need to use the prediction of `Rhad` as data input in the region $11.24\,\text{GeV} < \sqrt{s} < \sqrt{s_0}$. So the first thing $p(s)$ will need to do is suppress the region $11.24\,\text{GeV} < \sqrt{s} < \sqrt{s_0}$, which would reduce dependence on **Options A,C**. Finally, to reduce dependence on **Option B**, we need to reduce the contribution of the *BABAR* data in the region $M_{\Upsilon(4S)} < \sqrt{s} < 11.24\,\text{GeV}$.

To achieve the above goals, we will employ an analogue of the Legendre-polynomial approach of [22]. In that work, $p(s)$ was a Legendre-polynomial chosen to minimize the contribution above the narrow-resonances, which had large uncertainties. In our case, we will construct a Legendre-like Laurent polynomial consisting of linear combinations of three and four powers of s in the set $\mathcal{S} = \{s^{-3}, s^{-2}, s^{-1}, 1, s\}$ subject to a global constraint that reduces the contribution of the problematic energy regions. As an example, the order 3 Laurent polynomial is of the form $p(s) = \mathcal{P}_3^{(i,j,k)}(s, s_0) = A(s^i + Bs^j + Cs^k)$, and is determined by

$$\int_{s^*}^{s_0} \mathcal{P}_3^{(i,j,k)}(s, s_0) s^{-n}\, ds = 0, \tag{2.26}$$

[8]The situation for the charm mass case is very different, as one might expect: the high-energy expansion is an expansion in powers of m_f^2/s. Given that $m_b^2/m_c^2 \sim 25$, and that we evaluated the correlator in the charm case at $s = 25\,\text{GeV}^2$, we would need an $s = 25^2\,\text{GeV}^2 = 625\,\text{GeV}^2$ for the bottom correlator to achieve the same rate of convergence as in the charm case. Indeed, for the charm, the first three terms in the high-energy expansion differ from the exact tree-level result by less than 0.006% at $s_0 = 5^2\,\text{GeV}^2$, which is completely negligible.

			Uncertainties (MeV)				Options A, B and C (MeV)		
$p(s)$	$\bar{m}_b(10\,\text{GeV})$	$\sqrt{s_0}\,(\text{GeV})$	ΔExp.	$\Delta\alpha_s$	$\Delta\mu$	ΔTotal	ΔA	ΔB	ΔC
s^{-2}	3595	∞	12	8	2	14	34	-25	35
s^{-3}	3612	∞	9	4	1	10	20	-17	16
s^{-4}	3626	∞	7	5	6	10	12	-12	8
$\mathcal{P}_3^{(-3,-1,0)}(s_0,s)$	3624	16	6	6	2	9	1	-6	0
$\mathcal{P}_3^{(-3,-1,1)}(s_0,s)$	3624	16	6	6	2	9	2	-7	0
$\mathcal{P}_3^{(-3,0,1)}(s_0,s)$	3624	16	7	6	2	9	2	-7	0
$\mathcal{P}_3^{(-1,0,1)}(s_0,s)$	3625	16	8	5	4	10	4	-12	0
$\mathcal{P}_4^{(-3,-1,0,1)}(s_0,s)$	3623	20	6	6	3	9	0	-4	0

TABLE 2.4: The results for $\bar{m}_b(10\,\text{GeV})$ using a number of different kernels. The sources of uncertainties are from experiment (ΔEXP), the strong coupling constant ($\Delta\alpha_s$), and the variation of the renormalization scale by $\pm 5\,\text{GeV}$ about $\mu = 10\,\text{GeV}$ ($\Delta\mu$). We also include the uncertainties from calculating $\bar{m}_b(10\,\text{GeV})$ with and without *Options A, B,* or *C*. Following [71], these are not added to the total uncertainty.

for $n \in \{0,1\}$. This determines $\mathcal{P}_3^{(i,j,k)}$ up to an irrelevant constant term. Similar to the charm-quark case, including lower-powers of s in the set $\mathcal{S}$ produces poor convergence of the pQCD expansion, whilst including higher-powers of s brings in unknown $\mathcal{O}(\alpha_s^3)$ terms in the high-energy expansion. We choose s^* equal the last *BABAR* data point, $\sqrt{s^*} = 11.21\,\text{GeV}$.

Although is is obvious that such a kernel would suppress the region $\sqrt{s^*} < s < s_0$ (and hence reducing dependence on *Option A* and *Option C*), the kernel also suppresses the *BABAR* data relative to the narrow upsilon resonances. The reason for this is that the kernel diverges rapidly outside of the range $\sqrt{s^*} < s < s_0$.

2.1.6 Results

We give the results for some example kernels, with a full uncertainty breakdown, in Table 2.4. Our new approach gives very similar uncertainties to the popular kernels $p(s) = s^{-3}$ and $p(s) = s^{-4}$ when only considering the usual uncertainty metrics ($\Delta\alpha_s, \Delta\mu, \Delta\text{Exp}$). However, if one also factors in the uncertainties from *Options A,B,C*, then our method is far superior to the standard Hilbert-moment approach. The work [20, 71] obtained their final result using the kernel $p(s) = s^{-3}$, which is clearly highly sensitive to **Options A,B,C**.

One very important test that this method needs to pass is the following: we have introduced a large number of possible kernels that all depend on the arbitrary parameter s_0. Indeed, there are $\binom{5}{3} = 10$ possible kernels in the class $\mathcal{P}_3^{(i,j,k)}(s,s_0)$ and $\binom{5}{4} = 5$

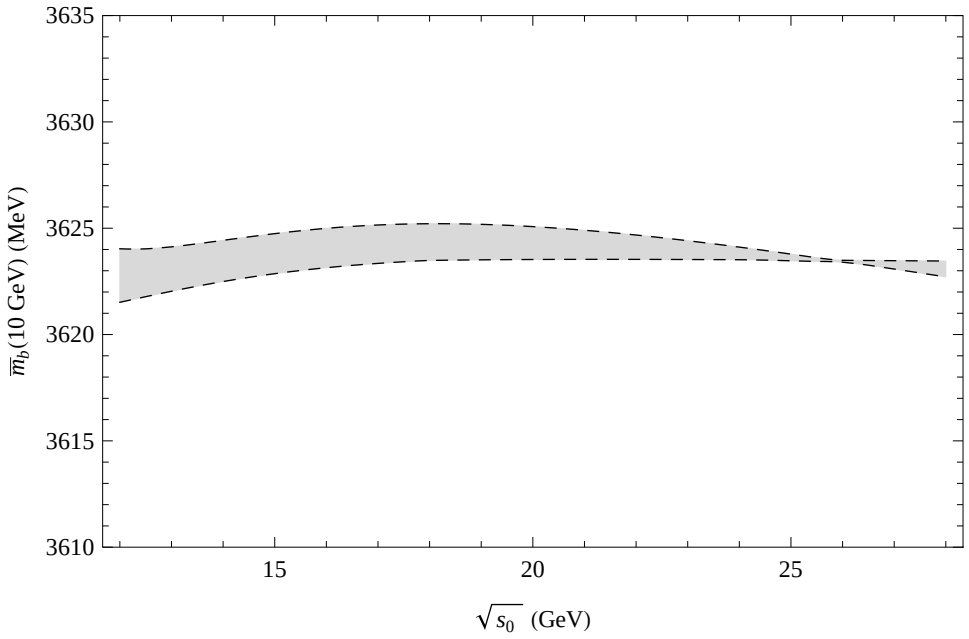

FIGURE 2.9: The range of values obtained for $\bar{m}_b(10\,\mathrm{GeV})$ using kernels of the form $\mathcal{P}_3^{(i,j,k)}(s, s_0)$ for varying s_0.

FIGURE 2.10: The range of values obtained for $\bar{m}_b(10\,\mathrm{GeV})$ using kernels of the form $\mathcal{P}_4^{(i,j,k,r)}(s, s_0)$ for varying s_0.

different kernels in the class $\mathcal{P}_4^{(i,j,k,r)}(s,s_0)$. Each of these kernels, with their different combinations of moments, put different emphasis on the low- and high-energy pQCD expansions, as well as the *BABAR* data. How sensitive are our results to particular choices of s_0 and kernel? To see the sensitivity, in Fig. 2.9 we plot the range of mass values obtained using all 10 kernels in the class $\mathcal{P}_3^{(i,j,k)}(s,s_0)$ against s_0. As can be seen, all of the values of the mass lie in the range $3621\,\text{MeV} \leq \bar{m}_b(10\,\text{GeV} \leq 3625\,\text{MeV}$ for a range of $12\,\text{GeV} < \sqrt{s_0} < 28\,\text{GeV}$. If instead we consider the 5 kernels in the class $\mathcal{P}_4^{(i,j,k,l)}(s,s_0)$ over a range of $18\,\text{GeV} < \sqrt{s_0} < 70\,\text{GeV}$, we obtain a mass range of $3621\,\text{MeV} \leq \bar{m}_b(10\,\text{GeV} \leq 3624\,\text{MeV}$. This is shown in Fig. 2.10. The fact that our method is so insensitive to the choice of s_0 and choice of kernel gives us confidence in this method. Indeed, we have even included regions of s_0 where the high-energy pQCD expansion is not guaranteed to converge, and our results are still consistent.

2.1.7 Conclusions

To obtain a final result, we choose the kernel producing the lowest total uncertainty. This turns out to be using the kernel $\mathcal{P}_3^{(-3,-1,0)}$, which gives

$$\bar{m}_b(10\,\text{GeV}) = 3624(9)\,\text{MeV}. \tag{2.27}$$

The total uncertainty is the uncertainty from varying μ, the strong coupling, and experiment all added in quadrature. We could also include the uncertainties from **Options A,B,C**, which would lead to $\bar{m}_b(10\,\text{GeV}) = 3623(10)\,\text{MeV}$, which has only slightly larger uncertainty. This situation can be contrasted to using the kernel $p(s) = s^{-3}$ (used by [20, 71]), where the uncertainty in the mass would more than double when including the **Options A,B,C** uncertainties.

We compare our result (2.27) with other results in the literature in Fig. 2.11. As can be seen, our result (2.27) is currently the most precise determination available, and is consistent with all LQCD determinations, as well as with the most precise sum rule approaches.

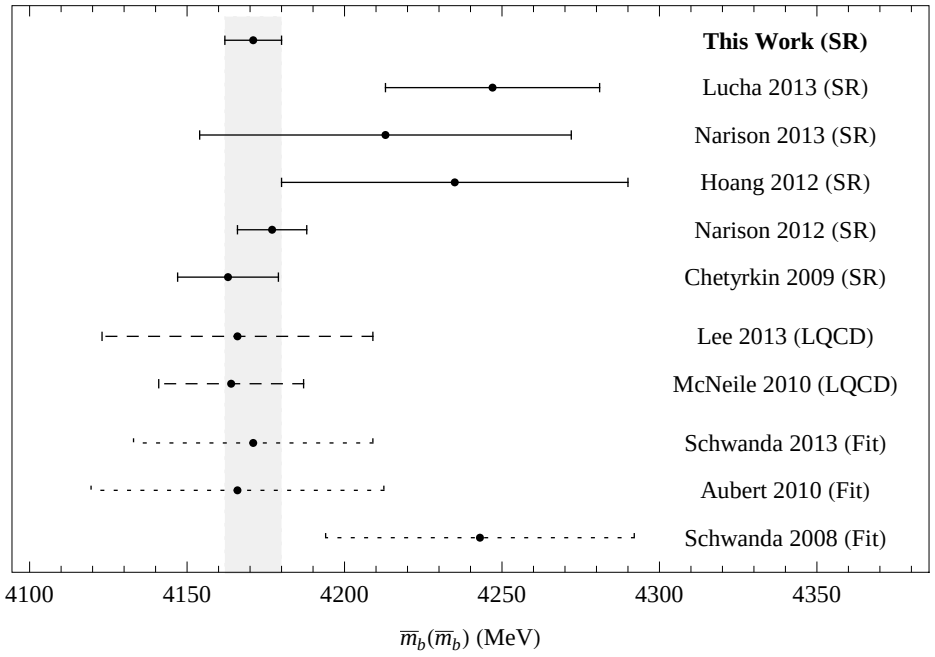

FIGURE 2.11: The value of $\bar{m}_b(\bar{m}_b)$ obtained in Eq. (2.27) compared the most recent determinations in the literature [20, 28, 53, 61, 72–77]. We have separated the results into three general class of method used to determine the bottom mass. These are sum rule approach (SR), lattice (LQCD), and global fits (fit).

2.2 The Strange Quark Mass

This section is based on our work [78]. The aim of this section will be to correct a serious shortcoming of a previous sum-rule calculation of the strange-quark mass [79], which extracted the strange-quark mass via an analysis of the pseudoscalar correlator. Unfortunately, the resulting perturbation expansion in powers of the strong coupling appears not converge, leading to a possibly large systematic uncertainty. We will now seek to remedy this situation.

As opposed to the rest of this thesis, we will need to consider the pseudoscalar correlator, which is defined by

$$\psi_5(q^2) = i \int d^4x\, e^{iqx} \langle 0|T[\partial^\mu A_\mu(x), \partial^\nu A_\nu^\dagger(0))|0\rangle. \tag{2.28}$$

Here $\partial^\mu A_\mu(x) = (m_s + m_{ud}) : \overline{s}(x)\, i\, \gamma_5\, u(x) :$ is the divergence of the axial-vector current, and $m_{ud} \equiv (m_u + m_d)/2$. The pseudoscalar correlator has the same analyticity properties as the vector correlator. Hence the sum rule (1.7) holds also for the pseudoscalar correlator. We will also only consider kernels $p(s)$ composed of positive moments, leading

to

$$\int_{s_{th}}^{s_0} p(s)\,\frac{1}{\pi}\mathrm{Im}\psi_5(s)\,\mathrm{d}s = -\frac{1}{2\pi i}\int_{|s|=s_0} p(s)\,\psi_5(s)\big|_{\mathrm{OPE}}\,\mathrm{d}s. \tag{2.29}$$

The OPE prediction for the correlator can be decomposed as[9]

$$\psi_5(s)\big|_{\mathrm{OPE}} = (\bar{m}_s + \bar{m}_{ud})^2\tilde{\psi}_5(s)\big|_{\mathrm{OPE}}, \tag{2.30}$$

$$\tilde{\psi}_5(s)\big|_{\mathrm{OPE}} = \Big(\psi_5(s)\big|_{\mathrm{pQCD}} + \psi_5(s)\big|_{\mathrm{d=2}} + \psi_5(s)\big|_{\mathrm{d=4}} + \ldots\Big). \tag{2.31}$$

The mass of the strange-quark can thus be directly written as[10]

$$\begin{aligned}\bar{m}_s = \Big[1 - \frac{\bar{m}_{ud}}{\bar{m}_s}\Big]^{-1}\Big(\int_{s_{th}}^{s_0} p(s)\,\frac{1}{\pi}\mathrm{Im}\psi_5(s)\,\mathrm{d}s\Big)^{1/2} \\ \times\Big(-\frac{1}{2\pi i}\int_{|s|=s_0} p(s)\,\tilde{\psi}_5(s)\big|_{\mathrm{OPE}}\,\mathrm{d}s\Big)^{-1/2}.\end{aligned} \tag{2.32}$$

The (renormalization group invariant) ratio $\bar{m}_s/\bar{m}_{ud}$ is known independently from LQCD. We use the PDG [41] value, which is completely dominated by LQCD results

$$\bar{m}_s/\bar{m}_{ud} = 27(1). \tag{2.33}$$

The strange-mass in (2.32) has the generic form

$$\bar{m}_s = A\cdot\left(a_0 + a_1\alpha_s + a_2\alpha_s^2 + a_3\alpha_s^3 + a_4\alpha_s^4\right)^{-1/2}, \tag{2.34}$$

as we will expand $\tilde{\psi}_5(s)\big|_{\mathrm{OPE}}$ in powers of the strong coupling. We will see in the next section that for a choice of kernel $p_3(s) = (s-s_0)(s-a)$, we get the following series for the strange-mass:

$$\bar{m}_s(2\,\mathrm{GeV}) = 248.3\left(1 + 2.59\alpha_s + 8.60\alpha_s^2 + 26.50\alpha_s^3 + 75.47\alpha_s^4\right)^{-1/2}. \tag{2.35}$$

Given that the strong coupling is $\alpha_s(2\,\mathrm{GeV}) \sim 0.3$, we can see that each term in the series is roughly the same size as the preceding term. This is not auspicious for the

[9] We do not include QED corrections in this case. As will be seen, as we do not have any experimental data in the resonance-threshold region, we will employ a model prediction $\mathrm{Im}\psi_5(s)$ which will not include QED corrections. One should therefore not include QED correction in the OPE prediction of the correlator.

[10] There is also a very small dependence on the strange mass arising from mass-correction contributions to $\psi_5(s)\big|_{\mathrm{d=2}}$. It was found not to matter if one just uses the PDG [1] value for the strange mass for these tiny mass corrections. We will do this to simplify the analysis.

purposes of convergence. Such a series was evaluated directly in [79], despite the series seemingly not converging.

There exist a number of mathematical techniques to increase the convergence of series that have been successfully applied to perturbative expansions appearing in Quantum Field Theory. A good overview of these methods can be found in [80]. The simplest of these methods is probably the use of Padè approximants, which has been successfully applied to expansions appearing in QCD [81–83]. The idea behind this method is that there exists an ambiguity in how one performs a series expansion. An order-3 expansion of some function can be the usual Taylor expansion $f(\alpha_s) = a_0 + a_1\alpha_s + a_2\alpha_s^2$, yet there is no *a priori* reason to prefer this expansion to the expansions $f(\alpha_s) = (\tilde{a}_0 + \tilde{a}_1\alpha_s)/(1 + \tilde{a}_2\alpha_s)$ or $f(\alpha_s) = (\hat{a}_0 + \hat{a}_1\alpha_s + \hat{a}_2\alpha_s^2)^{-1/2}$. Which of these expansions provides a better approximation to $f(\alpha_s)$ (or even whether the expansion converges) depends crucially on the analytic properties of $f(\alpha_s)$. An example of this phenomena is shown in Fig. 2.12.

An order k Padè approximant is a rational function approximation of the form

$$f(z) \approx [m/n] \equiv \frac{a_0 + a_1 z + \ldots + a_m z^m}{1 + b_1 z + \ldots + b_n z^n}, \quad m + n = k. \tag{2.36}$$

It should be noted that $[m/0]$ is simply the usual Taylor expansion of $f(z)$. Indeed, this $[m/0]$ approximant provides a great improvement in the convergence of (2.35):

$$\bar{m}_s(2\,\text{GeV}) = 248.3\left(1 - 1.30\alpha_s - 1.80\alpha_s^2 - 1.95\alpha_s^3 - 0.34\alpha_s^4\right). \tag{2.37}$$

This also leads to substantially different values of the mass. At $\mu = 2\,\text{GeV}$, the PDG strong coupling becomes $\alpha_s(2\,\text{GeV}) = 0.3047$, which gives

$$248.3\left(1 + 2.59\alpha_s + 8.60\alpha_s^2 + 26.50\alpha_s^3 + 75.47\alpha_s^4\right)^{-1/2} = 125\,\text{GeV}, \tag{2.38}$$

$$248.3\left(1 - 1.30\alpha_s - 1.80\alpha_s^2 - 1.95\alpha_s^3 - 0.34\alpha_s^4\right) = 94\,\text{GeV}. \tag{2.39}$$

It is thus extremely important to ensure that one uses the correct expansion technique if one wishes to determine the strange-quark mass precisely using sum rules.

The structure of this chapter will be as follows: we will calculate the strange-quark mass using three different kernels $p(s)$ that put different emphases on the OPE and the

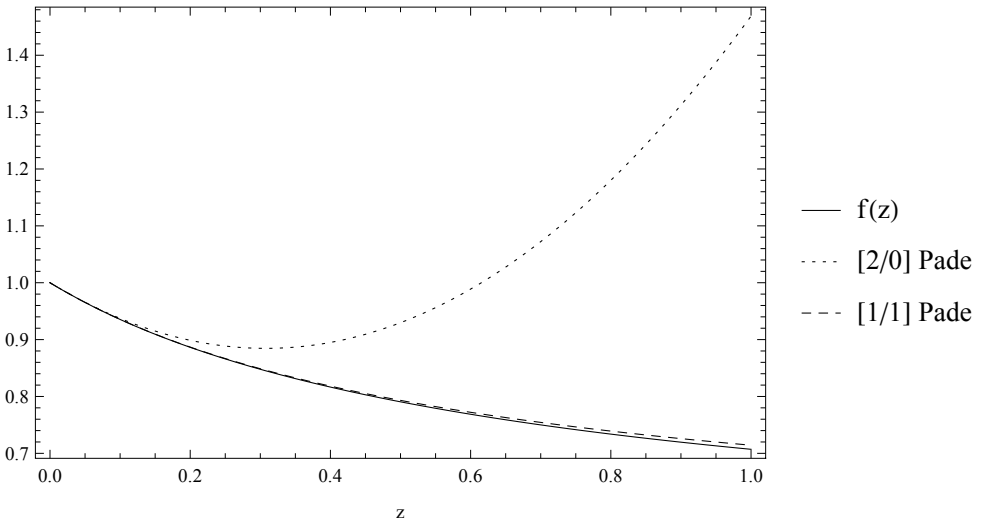

FIGURE 2.12: A plot of the function $f(z) = \sqrt{(\frac{z}{2}+1)(2z+1)}$ along with the [2/0] Padè expansion $f(z) \approx 1 - \frac{3z}{4} + \frac{39z^2}{32}$ (equivalent to the Taylor expansion) and the [1/1] Padè expansion $f(z) \approx (\frac{7z}{8}+1)/(\frac{13z}{8}+1)$. Example adapted from [84].

hadronic model. The kernel which reduces the total uncertainty the most will be taken as our final result. The convergence of this final result will then be analysed carefully.

2.2.1 Inputs

2.2.1.1 Correlator

The second derivative of $\psi_5(s)\big|_{\text{OPE}}$ is given in [85]. From this, we have $\psi_5(s)\big|_{\text{pQCD}}$ up to $\mathcal{O}(\alpha_s^4)$. Integrating this, we find (modulo an irrelevant term[11] $A + Bs$)

$$\begin{aligned}\psi_5(s)\big|_{\text{pQCD}} = \frac{-s}{16\pi^2}\Bigg[&6\,l_\mu - 12 \\ &+\frac{\alpha_s}{\pi}\Big(-6\,l_\mu^2 + 34\,l_\mu - 36.651\Big) \\ &+\left(\frac{\alpha_s}{\pi}\right)^2\Big(8.5\,l_\mu^3 - 95\,l_\mu^2 + 275.08\,l_\mu - 304.79\Big) \\ &+\left(\frac{\alpha_s}{\pi}\right)^3\Big(-13.813\,l_\mu^4 + 229.\,l_\mu^3 - 1165.4\,l_\mu^2 \\ &\quad + 2795.1\,l_\mu - 2966.2\Big) \\ &+\left(\frac{\alpha_s}{\pi}\right)^4\Big(24.172\,l_\mu^5 - 534.05\,l_\mu^4 + 3962.5\,l_\mu^3 \\ &\quad - 15231\,l_\mu^2 + 33532\,l_\mu\Big)\Bigg],\end{aligned} \tag{2.40}$$

[11] This term is irrelevant as $\psi_5(s)\big|_{\text{OPE}}$ only appears in a circular contour integral. Adding any analytic function to $\psi_5(s)\big|_{\text{OPE}}$ will leave the contour integral unchanged.

where $l_\mu = \log\left(-s/\mu^2\right)$.

The dimension-2 contribution to the OPE comes from mass-corrections. We take the $\mathcal{O}(\alpha_s^2)$ result for $\psi_5''(s)\big|_{\text{d=2}}$ from [85] and integrate to obtain

$$\psi_5(s)\big|_{\text{d=2}} = l_\mu \frac{\bar{m}_s^2}{96\pi^2}\Bigg[72 + \frac{\alpha_s}{\pi}\Big(384 - 144\, l_\mu\Big) \tag{2.41}$$

$$+ \left(\frac{\alpha_s}{\pi}\right)^2\Big(300\, l_\mu^2 - 1746\, l_\mu - 1848\zeta_3 + 5065\Big)\Bigg]. \tag{2.42}$$

The dimension-4 term in the OPE receives corrections from both the gluon condensate, the strange-quark condensate, the light-quark condensates, and mass corrections. We take the $\mathcal{O}(\alpha_s)$ result[12] for $\psi_5''(s)\big|_{\text{d=4}}$ from [85] and integrate to obtain

$$\psi_5(s)\big|_{\text{d=4}} = \frac{1}{16\pi^2 s}\Bigg[-2\pi^2\langle G^2\rangle - 8\pi^2\bar{m}_s\langle\bar{s}s\rangle + 16\pi^2\bar{m}_s\langle\bar{q}q\rangle + \bar{m}_s^4\{-3 - 6l_\mu\}$$

$$+ \frac{\alpha_s}{\pi}\Big(\langle G^2\rangle\{4\pi^2 l_\mu - 11\pi^2\} + \bar{m}_s\langle\bar{s}s\rangle\{16\pi^2 l_\mu - \frac{88\pi^2}{3}\}\Big) \tag{2.43}$$

$$+ \bar{m}_s\langle\bar{q}q\rangle\{\frac{224\pi^2}{3} - 32\pi^2 l_\mu\} + \bar{m}_s^4\{\frac{6520}{189} - \frac{346}{21}l_\mu\}\Big)\Bigg]. \tag{2.44}$$

The dimension-6 term in the OPE is not well known. We will use the $\mathcal{O}(\alpha_s)$ expression given in [85] which assumes vacuum-saturation,

$$\psi_5(s)\big|_{\text{d=6}} = -\frac{\bar{m}_s\langle\bar{u}uG\rangle}{2s^2} - \frac{\alpha_s}{\pi}\frac{16\left(\langle\bar{s}s\rangle^2 - 9\langle\bar{s}s\rangle\langle\bar{q}q\rangle + \langle\bar{q}q\rangle^2\right)}{27s^2}. \tag{2.45}$$

This approximation breaks down at next-to-next-to leading order [86], gives the incorrect sign for the ratio of the $d = 6$ vector- and axial-vector condensates [51, 87], and it underestimates the vector $d = 6$ condensate by a factor of 10 [51, 87]. We thus assume an order-of-magnitude uncertainty of 1000% on this $d = 6$ contribution.

We use the following inputs. The gluon condensate value is taken from Table 2.1, and the strong coupling is the PDG value $\alpha_s(M_Z) = 0.1184(7)$ [41]. We use the light-quark condensate value of [88–90]

$$\langle q\bar{q}\rangle = -(267 \pm 5)^3\,\text{MeV}^3. \tag{2.46}$$

[12] The result given in [85] contains some partial $\mathcal{O}(\alpha_s^2)$ and $\mathcal{O}(\alpha_s^3)$ information. Including these partial results does not change the strange-quark mass significantly.

For the strange-quark condensate, we use [85]

$$\langle \bar{s}s\rangle(2\,\mathrm{GeV}) = 0.8(3)\langle q\bar{q}\rangle. \tag{2.47}$$

Following [85] we use $\langle \bar{u}uG\rangle = 0.8\langle \bar{q}q\rangle$.

2.2.1.2 Hadronic Model

Unlike the case for the vector correlator, we don't have any experimental results for the pseudoscalar spectral function beyond the sharp $K^{\pm}$ pole. In order to proceed, we require a hadronic model for the resonance region beyond the kaon pole. The first step in constructing such a model is to obtain the correct threshold behaviour from chiral pertubation theory, as was proposed by [91]. This fixes the normalization of parametrization of the resonance. The chiral limit will be assumed. In our case, the threshold behaviour is given by [92]

$$\frac{1}{\pi}\mathrm{Im}\Psi_5(s)\big|_{K\pi\pi} = \frac{m_{K^\pm}^4}{2f_\pi^2}\frac{3}{2^8\pi^4}\frac{I(s)}{s(m_{K^\pm}^2-s)^2}\theta(s-m_{K^\pm}^2). \tag{2.48}$$

Here $I(s)$ is an integral function accounting for the $K^*(892)-\pi$ sub-channel. It is given by

$$\begin{aligned} I(s) = \int_{m_K^2}^{s}\frac{du}{u}(u-m_{K^\pm}^2)(s-u)\Big[(m_{K^\pm}^2-s)\big(u-\frac{s+m_{K^\pm}^2}{2}\big) \\ -\frac{1}{8u}(u^2-m_{K^\pm}^4)(s-u)+\frac{3}{4}(u-m_{K^\pm}^2)^2|F_{K^\pm}(u)|^2\Big], \end{aligned} \tag{2.49}$$

$$|F_{K^\pm}(u)|^2 = \frac{(m_{K^*}^2-m_{K^\pm}^2)^2+m_{K^*}^2\Gamma_{K^*}^2}{(m_{K^*}^2-u)^2+m_{K^*}^2\Gamma_{K^*}^2}. \tag{2.50}$$

The full hadronic spectral function can then be written as

$$\begin{aligned} \frac{1}{\pi}\mathrm{Im}\Psi_5(s)\big|_{\mathrm{had}} = 2f_{K^\pm}^2m_{K^\pm}^2\delta(s-m_{K^\pm}^2)+\frac{1}{\pi}\mathrm{Im}\Psi_5(s)\big|_{K\pi\pi}\frac{BW_1(s)+\lambda BW_2(s)}{1+\lambda} \\ +\frac{1}{\pi}\mathrm{Im}\Psi_5(s)\big|_{\mathrm{OPE}}\theta(s-s_0), \end{aligned} \tag{2.51}$$

where

$$BW_i(s) = \frac{\left(m_{K_i}^2-m_{K^\pm}^2\right)^2+\Gamma_{K_i}^2m_{K_i}^2}{\Gamma_{K_i}^2m_{K_i}^2+\left(s-m_{K_i}^2\right)^2}. \tag{2.52}$$

Kaon i	Mass m_i (MeV)	Width Γ_i (MeV)
$K_1(1460)$	~ 1460	~ 250
$K_2(1830)$	~ 1830	~ 250
$K^{\pm}$	493.677(16)	-
K^*	891.66(26)	50.8(9)

TABLE 2.5: The values of the input parameters for the hadronic model (2.51). All values are taken from the PDG [1].

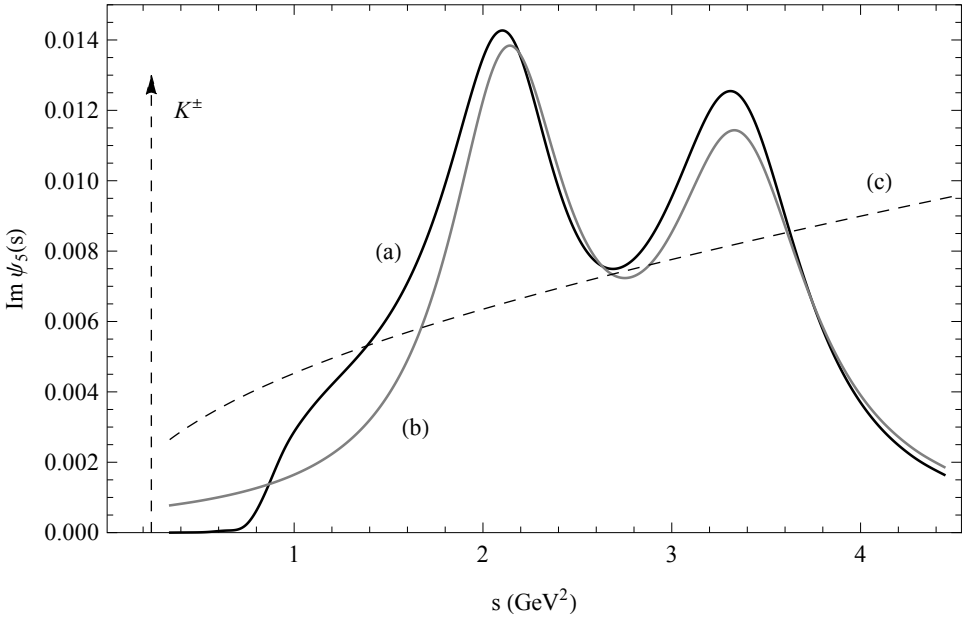

FIGURE 2.13: The hadronic spectral function given by the model (2.51) (*a*), the model used by [85] (*b*), and the pQCD prediction (*c*).

The parameter λ sets the relative weighting of the K_1. We choose $\lambda = 1$ to give an equal weighting. The kaon masses and widths used as input parameters for our hadronic model are given in Table 2.5. The pseudoscalar decay constants are taken from the PDG [1],

$$f_\pi = 92.21(14)\,\text{MeV}, \tag{2.53}$$

$$f_{K^\pm} = 110.4(6)\,\text{MeV}. \tag{2.54}$$

The hadronic model for the spectral function is plotted in Fig. 2.13. It is compared to the model used in [85]. We put a conservative 33% systematic uncertainty on this model prediction of the spectral function.

2.2.1.3 The choice of kernel $p(s)$

Given the large uncertainties induced by the hadronic model (2.51), we will want to minimize its contribution by an appropriate choice of kernel over which it will be integrated over. The first kernel is designed to suppress the two radial excitations of the Kaon, $K_1(1460)$ and $K_2(1830)$. Thus we choose

$$p_1(s) = (s - m_{K_1})(s - m_{K_2}). \tag{2.55}$$

This kernel was originally considered in [79]. The second kernel also suppresses the $K_1(1460)$ and $K_2(1830)$, but also vanishes at s_0. The motivation for the latter condition is that it is unclear where pQCD is meant to begin in Fig. 2.13. This pinching will make the sum rule less sensitive to this issue,

$$p_1(s) = (s - m_{K_1})(s - m_{K_2})(s - s_0). \tag{2.56}$$

This greater suppression of the model comes at the expense of bringing in the $d = 6$ condensate, which is extremely poorly known. Lastly, we have a kernel that vanishes at s_0 and somewhere between the $K_1(1460)$ and $K_2(1830)$

$$p_1(s) = (s - a)(s - s_0). \tag{2.57}$$

We choose $\sqrt{a} = 1.67\,\text{GeV}$. This will be found to be the optimum kernel.

2.2.2 Results

The results obtained for $\bar{m}_s(2\,\text{GeV})$ obtained using our three kernels given in equations (2.55)-(2.57) are shown in Table 2.6. The results are obtained by evaluating the series in (2.34) directly and by first expanding it as a Padè approximant (the two best Padè approximants are given in the Table). A full uncertainty breakdown is also given.
A note about the truncation uncertainty: for the [4/0] and [0/4] approximants, this uncertainty is simply taken to be the difference between the $\mathcal{O}(\alpha_s^4)$ and $\mathcal{O}(\alpha_s^3)$ results. For other approximants, this is not well-defined. Such an approximant has the form $[m/n]$ where $m + n = 4$ and $m, n \neq 0$. We will take $[m/n - 1]$ and $[m - 1/n]$ as our

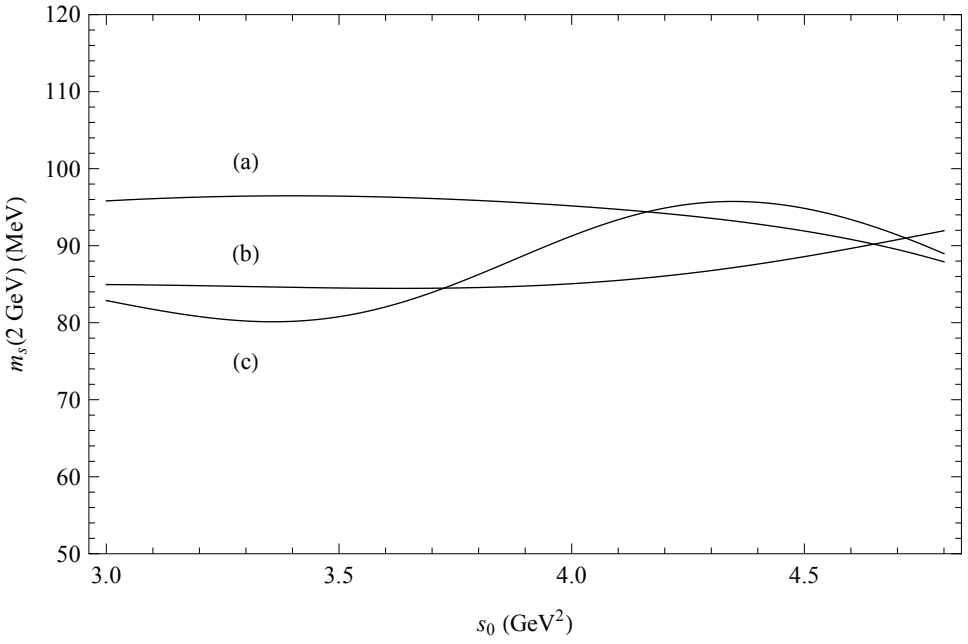

FIGURE 2.14: The strange-quark mass $\bar{m}_s(2\,\text{GeV})$ for varying s_0 was obtained using kernel $p_3(s)$, curve (a), $p_2(s)$, curve (b) and $p_1(s)$, curve (c). We used the [4/0] Padè approximant to expand (2.34).

		(MeV)							
Kernel	Expand	$\bar{m}_s(2\,\text{GeV})$	$\Delta\alpha_s$	$\Delta\langle G^2\rangle$	$\Delta_{d=6}$	Δs_0	Δmod	Δtrunc	Δtot
	None	117	2	2	6	18	5	9	22
$p_1(s)$	[4/0]	95	3	0.3	1	10	4	6	13
	[3/1]	90	4	1	2	10	6	2	13
	None	132	2	3	8	3	4	15	16
$p_2(s)$	[4/0]	86	5	2	8	4	2	11	15
	[3/1]	79	6	3	8	4	2	12	15
	None	125	2	2	4	5	8	12	16
$p_3(s)$	[4/0]	94	4	0.6	1	3	6	2	8
	[3/1]	94	4	1	2	4	6	4	9

TABLE 2.6: The results for $\bar{m}_s(2\,\text{GeV})$ obtained using three different kernels at $s_0 = \mu^2 = (4.2 \pm 0.5)\,\text{GeV}^2$. The results were obtained by either expanding the perturbative series using a Padè approximant ($[m/n]$), or not expanding ('None'). The uncertainties are from the strong coupling ($\Delta\alpha_s$), the gluon condensate ($\Delta\langle G^2\rangle$), the $d = 6$ condensate ($\Delta_{d=6}$), the variation in s_0 (Δs_0), the 33% systematic uncertainty on our model (Δmod), the truncation uncertainty (Δtrunc), and finally the uncertainties added in quadrature (Δtot).

$\mathcal{O}(\alpha_s^3)$ result, and take the mean difference between these and the $[m/n]$ result as our truncation uncertainty.

Our best result is using the kernel $p_3(s)$ from (2.57), and the [4/0] Padè approximant when expanding,

$$\bar{m}_s(2\,\text{GeV}) = 94(8)\,\text{MeV}. \tag{2.58}$$

It is noteworthy that the truncation uncertainty was reduced by a factor of six by expanding the poorly convergent series (2.35)

$$\bar{m}_s(2\,\text{GeV}) = 248.3\left(1 + 2.59\alpha_s + 8.60\alpha_s^2 + 26.50\alpha_s^3 + 75.47\alpha_s^4\right)^{-1/2} \tag{2.59}$$

to obtain the highly convergent (2.37)

$$\bar{m}_s(2\,\text{GeV}) = 248.3\left(1 + 2.59\alpha_s + 8.60\alpha_s^2 + 26.50\alpha_s^3 + 75.47\alpha_s^4\right)^{-1/2}. \tag{2.60}$$

Further support for this result is given by the fact that the next best Padè approximant, [3/1], gives exactly the same result for the mass. The series for this approximant is

$$\bar{m}_s(2\,\text{GeV}) = 248.3\left(\frac{1 - 1.47\alpha_s - 1.57\alpha_s^2 - 1.64\alpha_s^3}{1 - 0.17\alpha_s}\right). \tag{2.61}$$

Both the numerator and denominator appear convergent.

Finally, the results for all three kernels using the [4/0] approximant plotted for varying s_0 is given in Fig. 2.14.

2.2.2.1 The Convergence: varying μ

We found that the kernel $p_3(s)$ achieved a minimum total uncertainty, and we will thus further analyse this result. In order to do this, we will consider an alternative measure of convergence, which is varying the renormalization scale μ. This will lead to strange-mass at a different scale, which can then be run back to $\mu = 2\,\text{GeV}$ using the renormalization group equations (RGE). Although our final result $\bar{m}_s(2\,\text{GeV})$ should be independent of the arbitrary choice of μ used to perform our pQCD calculations, dependence arises due

Expansion Method	$\bar{m}_s(2\,\text{GeV})$	$\pm\Delta\mu$
[4/0] Padè	94	2
[3/1] Padè	94	2
[1/3] Padè	96	4
[0/4] Padè	116	6
No expansion	125	8
[2/2] Padè	180	~ 150

TABLE 2.7: The mass $\bar{m}_s(2\,\text{GeV})$ obtained using the kernel $p_3(s)$ using six different expansion methods for the series in (2.34). The results are given in order of how sensitive the method is to variations in the renormalization scale μ. We varied μ in the range $1.5\,\text{GeV} \leq \mu \leq 2.5\,\text{GeV}$.

to only using a truncated pQCD series.[13] We will vary the renormalization scale in the range $1.5\,\text{GeV} \leq \mu \leq 2.5\,\text{GeV}$. The exact size of the range one considers is somewhat arbitrary, thus the variation produced in the mass will also be somewhat arbitrary, making interpretations of this variation as an uncertainty difficult. The relative sizes of the variation in $\bar{m}_s(2\,\text{GeV})$ produced are better used as a guide to which expansion method produces better convergence.

The results for $\bar{m}_s(2\,\text{GeV})$ using six different expansion methods are shown in Table 2.7 (five Padè approximants and the result of evaluating (2.37) directly). We see that the method we chose of using the [4/0] Padè approximant also has 400% less dependence on μ compared to the method of not expanding (2.37). This provides additional support to the conclusion of the truncation analysis in the previous section.

There is another important result that can be seen in Table 2.7: the results with the smallest μ dependence are perfectly consistent. It would be a problem if different expansions converging well give inconsistent results for the mass.

2.2.3 Conclusion

We obtained a value for the strange-quark mass of

$$\bar{m}_s(2\,\text{GeV}) = 94(8)\,\text{MeV} \tag{2.62}$$

[13] Strictly, this is not the only reason: the pQCD series are known to by asymptotic. Hence adding more terms to the pQCD expansion does not continue to indefinitely produce better convergence. Thus it is likely for there to be some μ dependence at every order in perturbation theory.

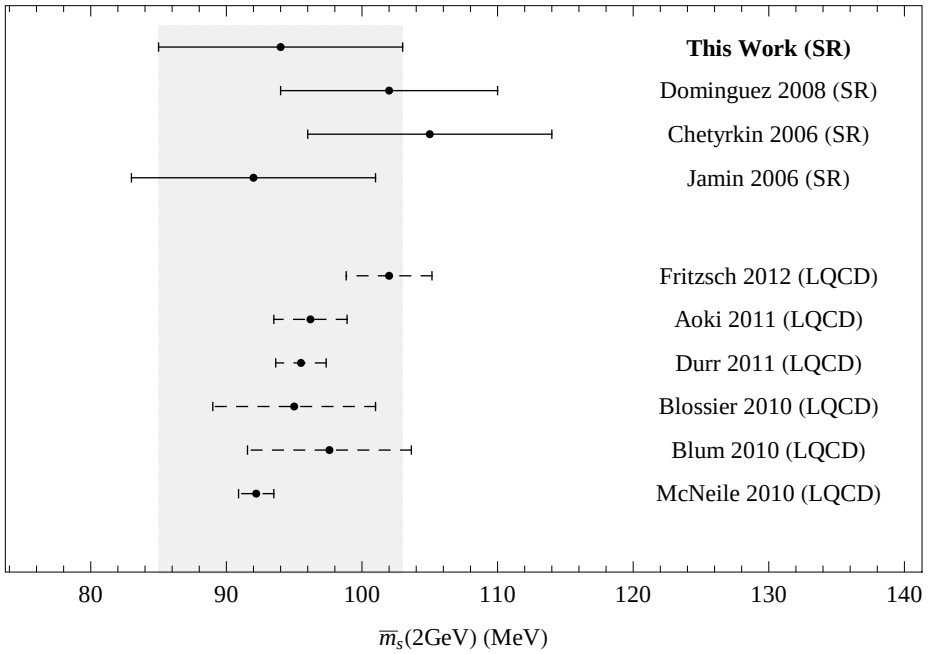

FIGURE 2.15: The strange-quark mass obtained in (2.62) compared to other sum rule [79, 85, 93] and LQCD [28, 64, 94–97] results.

by improving the convergence of the pQCD expansion (2.34) using Padè approximants. The excellent convergence of this result removes a major systematic uncertainty from the method of [79] arising from a poorly-convergent pQCD series. In addition to this, we have used updated inputs for the OPE prediction of the pseudoscalar correlator, a new kernel $p_3(s)$ (2.57) was introduced, and an estimate of the $d = 6$ term in the OPE (with generous uncertainties).

This result is compared to recent values for $\bar{m}_s(2\,\text{GeV})$ in the literature in Fig. 2.15. We find excellent agreement with both sum rule and LQCD results. The precision of sum rule methods are however not currently competitive with LQCD, primarily due to the lack of experimental data for the pseudoscalar spectral function.

Chapter 3

The Muon Anomalous Magnetic Moment

3.1 Introduction

The leptonic magnetic dipole moment $\vec{\mu}_l$, is given by

$$\vec{\mu}_l = g_l \frac{e}{2m_l}\vec{s}, \quad l \in \{e, \mu, \tau\}, \tag{3.1}$$

where g_l is the gyromagnetic ratio. This quantity has proven to be an extraordinarily powerful window into and test of new physics. The first major successes of the Dirac equation in 1928 was predicting $g_e = 2$ [98, 99], which was twice the value that was known to be associated with the angular momentum. This was soon experimentally confirmed. Soon after in 1948, a deviation from $g_e = 2$ was discovered by Kusch and Foley [100, 101], termed the *anomolous magnetic moment*.[1] This anomaly is customarily defined as

$$a_l = \frac{g_l - 2}{2} \tag{3.2}$$

Kusch and Foley found a value of $a_l = (1.19 \pm 0.10) \cdot 10^{-3}$. This result was explained by Schwinger shortly thereafter [102], who used quantum electrodynamics (QED) to

[1] We will refer to this as *the* $g-2$ *of the muon.*

calculate the one-loop correction

$$a_l = \frac{\alpha_{\text{em}}}{2\pi} + \ldots \approx 1.16 \cdot 10^{-3}. \tag{3.3}$$

This was one of the first tests of higher-order QED, and provided triumphant vindication for the QED program.

Today, the $g-2$ of the muon is of particular interest, as it currently represents one of the largest deviations between the Standard Model of Particle Physics and experiment. The Standard Model prediction is [103]

$$a_\mu^{\text{SM}} = 11\,659\,180.2(4.2)(2.6) \times 10^{-10}, \tag{3.4}$$

where the first uncertainty is from the lowest order hadronic contribution ($a_\mu^{\text{had,LO}}$), whilst the second uncertainty is from all other sources. This compares to average experimental value of the muon magnetic anomaly [1, 104],

$$a_\mu^{\text{exp}} = 11\,659\,208.9(6.3) \times 10^{-10}. \tag{3.5}$$

The discrepancy between experiment and theory is thus

$$\Delta a_\mu \equiv a_\mu^{\text{exp}} - a_\mu^{\text{SM}} = 28.7(8.0) \times 10^{-10}, \tag{3.6}$$

which represents a $3.6\,\sigma$ discrepancy between experiment and theory. Another recent analysis of the lowest-order hadronic contribution[105] leads to $a_\mu^{\text{SM}} = 11\,659\,182.8(4.9) \times 10^{-10}$, resulting in a $3.3\,\sigma$ discrepancy between experiment and theory.
For more information regarding the determinations of a_μ^{SM} and a_μ^{exp}, there exist excellent reviews of all aspects of the $g-2$ of the muon. The most comprehensive is [106]. Other general reviews include [1, 107, 108]. For a review focusing on possible supersymmetric contributions, see [109]. For an overview of the fascinating history of the theoretical and experimental efforts to understand the leptonic $g-2$ (and spin in general), see [110].

This discrepancy Δa_μ could be a sign of new physics, which makes makes it important to confirm the correctness of both a_μ^{SM} and a_μ^{exp}. On the experimental side, a new experiment is planned at Fermilab to begin taking data in 2016 with a four-fold increase

in precision over (3.5).[2] On the theoretical side, the hadronic contributions are the least under control, and are the largest source of uncertainty in (3.4). The reason for this is that QCD cannot be solved at low-energies, necessitating either the use of LQCD or experimental cross-section data. As LQCD does not have the requisite precision yet, the latter data-driven approach is standard [103].

In this chapter, we will focus on this lowest-order hadronic contribution $a_\mu^{\rm had,LO}$, which is given by

$$a_\mu^{\rm had,LO} = \int_0^\infty \tilde{K}(s) R(s)\, ds, \tag{3.7}$$

where [111]

$$\tilde{K}(s) = \frac{\alpha_{\rm em}^2}{3\pi^2 s} \int_0^1 dx \frac{x^2(1-x)}{x^2 + s(1-x)/m_\mu^2}, \tag{3.8}$$

and m_μ is the muon mass. It is plotted in Fig. 3.1. The structure of this chapter will be as follows: first, we will show that all of the heavy quark contributions to $a_\mu^{\rm had,LO}$ can be calculated to high-precision using sum rules. Second, we put together a complete collection of $e^+e^- \to$ hadrons data (and thus for $R(s)$ using in (3.7)). Lastly, we will the reduce the contribution of the low-energy $e^+e^- \to$ hadrons data to $a_\mu^{\rm had,LO}$ by using theoretical input in the form of the OPE. We will find that the discrepancy $\Delta a_\mu \equiv a_\mu^{\rm exp} - a_\mu^{\rm SM}$ is significantly reduced. In addition, we will find a serious discrepancy between the OPE and the current $e^+e^- \to$ hadrons data.

This chapter is based on our work [112–115].

3.2 The heavy-quark contribution to $a_\mu^{\rm had,LO}$

The standard approach to including the heavy-quark contribution to $a_\mu^{\rm had,LO}$ is via cross-section data [103]. However, we showed in our work [112] that one can obtain this heavy quark contribution purely from pQCD + the OPE, and with a greater precision than from cross-section data. This is certainly obvious for contributions very far from any resonance regions, but it is slightly counter-intuitive that you can also obtain the contributions to (3.7) of sharp resonances like the J/ψ, $\psi(2s)$ and Υ's.

[2] http://muon-g-2.fnal.gov/1-muon-g-2-collaboration-to-solve-mystery.shtml

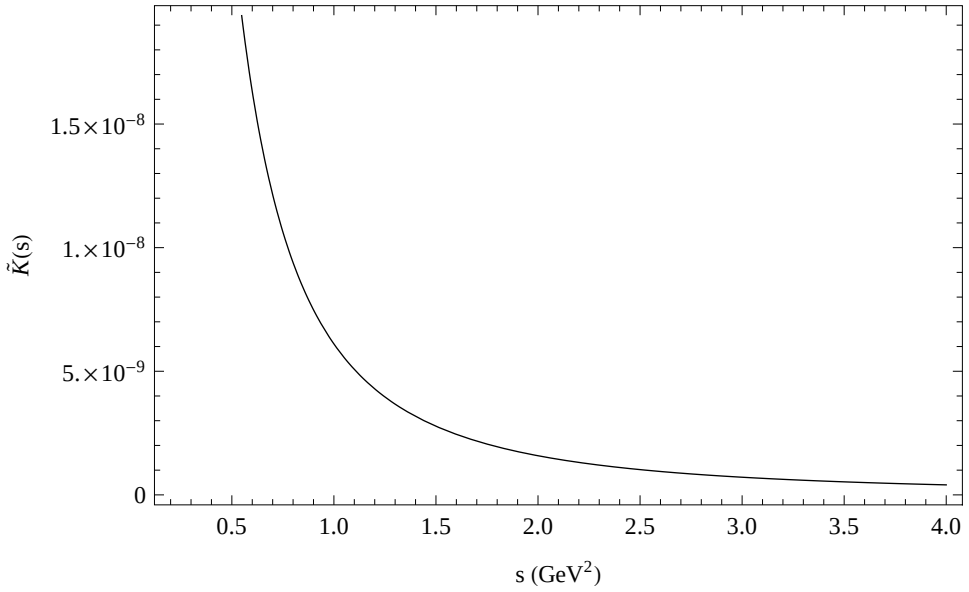

FIGURE 3.1: The integration kernel $\tilde{K}(s)$ used to determine $a_\mu^{\text{had,LO}}$.

The idea is to invert the mass-determination of the previous section: to determine the mass, (1.7) tells us that "integral over $R(s) \implies$ quark mass". However, we have just as well that "quark mass $\implies$ integral over $R(s)$", which is what we need for (3.7). Now if the only precision determinations of the heavy quark masses were via sum-rules like (1.7), then the last statement is tautological. However, we now have high-precision LQCD masses [28].

The only remaining problem is that the kernel $\tilde{K}(s)$ has a complicated analytic structure. There is however a simple solution: the shape of $\tilde{K}(s)$ in Fig. 3.1 looks roughly like some inverse power of s, which motivates us to approximate $\tilde{K}(s)$ by

$$K_c(s) = \frac{\alpha_{\text{em}}^2}{3\pi^2 s}\left[\frac{a_1}{s} + \frac{a_2}{s^2}\right]. \tag{3.9}$$

For the charm case, we want the contribution from the resonance region $M_{J/\psi}^2 < s < (5\,\text{GeV})^2$ (the rest of the charm is trivially obtained using pQCD directly using (3.7)), and thus fit $K_c(s)$ to $\tilde{K}(s)$ in this region. We find $a_1 = 0.003712\,\text{GeV}^2$ and $a_2 = -0.0005122\,\text{GeV}^4$. The maximum difference between $K_c(s)$ and $\tilde{K}(s)$ is 0.02%, which immediately gives a rigorous bound on the uncertainties when integrating over the approximated kernel $K_c(s)$. We then have that the total charm contribution to (3.7)

is

$$a_\mu^{\text{had,LO}}\big|_c \approx 6\pi i \int_{|s|=s_0} \Pi^{(c)}_{\text{OPE}}(s)\, K_c(s)\, \mathrm{d}s \tag{3.10}$$

$$+ 12\pi^2\, \text{Res}[\Pi^{(c)}_{\text{OPE}}(s)\, K_c(s), s=0] + \int_{s_0}^{\infty} \tilde{K}(s) R_c(s)\, ds \tag{3.11}$$

$$= 14.4(1) \times 10^{-10} \tag{3.12}$$

where $s_0 = (5\,\text{GeV})^2$. The uncertainty quoted above is the uncertainty from the strong coupling, the gluon condensate and varying the scale μ by $\pm 1\,\text{GeV}$, as we did for the charm mass. Our result using the approximation $\tilde{K}(s) \approx K_c(s)$ can only differ from the exact result by 0.02%, or 0.003×10^{-10}, which is completely negligible.
As we cross the bottom-threshold for the high-energy integral, we decouple our coupling and charm mass to a $n_f = 5$ theory using RunDec [42].[3]

The case of the bottom is exactly the same. Using

$$K_b(s) = \frac{\alpha_{\text{em}}^2}{3\pi^2 s}\left[\frac{b_1}{s} + \frac{b_2}{s^2}\right] \tag{3.13}$$

and fitting in the region $M_\Upsilon^2 < s < (12\,\text{GeV})^2$, we find the fit parameters $a_1 = 0.003719\,\text{GeV}^2$ and $a_2 = -0.0007637\,\text{GeV}^4$. The maximum deviation between the fitted and exact kernel is now 0.0005%, which for are practical purposes is exact. We calculate

$$a_\mu^{\text{had,LO}}\big|_b \approx 6\pi i \int_{|s|=s_0} \Pi^{(b)}_{\text{OPE}}(s)\, K_b(s)\, \mathrm{d}s \tag{3.14}$$

$$+ 12\pi^2\, \text{Res}[\Pi^{(b)}_{\text{OPE}}(s)\, K_b(s), s=0] + \int_{s_0}^{\infty} \tilde{K}(s) R_b(s)\, ds \tag{3.15}$$

$$= 0.29(1) \times 10^{-10} \tag{3.16}$$

3.3 Compiling an $e^+e^- \to$ hadrons data collection

There are two types of experimental information of the R-ratio in the literature, *inclusive measurements* and *exclusive measurements*. The former measures every possible hadronic final state, whilst the latter measures only a single final state. We have high-precision inclusive data above $\sqrt{s} = 2\,\text{GeV}$ from BES [55, 116], whilst below this there

[3] We do not find it necessary to decouple across the top-threshold.

only exist high-precision exclusive state measurements. We are thus required to create a data compilation including all possible hadronic final states that is valid below $\sqrt{s} = 2\,\text{GeV}$.

The data collection we will use was first compiled in our work [113] for the purposes of determining the vacuum condensates. The philosophy behind compiling the collection is to use the recent measurements from *BABAR* where possible. There exist some channels and some energy regions for which there is no *BABAR* data. In this case we make use of the most recent alternative data. Finally, there exist some channels for which there exists no data, and we will need to estimate this missing data using isospin relations. The total collection is given in Table 3.1.

One important feature of our approach is that there are no overlapping data, which would require averaging procedures. Such averaging procedures have been used by [103] and [105] for example. These approaches are essential if one wants to obtain the smallest possible uncertainty in $a_\mu^{\text{had,LO}}$, as many systematic uncertainties are correlated if the same experimental facility has been used (we will use the conservative assumption that systematic uncertainties for different channels measured by the same experimental group are 100% correlated). Thus averaging many data sets reduces the linear addition of correlated data. We will therefore have far higher uncertainties in $a_\mu^{\text{had,LO}}$ than those obtained by [103] and [105]. This will be a virtue, as we will demonstrate that even our high-uncertainty data collection is inconsistent witht the OPE, giving confidence that other approaches to compiling the data will also be inconsistent.

3.3.1 Handling the Data

3.3.1.1 Integrating the Data and Uncertainties

For most of the data sets, the method of numerical integration is not important. However, some of the very narrow resonances have limited resolution, and so one has to be careful how one integrates these data. It was pointed out in [139] that linear interpolation overestimates Breit-Wigner shapes, and it was recommended in [103] that quadratic interpolation should be used for this case. However, we found that a first-degree spline interpolation of the data is superior when dealing with Breit-Wigner type shapes, which we will use.

Number	$e^+e^- \to$	Reference	Data Range $\sqrt{s}$ (GeV)	Vacuum Pol.
1	$\pi^0\gamma$	CMD-2 (2005) [117]	0.6 – 1.31	Dressed
2	$\eta\gamma$	CMD-2 (2005) [117]	0.6 – 1.38	Dressed
3	$\pi^+\pi^-$	BaBar (2009) [118, 119]	0.31 – 2.95	Bare
4	$\pi^+\pi^-\pi^0$	BaBar (2004) [120]	1.06 – 2.99	Dressed
		CMD-2 (2006) [121]	1.01 – 1.06	Dressed
		SND (2002) [122]	0.98 – 1.01	Dressed
		SND (2003) [123]	0.66 – 0.98	Dressed
5	$2(\pi^+\pi^-)$	BaBar (2005) [124]	0.62 – 4.45	Bare
6	$\pi^+\pi^-2(\pi^0)$	BaBar (2010) [125]	0.76 – 3.31	Dressed
		SND (2009) [126]	0.66 – 0.94	Dressed
7	$2\pi^+2\pi^-\pi^0$	BaBar (2007) [127]	1.03 – 2.98	Dressed
8	$3(\pi^+\pi^-)$	BaBar (2006) [128]	1.3 – 4.5	Dressed
9	$2(\pi^+\pi^-\pi^0)$	BaBar (2006) [128]	1.3 – 4.5	Dressed
10	$\eta(\pi^+\pi^-)$	BaBar (2007) [127]	1.03 – 2.98	Dressed
11	$\eta\omega$	BaBar (2006) [128]	1.25 – 3.25	Dressed
12	$\eta(2\pi^+2\pi^-)$	BaBar (2007) [127]	1.31 – 2.89	Dressed
13	$\omega\pi^0(\omega \to \pi^0\gamma)$	CMD-2 (2003) [129]	0.92 – 1.38	Bare
14	K^+K^-	CMD-2 (2008) [130]	1.011 – 1.034	Dressed
		SND (2007) [131]	1.04 – 1.38	Dressed
		DM2 (1988) [132]	1.38 – 2.40	?
15	$K^0_sK^0_L$	SND (2001) [133]	1.01 – 1.06	Dressed
		SND (2006) [134]	1.04 – 1.38	Dressed
		DM1 (1981) [135]	1.4 – 2.1	?
16	$\eta\phi$	BaBar (2008) [136]	1.57 – 3.45	Dressed
17	$p\bar{p}$	BaBar (2006) [137]	1.88 – 4.2	Dressed
18	$n\bar{n}$	Fenice (1998) [138]	1.9 – 2.44	Dressed
19	Inclusive	BES (2002) [55]	2 – 5	Bare
		BES (2009) [116]	2.6 – 3.65	Bare
20	$\pi^+\pi^-$ (χpT)	*	0.14 – 0.31	
21	$\pi^+\pi^-3\pi^0$	*	1.03 – 2.98	
22	$\pi^+\pi^-(4\pi^0)$	*	1.3 – 4.5	
23	$\omega\pi^+\pi^-$,$\omega 2\pi^0(\omega \to \pi^0\gamma)$	*	1.15 – 2.53	
24	$\omega(\text{non} - 3\pi, \pi\gamma, \eta\gamma)$	*	0.7 – 0.8	
25	$\phi(\text{non} - K\overline{K}, 3\pi, \pi\gamma, \eta\gamma)$	*	1.01 – 1.03	
26	$\eta\pi^+\pi^-(2\pi^0)$	*	1.3 – 2.9	
27	$K\overline{K}\pi$	*	1.3 – 4.7	
28	$K\overline{K}2\pi$	*	1.4 – 4.3	
29	$K\overline{K}3\pi$	*	1.6 – 4.5	

TABLE 3.1: Data collection for $e^+e^- \to$ hadrons. Stars ($*$) indicate that the final state had not been measured, and was estimated. The treatment of vacuum polarizations is given in Appendix 3.3.1.2. Question marks indicate that we do not know which corrections have been applied by the experimentalists.

For the systematic uncertainties, we make the most conservative assumption that cross-sections in different channels obtained from the same experimental collaboration are 100% correlated, meaning that we add them linearly. Different experiments are assumed to be independent. Within some channel, the systematic uncertainties from an experiment are assumed to be 100% correlated, whilst the statistical uncertainties are independent. The channel where this is not the case is the $e^+e^+ \to \pi^+\pi^-$ channel, where we are supplied with correlation matrices for the statistical uncertainties [118, 119].

3.3.1.2 Vacuum Polarization and Final State Radiation

When using the cross-section data in our dispersion relation (3.7), we require the so-called 'undressed' (or 'bare') cross-section,

$$\sigma_0(s) = \sigma_0(e^+e^- \to \gamma^* \to \text{hadrons}(+\gamma)) \tag{3.17}$$

However, $\sigma_0(s)$ is often not given by experimental groups. The two major issues are that

- Final State Radiation (FSR) has not been added.
- Hadronic vacuum polarization has been included.

Sometimes (especially for older experiments) the situation with these corrections is not even mentioned.

For the case of the FSR, we have that the *BABAR* [118, 119] data for $e^+e^- \to \pi^+\pi^-$ has already included FSR, but the rest of the data either haven't mentioned the FSR corrections or have not added them. We will follow [140] and apply FSR corrections only to the $e^+e^- \to K^+K^-$ final state (for which we have an analytical expression). For the rest of the data, we will not add FSR but rather add an additional 1% systematic uncertainty on all of the data. The motivation for this is that the FSR is expected to contribute roughly 1% to the cross-section.
The FSR contribution to $e^+e^- \to K^+K^-$ can be found in [141], and is

$$\sigma_{\text{FSR}}(s) = \left(1 + \eta(s)\frac{\alpha_{\text{em}}}{\pi}\right) \tag{3.18}$$

where

$$\eta(s) = \frac{\beta^2+1}{\beta}\left[4\mathrm{Li}_2\left(\frac{1-\beta}{\beta+1}\right) + 2\mathrm{Li}_2\left(-\frac{1-\beta}{\beta+1}\right)\right. \tag{3.19}$$

$$\left. - 3\log\left(\frac{2}{\beta+1}\right)\log\left[\frac{\beta+1}{1-\beta}\right] - 2\log(\beta)\log\left(\frac{\beta+1}{1-\beta}\right)\right] \tag{3.20}$$

$$- \frac{3\left(\beta^2+1\right)}{2\beta^2} - 3\log\left(\frac{4}{1-\beta^2}\right) + \frac{\left(\frac{5}{4}\left(\beta^2+1\right)^2 - 2\right)\log\left(\frac{\beta+1}{1-\beta}\right)}{\beta^3} \tag{3.21}$$

$$- 4\log(\beta) \tag{3.22}$$

and

$$\beta = \sqrt{1 - \frac{4m_K^2}{s}} \tag{3.23}$$

As we are not entirely sure if the full FSR has been added, we follow [140] and only apply half the correction and have a 100% uncertainty on the FSR correction,

$$\sigma_{\mathrm{FSR}}(s) = \left(1 + \frac{1}{2}\eta(s)\frac{\alpha_{\mathrm{em}}}{\pi}\right) \pm \frac{1}{2}\eta(s)\frac{\alpha_{\mathrm{em}}}{\pi}. \tag{3.24}$$

Here $m_K = 0.4937\,\mathrm{GeV}$ is the kaon mass. Adding the above FSR correction increases $a_\mu^{\mathrm{had,LO}}$ by about 0.42×10^{-10}.

Now we need to deal with the vacuum polarization. We show in Table 3.1 which final states have not had the vacuum polarization removed. The undressed cross-section is related to the Born cross-section by

$$\sigma_0 = \left(\frac{\alpha(0)}{\alpha(s)}\right)^2 \sigma_{\mathrm{born}} = |1 - \Pi'(s)|^2 \sigma_{\mathrm{born}} \tag{3.25}$$

where $\Pi'(s)$ is the vacuum polarization function $\Pi'(s) \equiv \Pi(s) - \Pi(0)$. We obtain $\Pi(s)$ by a dispersion relation integrating over hadronic data. We make use of a collection for $\Pi'(s)$ supplied to us by S. Eidelman, which is plotted (without uncertainties) in Fig. 3.2. We will also make use $\sigma \equiv \sigma_0$ from now on to simplify notation.

3.3.2 Missing Data

Some of the exclusive channels are as yet unmeasured. Here we give the estimated values of the missing channels. The estimates are mostly based on isospin-arguments, based

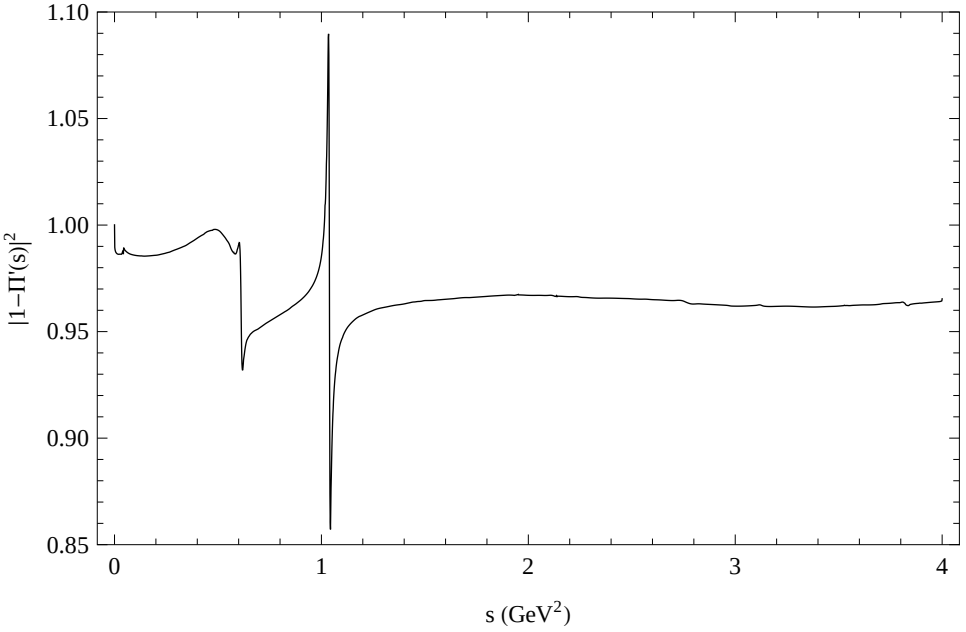

FIGURE 3.2: The hadronic vacuum polarization correction.

primarily on the analysis of [103], where further details can be found. We also assign a 33% model error onto all of these data sets, unless stated otherwise.

20. We don't have data for the $\pi^+\pi^-$ final-state at the lowest energies, so we will use the prediction of Chiral Perturbation Theory (χpT). In this case, we have $\sigma(\pi^+\pi^-) = \pi\alpha^2\beta_0^3|F_\pi^0|^2/(3s)$, where $\beta_0 = (1-4m_\pi^2/s)^{1/2}$. The form-factor is of the form $F_\pi^0 = 1 + \frac{1}{6}\langle r^2\rangle_\pi s + c_1 s^2 + c_2 s^3 + \mathcal{O}(s^4)$. These constants are found by fitting the form-factor to spacelike data, with the result $\langle r^2\rangle_\pi = (0.439\pm0.008)\text{fm}^2$, $c_1 = (6.8\pm1.9)\text{GeV}^{-4}$ and $c_2 = (-0.7\pm6.8)\text{GeV}^{-8}$ [139].

21. We determine $\sigma(2\pi^+2\pi^-\pi^0)_{\eta-\text{excl.}}$ in §3.3.2.1.1. We can use this to obtain the missing channel $\sigma(\pi^+\pi^-3\pi^0)_{\eta-\text{excl.}} = \frac{1}{2}\sigma(2\pi^+2\pi^-\pi^0)_{\eta-\text{excl.}}$.

22. $\sigma(\pi^+\pi^-4\pi^0) = 0.0625\,\sigma(3\pi^+3\pi^-)+0.145\,\sigma(2\pi^+2\pi^-2\pi^0)_{\eta-\text{excl}}$, where $\sigma(2\pi^+2\pi^-2\pi^0)_{\eta-\text{excl}}$ is determined in §3.3.2.1.2.

23. We have $\sigma(\omega\pi^+\pi^-)$ from BaBar (2007) [127]. However, the dominant three-pion decay of the ω already appears in the five-pion final state. Thus we calculate the contribution for $\omega\to\pi^0\gamma$, which we obtain using $\sigma(\omega\pi^+\pi^-\to\pi^+\pi^-\pi^0\gamma) = \sigma(\omega\pi^+\pi^-)\times\mathcal{B}(\omega\to\pi^0\gamma)$ where $\mathcal{B}(\omega\to\pi^0\gamma) = 0.0828\pm0.0028$. Then from isospin, we have that $\sigma(\omega2\pi^0\to3\pi^0\gamma) = 0.5\,\sigma(\omega\pi^+\pi^-\to\pi^+\pi^-\pi^0\gamma)$.

24. The cross-section $\sigma(\omega \to \pi^+\pi^-\pi^0)$ can be taken from [142]. This is the major decay mode of the ω, with $\mathcal{B}(\omega \to \pi^+\pi^-\pi^0) = 0.892 \pm 0.007$. In addition to this final state, we have already accounted for the $\pi^0\gamma$, $\pi^+\pi^-$, and $\eta\gamma$ final states. We thus estimate the unnaccounted for ω decays as being $\sigma(\omega \to \pi^+\pi^-\pi^0) \times \mathcal{B}(\text{non} - 3\pi, \pi\gamma, \eta\gamma)/\mathcal{B}(\omega \to \pi^+\pi^-\pi^0)$, where $\mathcal{B}(\text{non} - 3\pi, \pi\gamma, \eta\gamma) = 0.0094$.

25. We have already accounted for ϕ to $K\bar{K}$, 3π, $\pi\gamma$ and $\eta\gamma$. Hence there is a contribution which we are missing, found from $\mathcal{B}(\text{missing}) = 1 - \mathcal{B}(\phi \to K\bar{K}) - \mathcal{B}(\phi \to 3\pi) - \mathcal{B}(\phi \to \pi\gamma) - \mathcal{B}(\phi \to \eta\gamma) = 0.0014$. Hence we calculate $\sigma(\phi(\text{non} - K\overline{K}, 3\pi, \pi\gamma, \eta\gamma)) = \sigma(\phi \to K^+K^-)\mathcal{B}(\text{missing})/\mathcal{B}(\phi \to K^+K^-) = 0.003\,\sigma(\phi \to K^+K^-)$.

26. We estimate that $\sigma(\eta 2\pi^+2\pi^-) = \sigma(\eta\pi^+\pi^-2\pi^0)$.

27. We have $\sigma(K\overline{K}\pi) = 3\sigma(K^0_sK^\pm\pi^\mp) + \sigma(\phi\pi^0) \times \mathcal{B}(\phi \to K\overline{K})$. Here $\sigma(K^0_sK^\pm\pi^\mp)$ and $\sigma(\phi\pi^0)$ are obtained from BaBar (2008) [136]. We also have $\mathcal{B}(\phi \to K\overline{K}) = 0.831 \pm 0.003$. We assign a 33% systematic uncertainty on the final cross-section.

28. $\sigma(K\overline{K}2\pi) = 9\sigma(K^+K^-2\pi^0) + \frac{9}{4}\sigma(K^+K^-\pi^+\pi^-)$. The have $\sigma(K^+K^-2\pi^0)$ and $\sigma(K^+K^-\pi^+\pi^-)$ from BaBar (2007) [143]. To estimate an uncertainty for this result, we make use of a very different procedure found in [140], which uses the inclusive data K_SX (DM1 Collaboration, [135]) as a starting point. The difference in cross-section between these methods is around 17%, which we take to be the systematic uncertainty.

29. We estimate that $\sigma(K^0\bar{K}^0\pi^+\pi^-\pi^0)_{\eta-\text{excl}} = \sigma(K^+K^-\pi^+\pi^-\pi^0)_{\eta-\text{excl}}$. Taking these two processes as the primary contributors, we get $\sigma(K\overline{K}3\pi) = 2\sigma(K^+K^-\pi^+\pi^-\pi^0)_{\eta-\text{excl}}$, where we obtain $\sigma(K^+K^-\pi^+\pi^-\pi^0)_{\eta-\text{excl}}$ in §3.3.2.1.3.

3.3.2.1 Removing η

In estimating unmeasured final states in the previous section, we had to remove the η-contribution from some final states to employ the Pais isospin-class analysis of [103]. We just give here the results. Note that to avoid double counting, we must use these η-removed cross-section in our integrals.

Channel	This work	Hagiwara *et al.*[105] (2011)	Davier *et al.*[103] (2011)
$\pi^+\pi^-$	500.83 ± 6.94 (KLOE) 513.92 ± 3.8 (BABAR)	505.65 ± 3.09	507.80 ± 2.84
$\pi^+\pi^-\pi^0$	47.02 ± 1.97	47.38 ± 0.99	46.00 ± 1.48
K^+K^-	21.59 ± 0.51	22.09 ± 0.46	21.63 ± 0.73
$\pi^+\pi^-2\pi^0$	18.05 ± 1.49	18.62 ± 1.15	18.01 ± 1.24
$2\pi^+2\pi^-$	13.03 ± 0.67	13.50 ± 0.44	13.35 ± 0.53
$K^0_S K^0_L$	12.70 ± 0.55	13.32 ± 0.16	12.96 ± 0.39
Sum of isospin channels	6.01 ± 0.89	5.98 ± 0.42	6.06 ± 0.46
$\pi^0\gamma$	4.65 ± 0.33	4.54 ± 0.14	4.42 ± 0.19
$\eta\pi^+\pi^-$	1.22 ± 0.11	0.88 ± 0.10	1.15 ± 0.19
$\omega\pi^0$	0.86 ± 0.04	0.76 ± 0.03	0.89 ± 0.07
$\eta\gamma$	0.55 ± 0.16	0.69 ± 0.02	0.64 ± 0.02
$\eta\omega$	0.49 ± 0.05	0.38 ± 0.06	0.47 ± 0.06
$\eta\phi$	0.36 ± 0.04	0.33 ± 0.03	0.36 ± 0.03
$3\pi^+3\pi^-$	0.12 ± 0.01	0.11 ± 0.01	0.12 ± 0.01
$\phi(\rightarrow$ unaccounted)	0.05 ± 0.02	0.04 ± 0.04	0.05 ± 0.00
$\eta 2\pi^+2\pi^-$	0.03 ± 0.02	0.02 ± 0.00	0.02 ± 0.01
$\eta 2\pi^+2\pi^-$	0.03 ± 0.02	0.02 ± 0.00	0.02 ± 0.01
Total	627.58 ± 7.89 (KLOE) 640.69 ± 6.54 (BABAR)	634.28 ± 3.53	633.93 ± 3.61

TABLE 3.2: The contributions from different channels to a_μ (units of 10^{-10}) for energies up to 1.8 GeV. The contributions to the 'Sum of isospin channels' can be found in Table 2 of Ref. [105]. We give our result for the $e^+e^- \rightarrow \pi^+\pi^-$ channel both when using the *BABAR* [118, 119] or the KLOE [144] data.

1. $\sigma(2\pi^+2\pi^-\pi^0)_{\eta-\text{excl.}} = \sigma(2\pi^+2\pi^-\pi^0) - \sigma(\eta\pi^+\pi^-) \times \mathcal{B}(\eta \rightarrow \pi^+\pi^-\pi^0)$, where $\mathcal{B}(\eta \rightarrow \pi^+\pi^-\pi^0) = 0.2274 \pm 0.0028$ and where $\sigma(2\pi^+2\pi^-\pi^0)$ is obtained from BaBar (2007) [127].

2. $\sigma(2\pi^+2\pi^-2\pi^0)_{\eta-\text{excl.}} = \sigma(2\pi^+2\pi^-2\pi^0) - \sigma(\eta\omega) \times \mathcal{B}(\eta \rightarrow \pi^+\pi^-\pi^0) \times \mathcal{B}(\omega \rightarrow \pi^+\pi^-\pi^0)$, where $\mathcal{B}(\omega \rightarrow \pi^+\pi^-\pi^0) = 0.892 \pm 0.007$, $\sigma(2\pi^+2\pi^-2\pi^0)$ was measured by BaBar [128], and $\sigma(\eta\omega)$ was also taken from [128].

3. We calculate $\sigma(K^+K^-\pi^+\pi^-\pi^0)_{\eta-\text{excl}} = \sigma(K^+K^-\pi^+\pi^-\pi^0) - \sigma(\phi\eta) \times \mathcal{B}(\phi \rightarrow K^+K^-) \times \mathcal{B}(\eta \rightarrow \pi^+\pi^-\pi^0)$, where $\mathcal{B}(\phi \rightarrow K^+K^-) = 0.489 \pm 0.01$ and $\mathcal{B}(\eta \rightarrow \pi^+\pi^-\pi^0) = 0.2274 \pm 0.0028$. We obtain $\sigma(K^+K^-\pi^+\pi^-\pi^0)$ from BaBar (2007) [127], and $\sigma(\phi\eta)$ is taken from BaBar (2008) [136].

3.4 The low-energy contribution to $a_\mu^{\text{had,LO}}$

We now have a complete set of data for the low-energy region $0\,\text{GeV} < \sqrt{s} < 2\,\text{GeV}$. A channel-by-channel contribution breakdown to $a_\mu^{\text{had,LO}}$ of our data set is given in Table

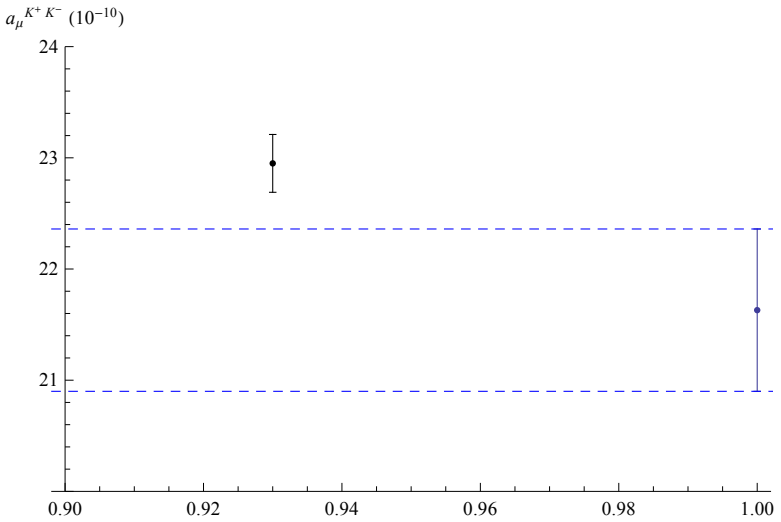

FIGURE 3.3: The contribution to $a_\mu^{\text{had,LO}}$ of the $e^+e^- \to K^+K^-$ channel, from new high-precision *BABAR* measurement [145] (the upper value), compared to the previous world average [103] (lower value). This represents a $1.6\,\sigma$ discrepancy between the two determinations.

3.2, and compared to two recent data sets in the literature [103, 105]. In this section, we will introduce a technique to reduce the contribution of these data in favour of pQCD + the OPE. We will follow closely our work [114, 115].

3.4.1 Introduction

A plausible explanation for the discrepancy $\Delta a_\mu \equiv a_\mu^{\text{exp}} - a_\mu^{\text{SM}} = 28.7(8.0) \times 10^{-10}$ in (3.6) is that there is some systematic error in the experimentally determined hadronic cross-section that enters into (3.7). One reason for this is that there are many examples of hadronic cross-section data being inconsistent with each other. An example from the $e^+e^- \to K^+K^-$ channel is shown in Fig. 3.3. Another example is for the dominant $e^+e^- \to \pi^+\pi^-$ channel. For the energy range $(1 - 0.85)\,\text{GeV}^2$, the 2010 KLOE Collaboration[144] found $a_\mu^{\pi^+\pi^-} = (478.5 \pm 7.0) \times 10^{-10}$, compared to the *BABAR* Collaboration[118] measurement of $a_\mu^{\pi^+\pi^-} = (491.4 \pm 3.7) \times 10^{-10}$. This consitutes a serious $1.6\,\sigma$ discrepancy.

These inconsistencies in the hadronic cross-section data motivate us to reduce our dependence on these data. One approach is calculating $a_\mu^{\text{had,LO}}$ in the framework of LQCD. Although there is currently much effort underway in this direction [146–148], these results are far from being precise enough to give any insight into the discrepancy (3.6). In this context, we have looked at hybrid method that quenches the low-energy e^+e^+

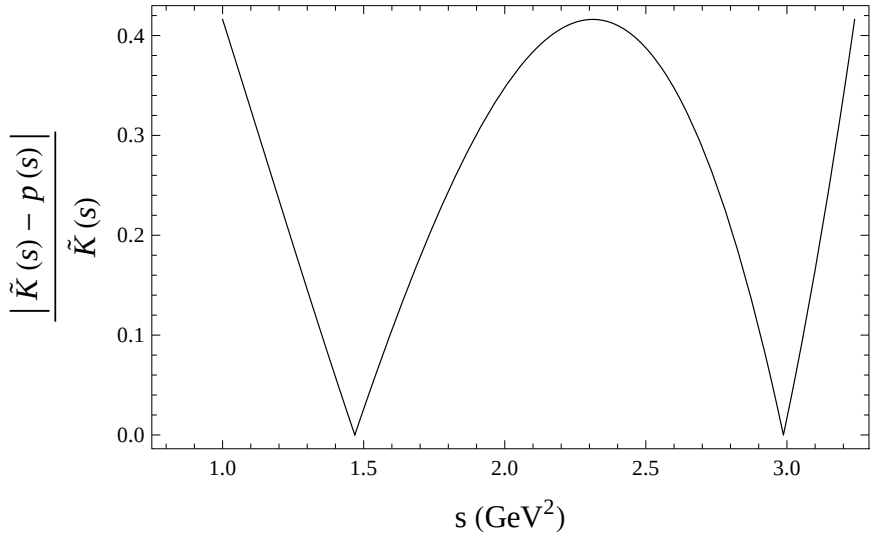

FIGURE 3.4: The magnitude of the ratio of integration kernels used in (3.27) and (3.7).

data contribution to $a_\mu^{\text{had,LO}}$ by including theoretical input in the form the Operator Product Expansion (OPE) [114, 115].[4] This procedure reduces the discrepancy Eq. (3.6) to $\Delta a_\mu = 19.2(8.0) \times 10^{-10}$ based on two assumptions:

1. There is no dimension $d = 2$ term (beyond mass corrections) in the OPE,
2. The validity of quark-hadron duality.

The sensitivity of our conclusions on these assumptions will be tested by looking at a quantitative duality-violating model, as well as a proposed hypothetical $d = 2$ term in the OPE. It was found that these models are unable to significantly modify our reduction in the discrepancy Δa_μ.

3.4.2 The Method

We will focus on the region below $\sqrt{s} = 1.8\,\text{GeV}$, which accounts for about 92% of the contribution to (3.7). It is usually assumed that pQCD is valid above $\sqrt{s} = 1.8\,\text{GeV}$ [103], though we will test this assumption later.

Let us consider a correlator defined via (1.1) and the EM current $j_\mu^{\text{em}}(x) = \sum_f Q_f \bar{f}(x)\gamma_\mu f(x)$, with the sum going over the light quarks $f = \{u, d, s\}$. Letting $p(s)$ be composed only of non-negative powers of s, our sum rule (1.7) allows us to write the low-energy piece

[4] A similar technique was first proposed in an unpublished work [149].

of (3.7) as

$$\tilde{a}_\mu^{\text{had,LO}}(s_0) = \int_0^{s_0} \tilde{K}(s)R(s)\,ds \tag{3.26}$$

$$= \int_0^{s_0} \left[\tilde{K}(s) - p(s)\right] R(s)\,ds + 6\pi i \oint_{|s|=s_0} p(s)\Pi_{\text{OPE}}(s)\,ds. \tag{3.27}$$

We have gained the ability to choose $p(s)$, and hence choose which e^+e^- data to suppress, at the cost of a contour integral over the correlator. There are a number of considerations in selecting $p(s)$. First, evey power of s^n that $p(s)$ contains will lead to a $d = 2(n+1)$ term in the OPE contributing to (3.27). As all terms above $d = 4$ are very poorly known, we will only use kernels of the form $p(s) = a + bs$. Higher dimensional terms in the OPE do contribute, as there are logarithmic momentum terms at $\mathcal{O}(\alpha_s^2)$, but their contribution is heavily suppressed. We will verify this assumption for the $d = 6$ term.

The second consideration is the fact that the region $1\,\text{GeV} < \sqrt{s} < 1.8\,\text{GeV}$ has the most poorly known data, both in terms of large uncertainties and channels for which we don't have data. It is also the only region that is feasibly suppressed with a linear kernel: $\tilde{K}(s)$ is roughly approximated be $\tilde{s}^{-2}$, thus the smaller the s, the greater the curvature and the worse the fit. In addition, the magnitude of such a kernel becomes very large in the poorly known $[1, 1.8]\,\text{GeV}$ region, emphasizing this data. This destroys any usefulness of the method.

We will therefore choose $p(s)$ to minimize the contribution of the region $1\,\text{GeV} < \sqrt{s} < 1.8\,\text{GeV}$, which we do by demanding that the quantity

$$\text{Max}\left|\frac{\tilde{K}(s) - p(s)}{\tilde{K}(s)}\right|, \quad (1\,\text{GeV} < \sqrt{s} < 1.8\,\text{GeV}) \tag{3.28}$$

is minimized.[5] This determines $p(s)$ to be

$$p(s) = 4.996 \times 10^{-9} - 1.432 \times 10^{-9} s. \tag{3.29}$$

We can see from Fig. 3.4 that our new kernel $\tilde{K}(s) - p(s)$ suppresses all the data in the interval $1\,\text{GeV} < \sqrt{s} < 1.8\,\text{GeV}$ by a factor of at least 2.5 compared to the standard kernel $\tilde{K}(s)$. All of the data below 1 GeV is also suppressed, but by a smaller factor.

[5] One can use other minimization philosophies, like least-squares fitting. We chose this philosophy as it provides the best bounds on the contributions. We checked that least-squares minimization had negligible effect on our final results.

3.4.3 Theoretical Input

The OPE for the light-quarks includes the quark condensates, which are not found in the heavy-quark OPE we used previously.[6] We will parameterize the OPE prediction of the light-quark correlator $\Pi(s)$ in the customary form

$$\Pi_{\rm OPE}(s) = \sum_{n=0} C_{2n}(s,\mu^2)\langle \mathcal{O}_{2n}(\mu^2)\rangle + \Pi_{\rm qed}(s). \tag{3.30}$$

The first-term is just pQCD,

$$C_0(s,\mu^2)\langle \mathcal{O}_0(\mu^2)\rangle \equiv \Pi_{\rm pQCD}(s) = \sum_{i=u,d,s} \frac{Q_i^2}{16\pi^2}\left(\frac{20}{3} - 4\log\left(-\frac{s}{\mu^2}\right) + \mathcal{O}(\alpha_s)\right). \tag{3.31}$$

Here $Q_T^2 = \sum_{i=u,d,s} Q_i^2 = 2/3$. Unlike the case for the heavy-quark correlator, we know the pQCD light-quark correlator to $\mathcal{O}(\alpha_s^4)$. The complete expression is given by [150].[7] There exists a well-known [151] ambiguity of how to evaluate the contour integral over $\Pi_{\rm pQCD}(s)$ in (1.7): one can either fix the scale μ and then perform the contour integral (Fixed Order Perturbation Theory (FOPT)), or one can first choose a running scale $\mu = i\sqrt{s}$ before performing the contour integral (Contour Improved Perturbation Theory (CIPT)). For the CIPT approach, the coupling α_s becomes a function of s, and one must use the renormalization group to solve for α_s along the contour. We give the full details of this precedure in the Appendix §A.3. For the FOPT approach, we will use $\mu = M_\tau$. Both FOPT and CIPT will be used to integrate over $\Pi_{\rm pQCD}(s)$, and their mean taken as the final result. The half of the difference between the FOPT and CIPT result will be taken as a systematic uncertainty. This ensures that our result is consistent with both the FOPT and CIPT approaches.

We assume that the $d = 2$ term in the OPE, $C_2(s,\mu^2)\langle \mathcal{O}_2(\mu^2)\rangle$, receives contributions only from mass-corrections. We use the the three-loop $\mathcal{O}(m_s^2)$ result,[152, 153] neglecting the contributions from the up and down quarks, giving

$$C_2\langle \mathcal{O}_2\rangle = \sum_{i=u,d,s} Q_i^2 \frac{\bar{m}_i^2(\mu)}{4\pi^2}\Big(6 + \mathcal{O}(\alpha_s)\Big) \tag{3.32}$$

[6] This ultimately arises from the fact that there is no chiral symmetry for the heavy quarks.

[7] The reference supplies a link to http://www.ttp.kit.edu/Progdata/ttp10/ttp10-42/ where the full correlator is helpfully supplied as a Mathematica file.

For the quark masses, we will use the PDG values [1] $\bar{m}_u(2\,\text{GeV}) = (2.3 \pm 0.7)\,\text{MeV}$, $\bar{m}_d(2\,\text{GeV}) = (4.8 \pm 0.7)\,\text{MeV}$ and $\bar{m}_s(2\,\text{GeV}) = (95 \pm 5)\,\text{MeV}$.

The dimension-4 term in (3.30) is given by [154],

$$C_4\langle\mathcal{O}_4\rangle = \frac{1}{s^2}\sum_{i=u,d,s} Q_i^2\Big[\left(\frac{1}{12} - \frac{11}{216}\frac{\alpha_s(\mu)}{\pi}\right)\langle\frac{\alpha_s}{\pi}G^2\rangle + \left(2 - \frac{2}{3}\frac{\alpha_s(\mu)}{\pi} + \mathcal{O}(\alpha_s^2)\right)\bar{m}_i(\mu)\langle\bar{q}_i q_i\rangle(\mu)\Big]. \tag{3.33}$$

The Wilson coefficient for the gluon condensate is known only up to $\mathcal{O}(\alpha_s)$, whilst the coefficient for the quark condensate is known to $\mathcal{O}(\alpha_s^2)$ [154]. We gave various gluon condensate determinations in Table 2.1, and will use the conservative estimate

$$\langle\frac{\alpha_s}{\pi}G^2\rangle = 0.015 \pm 0.015\,\text{GeV}^4. \tag{3.34}$$

The light-quark condensate is taken from (2.46) whilst the strange-quark condensate is from (2.47). It turns out that the contribution from the quark condensates is virtually negligible compared to the gluon condensate.

The QED contributions are

$$\Pi_{\text{qed}}(s) = \sum_{i=u,d,s} Q_i^4 \frac{3}{16\pi^2}\left(\frac{55}{12} - 4\zeta_3 - \log\left(\frac{-s}{\mu^2}\right)\right)\frac{\alpha_{\text{em}}}{\pi} \tag{3.35}$$

The magnitude of the contributions to $\tilde{a}_\mu^{\text{had,LO}}(s_0)$ from each of these pieces in the OPE is given in Table 3.3.

3.4.3.1 An estimate of $C_6\langle\mathcal{O}_6\rangle$

In this subsection, we will want to verify that the contribution from $C_6\langle\mathcal{O}_6\rangle$ can be neglected. Its contribution to the OPE (3.30) is [155]

$$\begin{aligned} C_6\langle\mathcal{O}_6\rangle = \frac{1}{s^3}\sum_f Q_f^2\Big[&8\pi^2\left(1 - \frac{91}{72}\log\left[\frac{-s}{\mu^2}\right]\frac{\alpha}{\pi}\right)\frac{\alpha}{\pi}\langle A_\mu^a A^{a\mu}\rangle \\ &+ \frac{32\pi^2}{9}\left(1 - \frac{643}{288}\log\left[\frac{-s}{\mu^2}\right]\frac{\alpha}{\pi}\right)\frac{\alpha}{\pi}\langle V_\mu^a V^{\mu a}\rangle \\ &- \frac{16\pi^2}{27}\left(\log\left[\frac{-s}{\mu^2}\right]\left(\frac{\alpha}{\pi}\right)^2\right)\langle A_\mu A^\mu\rangle - \frac{8\pi^2}{3}\left(\log\left[\frac{-s}{\mu^2}\right]\left(\frac{\alpha}{\pi}\right)^2\right)\langle V_\mu V^\mu\rangle\Big]. \end{aligned} \tag{3.36}$$

	Contribution to $\tilde{a}_\mu^{\mathrm{had,LO}}(s_0)(\times 10^{-10})$
Π_{pQCD}	206.25
$C_2\langle\mathcal{O}_2\rangle$	-1.65
$C_4\langle\mathcal{O}_4\rangle$	0.41
$C_6\langle\mathcal{O}_6\rangle$	≈ -0.0158
$\Pi_{\mathrm{qed}}(s)$	0.40

TABLE 3.3: Breakdown of OPE contributions to $\tilde{a}_\mu^{\mathrm{had,LO}}(s_0)$ at $s_0 = 1.8^2\,\mathrm{GeV}^2$. Contour integrals performed using FOPT.

Its contribution to $\tilde{a}_\mu^{\mathrm{had,LO}}(s_0)$ is $6\pi i \oint_{|s|=s_0} p(s) C_6\langle\mathcal{O}_6\rangle\, ds$, where $p(s)$ is the quenching-kernel (4.18). Very little is known about $\langle A_\mu^a A^{a\mu}\rangle, \langle V_\mu^a V^{a\mu}\rangle$ etc. One way to make progress is to invoke the so-called vacuum saturation approximation, which means assuming

$$\langle A_\mu^a A^{a\mu}\rangle = -\langle V_\mu^a V^{a\mu}\rangle = \frac{4}{9}\langle\overline{\psi}\psi\rangle^2 \tag{3.37}$$

$$\langle A_\mu A^\mu\rangle = -\langle V_\mu V^\mu\rangle = \frac{2}{9}\langle\overline{\psi}\psi\rangle^2 \tag{3.38}$$

Using a rough value of $\langle\overline{\psi}\psi\rangle = (-0.24)^3\,\mathrm{GeV}^3$ for all three light quark condensates, and vacuum saturation, we find

$$6\pi i \oint_{|s|=s_0} p(s)\frac{C_6\langle\mathcal{O}_6\rangle}{s^3}\, ds = -0.00158\cdot 10^{-10} \tag{3.39}$$

which is entirely negligible in our context. However, there is evidence that this approximation is off by a large factor. One approach is to introduce a 'fudge-factor', making the replacement $\langle\overline{\psi}\psi\rangle^2 \to \lambda\langle\overline{\psi}\psi\rangle^2$. It has been argued by [155] that $\lambda \sim 3-9$. Using a conservative value of $\lambda = 10$, one trivially obtains

$$6\pi i \oint_{|s|=s_0} p(s)\frac{C_6\langle\mathcal{O}_6\rangle}{s^3}\, ds = -0.0158\cdot 10^{-10} \tag{3.40}$$

which is still negligible. We will therefore ignore the contribution of $C_6\langle\mathcal{O}_6\rangle$. We will assume that the contributions from $C_8\langle\mathcal{O}_8\rangle$ and higher are also negligible.

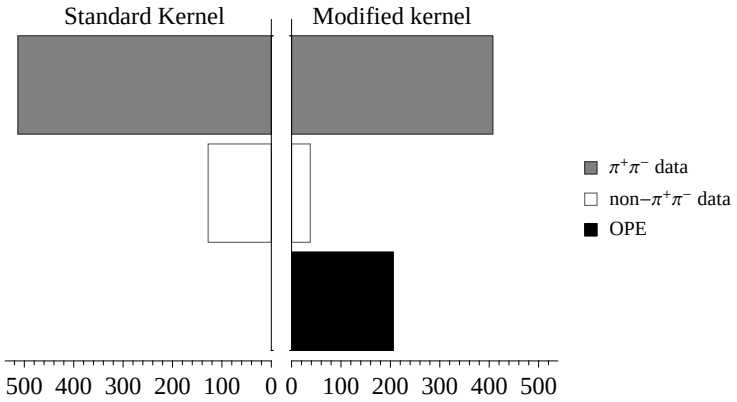

FIGURE 3.5: A breakdown of the contributions to $a_\mu^{\text{had,LO}}$ (in units of 10^{-10}) using both the standard approach Eq. (3.7) and the quenched kernel approach (3.27).

3.4.4 Results

Using the standard kernel $\tilde{K}(s)$ in Eq. (3.7), and integrating up to $\sqrt{s_0} = 1.8\,\text{GeV}$, we find

$$a_\mu^{\text{had,LO}}(s_0) = (640.7 \pm 6.5_{\Delta\text{data}}) \cdot 10^{-10}, \tag{3.41}$$

where the error is the combined statistical and systematic error from the e^+e^- data.

Using instead the quenched-kernel approach, i.e. Eq. (3.27), with $\sqrt{s_0} = 1.8\,\text{GeV}$, we have that the average of the FOPT and CIPT approach is

$$\begin{aligned}\tilde{a}_\mu^{\text{had,LO}}(s_0) &= (650.2 \pm 3.1_{\Delta\text{data}} \pm 1.7_{\Delta\text{conv}} \pm 0.9_{\Delta\alpha_s} \pm 1.3_{\Delta\langle G^2\rangle} \pm 0.8_{\Delta\text{int}}) \cdot 10^{-10} \\ &= (650.2 \pm 4.0) \times 10^{-10},\end{aligned} \tag{3.42}$$

The uncertainties: Δconv is the difference between the $\mathcal{O}(\alpha_s^4)$ and $\mathcal{O}(\alpha_s^3)$ pQCD results, $\Delta\alpha_s$ is the uncertainty from the strong coupling, $\Delta\langle G^2\rangle$ is the uncertainty in the gluon condensate, and finally Δint is half the difference between using FOPT and CIPT.

Before concluding how much our method reduces the discrepancy (3.6), we need to deal with one more small issue, that of higher-order $\mathcal{O}(\alpha_{\text{em}}^3)$ hadronic corrections to the muon $g-2$. The reason for this is that the calculation of these corrections makes use of the same e^+e^- data as does the $\mathcal{O}(\alpha_{\text{em}}^2)$ leading-order contribution (3.7). We thus use the same procedure as we used for leading-order contribution (3.7) of suppressing the e^+e^- data in favour of the OPE. The kernels used to integrate the e^+e^- data can be found

in [156].[8] One finds that the difference between the standard kernel approach, $a_\mu^{\text{had,NLO}}$, and the quenched kernel approach, $\tilde{a}_\mu^{\text{had,NLO}}$, is

$$\tilde{a}_\mu^{\text{had,NLO}} - a_\mu^{\text{had,NLO}} = -0.2 \times 10^{-10}. \tag{3.43}$$

Combining this with (3.42), we find that the our modified approach reduces the discrepancy (3.6) to

$$\Delta a_\mu \equiv a_\mu^{\text{exp}} - \tilde{a}_\mu^{\text{SM}} = 19.2(8.0) \times 10^{-10}. \tag{3.44}$$

This is now a lower $2.4\,\sigma$ effect.[9]

Our analysis of $a_\mu^{\text{had,LO}}$ only produces an interesting result if there is a discrepancy between the OPE and the e^+e^- data. This discrepancy can be seen in Fig. 3.6, which shows the difference $\tilde{a}_\mu^{\text{had,NLO}} - a_\mu^{\text{had,NLO}}$ plotted for varying s_0. If the data were consistent with the OPE, this quantity ought to be consistent with 0, which it is not for any value of s_0. The conclusion that there is such an inconsistency between the OPE and the data is fundamental to our analysis, and we will now look carefully at the assumptions we made in our analysis, and see how sensitive our conclusion is to these.

3.4.5 A Critical Examination of Our Assumptions

As already stated in the introduction, our analysis makes two important assumptions:

1. There is no dimension $d = 2$ term (beyond mass corrections) in the OPE,
2. The validity of quark-hadron duality.

We found in Fig. 3.6 a clear discrepancy between the OPE and the e^+e^- data. In this subsection we give a critical discussion of whether a violation of these assumptions could bring the OPE and e^+e^- into agreement.

[8] The next-to-leading order contribution is parametrized as $\tilde{a}_\mu^{\text{had,NLO}} = a^{(2a)} + a^{(2b)} + a^{(2c)}$ in [156]. Both $a^{(2a)}$ and $a^{(2b)}$ can be written in the form $a^{(2i)} = \int_0^\infty ds\, \tilde{K}_i(s) R(s)$ for $i = a, b$. The fitting kernels were found to be $p_a(s) = (-1.633 + 4.50s) \times 10^{-11}$ and $p_b(s) = (7.11 - 2.01s) \times 10^{-11}$. The term $a^{(2c)}$ is a double integral over two kernels. It is not obvious how to use our fitting approach for this term. Luckily, it is of $\mathcal{O}(100)$ smaller than either $a^{(2a)}$ or $a^{(2b)}$, meaning we can ignore it.

[9] This statement is not entirely rigorous: the discrepancy (3.6) used the e^+e^- data set of [103]. We would need to run our fitting method on the dataset of [103] to conclude this.
Also, we assumed that the uncertainty in Δa_μ stays the same, which won't exactly be the case: for our dataset, the fitting method reduces the uncertainty in the $a_\mu^{\text{had,LO}}$ by roughly a third, as can be seen from (3.41) and (3.42). Assuming a similar reduction in uncertainty would happen when using the dataset of [103], we would have a $2.6\,\sigma$ discrepancy for Δa_μ instead, which still represents a significant 1σ reduction.

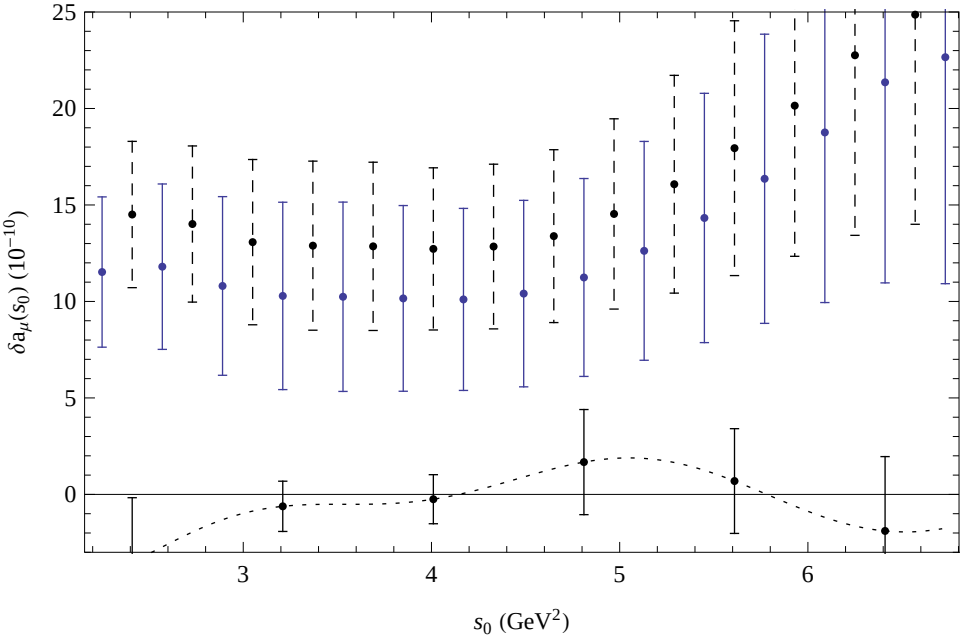

FIGURE 3.6: The difference between the fitted and non-fitted results, $\delta a_\mu(s_0) \equiv \tilde{a}_\mu^{\rm had,LO}(s_0) - a_\mu^{\rm had,LO}(s_0)$, as a function of s_0. Cauchy's Theorem demands that $\delta a_\mu(s_0) = 0$. The contour integral Eq. (3.27) was performed using FOPT. The dashed (solid) error bar is the result from using the 2010 KLOE [144] (*BABAR* [118, 119]) data in the $e^+e^- \to \pi^+\pi^-$ channel. The dotted line shows the contribution to $\delta a_\mu(s_0)$ from possible duality violations given by the model Eq. (3.46). The uncertainties cited for the model arise from the model fit parameters, and we conservatively added these uncertainties linearly as we don't know their individual correlations.

3.4.5.1 The Dimension-2 Term in the OPE

The usual reason given for $C_2\langle\mathcal{O}_2\rangle$ only receiving contributions from mass corrections is that there are no $d = 2$ gauge-invariant operators involving quark and gluon fields in QCD. One can however not *a priori* exclude additional contributions to $C_2\langle\mathcal{O}_2\rangle$ [157].

The evidence that there is no $C_2\langle\mathcal{O}_2\rangle$ term comes from LQCD [158], as well as from QCD sum rule analyses[87, 159] of the τ-decay data obtained by the ALEPH collaboration [50].

Let us relax this assumption and consider a model proposed for an effective $d = 2$ term [157],

$$C_2\langle\mathcal{O}_2\rangle = \sum_{i=u,d,s} Q_i^2 \frac{1}{16\pi^2}\frac{\alpha_s}{\pi}\lambda^2\left(\frac{128}{3} - 32\zeta_3\right), \tag{3.45}$$

where λ^2 is identified as a 'tachyonic gluon mass' ($\lambda^2 < 0$). The gluon mass was estimated to lie in the range $-0.085\,\text{GeV}^2 < \frac{\alpha_s}{\pi}\lambda^2 < -0.034\,\text{GeV}^2$ [157]. Including this term into the OPE (3.30) would *increase* our result (3.42) by $(3.6 - 8.9) \times 10^{-10}$, significanlty

decreasing the discrepancy Δa_μ. It would thus also significantly increase the discrepancy in Fig. 3.6.

3.4.5.2 Duality Violations

The use of the OPE in the deep Euclidean region is entirely rigorous. However, the contour integral in (3.27) involves integrating the OPE expression for the correlator also near the Minkowski axis, and here the validity of the OPE is not guaranteed. Let us define the difference between the exact correlator and the expression given by the OPE as $\Delta_{\rm DV} = \Pi(s) - \Pi_{\rm OPE}(s)$. Then the exact result for the contour integral (3.27) is $\oint_{|s|=s_0} p(s)\,[\Pi_{\rm OPE}(s) + \Delta_{\rm DV}]\,ds$. The assumption we made in (3.27) was that the integral over $\Delta_{\rm DV}$ is zero. This assumption is referred to as *global quark-hadron duality*. We will give two pieces of evidence that violations of this duality assumption won't invalidate our conclusions:

1. We use a recent quantitative model of duality violations [160] that was derived using very some fairly general features that such duality violations should follow, to estimate the magnitude of possible duality violations. The model is of the form

$$\frac{1}{\pi}{\rm Im}\Delta_{\rm DV}(s) = \frac{2}{3}\Big[\frac{5}{6}\kappa_V e^{-\gamma_V s}\sin(\alpha_V + \beta_V s) + \frac{1}{6}\kappa_V e^{-\gamma_V s}\sin(\alpha'_V + \beta_V s)\Big]. \quad (3.46)$$

   The coefficients in the above, obtained by fitting to the BES inclusive data [55, 116] can be found in [160]. The contribution of these duality violations to (3.27) is then obtained using ($\sqrt{s_0} = 1.8\,{\rm GeV}$)

$$\begin{aligned} 6\pi i \oint_{|s|=s_0} p(s)\Delta_{\rm DV}\,ds &= -12\pi \int_{s_0}^{\infty} p(s){\rm Im}\Delta_{\rm DV}(s)\,ds \\ &= -0.59(59)\cdot 10^{-10}. \end{aligned} \quad (3.47)$$

   This is too small by an order of magnitude to bring the data and the OPE in Fig. 3.6 into agreement.[10] The duality violating contribution for varying s_0 is plotted in Fig. 3.6.

[10] One note regarding the uncertainty in the above, it was obtained by varying the parameter errors obtained from the fit of the model to the data, and adding these variations in quadrature. As the uncertainties are likely correlated, one can obtain an upper bound on the uncertainty of $6\pi i \oint_{|s|=s_0} p(s)\Delta_{\rm DV}\,ds$ by assuming that the uncertainties in the model parameters are 100% correlated. One then obtains for (3.47) a result of -0.59(1.25), which is still far too small to bring about consistency.

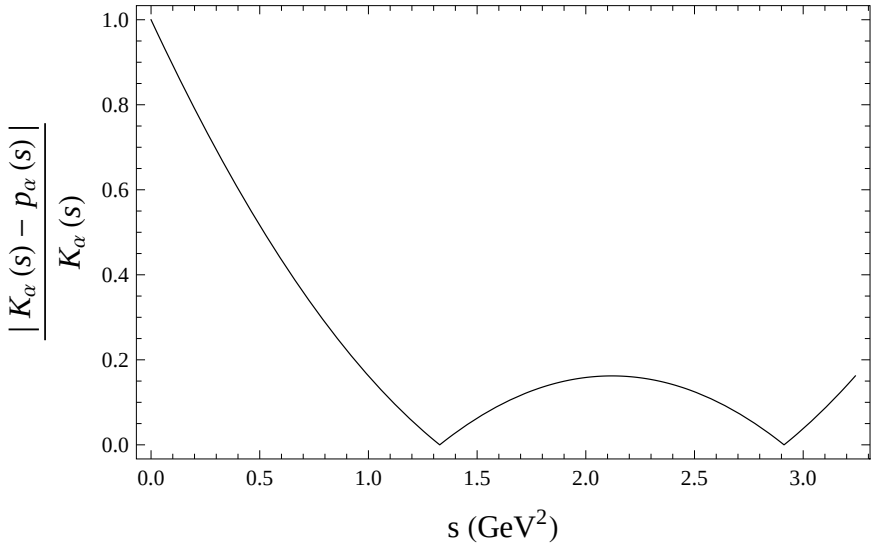

FIGURE 3.7: The magnitude of the ratio of integration kernels used to integrate over the e^+e^- data to determine $\Delta\alpha_{\rm had}(M_Z^2)$ in the standard approach (3.49) versus the quenched approach.

2. We expect on general grounds [160] that the contribution of the duality violations vanishes as $s_0 \to \infty$. This is certaintly true of the model (3.47). However, increasing s_0 seems to worsen the agreement between the OPE and the e^+e^- data in Fig. 3.6. It can also be noted that the 2009 BES Collaboration [116] supplied three high-precision measurements of $R(s)$ 2.60, 3.07 and 3.65 GeV. Each of these is perfectly in agreement with pQCD, giving additional evidence that pQCD is valid at the right-side of Fig. 3.6.

We thus believe that there is good evidence that the discrepancy between the OPE and the e^+e^- is real, with the e^+e^- cross-section data being too small. Partially suppressing this (possibly) problematic data lead to reduction in the discrepancy (3.6) between the Standard Model and experimental results for the $g-2$ of the muon, Δa_μ, from $3.6\,\sigma$ to $2.4\,\sigma$. It might be hoped that a 100% suppression of the e^+e^- data would lead to a further decrease in Δa_μ.

3.4.6 A common objection: the Higgs Mass

We have argued that there is good evidence that the $e^+e^- \to$ hadrons cross-section data is *too small*, and that this is a plausible explanation for the current discrepancy $\Delta a_\mu \equiv a_\mu^{\rm exp} - a_\mu^{\rm SM}$. However, W.J. Marciano *et al.* [161] produced a well-known analysis that showed that simple increases to $\sigma(e^+e^- \to \text{hadrons})$ required to set $\Delta a_\mu = 0$ have

the effect of also increasing the hadronic contribution to the QED coupling, $\Delta\alpha_{\rm had}(M_Z^2)$, given by

$$\Delta\alpha_{\rm had}(M_Z^2) = \frac{\alpha_{\rm em} M_Z^2}{3\pi} P \int \frac{R(s)}{s(M_Z^2 - s)} ds. \tag{3.48}$$

This is a key input parameter for Standard Model fits to electroweak precision data, which have been used to determine the Higgs mass [162, 163], and is strongly negatively correlated[11] with the Higgs mass obtained in this way. The most recent of such fit [163] obtains $M_H = 94^{+25}_{-22}\,\text{GeV}$, which can be compared with the likely Higgs found by the ATLAS Collaboration $M_H = 125.3(0.6)\,\text{GeV}$ [164] and the CMS Collaboration $M_H = 126(0.6)\,\text{GeV}$ [165]. This already represents a $\sim 1.3\,\sigma$ discrepancy between the fitted and observed Higgs masses. Thus increasing $\sigma(e^+e^- \to \text{hadrons})$ increases $\Delta_{\rm had}(M_Z)$ which further decreases the already too small fitted Higgs mass. This could then still be a sign of new physics. Therefore it is of interest to know the shift in $\Delta\alpha_{\rm had}(M_Z^2)$ if we perform the same analysis on $\Delta_{\rm had}(M_Z)$ as we did for $a_\mu^{\rm had,LO}$. We follow exactly the same analysis, except with the replacement

$$\tilde{K}(s) \to K_\alpha(s) = \frac{\alpha_{\rm em} M_Z^2}{3\pi} \frac{1}{s(M_Z^2 - s)} \tag{3.49}$$

which leads to a fitting kernel of $p_\alpha(s) = 0.0008490 - 0.0002002\,s$. The suppression is shown in Fig. 3.7. The greater suppression of the data compared to Fig. 3.4 is due to the kernel $K_\alpha(s)$ going roughly as $\sim 1/s$, whilst the $g-2$ kernel goes as $\sim 1/s^2$, which implies that the curvature is smaller for $K_\alpha(s)$ implying that a straight-line will fit it better. Let us define $\delta\alpha_{\rm had}$ as the difference between $\Delta\alpha_{\rm had}(M_Z^2)$ obtained using the standard approach (3.49) and using the fitted kernel $K_\alpha(s) - p_\alpha(s)$. We find

$$\delta\alpha_{\rm had} = 1.7 \times 10^{-4}. \tag{3.50}$$

The above is the average between FOPT and CIPT. We neglect the uncertainties, as they are not important in what follows. To determine rigorously how this changes the Higgs mass, one would need to use GFITTER [162, 163]. However, we can give a simple estimate by approximating the functional dependence of M_H on $\Delta\alpha_{\rm had}(M_Z^2)$ to be linear for small changes in $\Delta\alpha_{\rm had}(M_Z^2)$. We are given two[12] pairs $\{\Delta\alpha_{\rm had}(M_Z^2), M_H\}$ in [103] obtained using GFITTER and where only $\Delta\alpha_{\rm had}(M_Z^2)$ is being varied, {{274.21 ×

[11] The exact correlation between $\ln M_H$ and $\Delta\alpha_{\rm had}(M_Z^2)$ is -0.395 [162].
[12] There is actually a third pair in the Erratum of [103].

$10^{-4}, 96\,\text{GeV}\}, \{276.8 \times 10^{-4}, 84\,\text{GeV}\}$. We immediately have that (3.50) reduces the Higgs mass by approximately 8 GeV. This would mean the fitted value [163] goes to $M_H \sim 86^{+25}_{-22}\,\text{GeV}$ which is now a $1.6\,\sigma$ discrepancy.[13] Thus our fitting procedure that suppresses the e^+e^- data has increased the discrepancy between the fitted Higgs and observed Higgs by about 0.3σ, whilst decreasing the discrepancy $\Delta a_\mu \equiv a_\mu^{\text{exp}} - a_\mu^{\text{SM}}$ by about 1.2σ. This can be considered an overall improvement to the tension between the Standard Model and experiment.

However, there is still a tension both for the Higgs and $g-2$ between the Standard Model prediction and experiment. Assuming that the Standard Model is correct, there are a large number of possible scenario's that bring consistency. We list the most plausible:

1. a_μ^{exp} from [1, 104] is wrong. This will only have a chance of being corrected beyond 2016 by the new Fermilab experiment.

2. The problem comes from the non-$a_\mu^{\text{had,LO}}$ hadronic contributions $g-2$ of the muon. The hadronic contributions are

$$a_\mu^{\text{had}} = a_\mu^{\text{had,LO}} + a_\mu^{\text{had,HO}} + a_\mu^{\text{had,1-by-1}} \tag{3.51}$$

   where (taking the results from [105] the lowest-order hadronic contribution is about $a_\mu^{\text{had,LO}} = (694.91 \pm 4.27) \times 10^{-10}$, the higher-order hadronic contributions are $a_\mu^{\text{had,LO}} = (9.84 \pm 0.07) \times 10^{-10}$ and the light-by-light scattering contribution $a_\mu^{\text{had,1-by-1}} = 10.5(2.6) \times 10^{-10}$. The higher-order contributions also make use of the e^+e^- cross-section data. This contribution is well under control given its size. There are issues with the light-by-light scattering contribution however, which is currently obtained via models. The result of $a_\mu^{\text{had,1-by-1}} = 10.5(2.6) \times 10^{-10}$ quoted by [105] comes from [166], who write that

> Combining results of different models with educated guesses on the errors we come to the estimate $a_\mu^{\text{had,1-by-1}} = 10.5(2.6) \times 10^{-10}$.

   Yet these uncertainties would have to be off by a factor of ten in order to explain the discrepancy $\Delta a_\mu \equiv a_\mu^{\text{exp}} - a_\mu^{\text{SM}} = 28.7(8.0) \times 10^{-10}$, which seems unlikely, even if they have been guessed.

[13] Assuming of course that the uncertainties don't change much.

3. The discrepancy Δa_μ comes primarily from $a_\mu^{\mathrm{had,LO}}$. This immediately implies that the e^+e^- cross-section data is too small. Then we have the following options:

   (a) The only problem is with the e^+e^- cross-section data. As the kernels used to determine $a_\mu^{\mathrm{had,LO}}$ and $\Delta_{\mathrm{had}}(M_Z)$ are quite different ($\sim 1/s^2$ versus $\sim 1/s$), it is possible to increase one without increasing the other. As pointed out by Marciano *et al.* [161],

   > It is interesting to note that there are more complex scenarios where it is possible to bridge the Δa_μ discrepancy without significantly affecting M_H. For instance, we may envisage an increase of $\sigma(s)$ at low s combined with a decrease at high s in such a manner that their overall contribution to $\Delta\alpha_{\mathrm{had}}(M_Z^2)$, and therefore to M_H, approximately cancels. Since the contributions to $a_\mu^{\mathrm{had,LO}}$ are more heavily weighted at low s, it is then possible to further adjust the positive and negative shifts to bridge the muon $g-2$ discrepancy.

   Our approach to suppress the e^+e^- gives some support for this scenario for the $g-2$ case, as $a_\mu^{\mathrm{had,LO}}$ increased when the data were partially suppressed. However, $\Delta_{\mathrm{had}}(M_Z)$ also increased, worsening the situation with the Higgs mass. If only the data were the problem, we might expect a partial suppression of the data to improve the situation with a too small Higgs, which is not the case.

   (b) The e^+e^- cross-section is too small *and* the top-quark mass is too small. This possibility was not mentioned by Marciano *et al.* [161], and it is this possibility that we think is the most plausible. The fit to the Higgs mass is very sensitive to both $\Delta\alpha_{\mathrm{had}}(M_Z^2)$ and the top mass. The top mass used by GFITTER [163] is $m_t = (173.18 \pm 0.94)\,\mathrm{GeV}$ from the Tevatron [167]. There are a number of problems with the top quark mass. One major issue is the problem of mass definitions. Most calculations (like the Tevatron measurement) rely on Monte Carlo generators to extract m_t, and there are difficulties in relating this Monte Carlo mass to the pole mass. It is usually assumed that the Monte Carlo mass is the same as the pole mass, but the true pole mass could be 1 GeV higher than the mass in current Monte Carlo generators [168].
   The GFITTER group also notes,

The theoretical uncertainties arising from nonperturbative colour-reconnection effects in the fragmentation process [169, 170], and from ambiguitities in the top-mass definition [171, 172], affect the (kinematic) top mass measurement. Their quantitative estimate is difficult and may reach roughly 0.5 GeV each, where the systematic error due to shower effects could be larger [169].

An approximate dependence of the Higgs mass on the top mass is given in [161], from which we have that a change of Δm_t leads to a change in the fitted Higgs mass of $\Delta M_H \approx 11.2 \Delta m_t$. From the above discussion of the uncertainties, the top mass could easily be systematically shifted downwards by $\sim 2\,\text{GeV}$ or more. Removing this bias would lead to an increase in M_H by a very significant 22 GeV.

If the Standard Model is correct, and the a_μ^{exp} from [1, 104] is correct, then we think $3(b)$ is the most likely of the scenario's. It is very hard to see how we can achieve consistency both for the $g-2$ of the muon and for the fitted Higgs mass unless the current value top-quark $m_t = (173.18 \pm 0.94)\,\text{GeV}$ [167] is too small by $\sim 2\,\text{GeV}$.

Chapter 4

The Running of the Electromagnetic Coupling

4.1 Introduction

The running of the QED coupling $\alpha_{\rm em}$ can be parameterized by

$$\alpha_{\rm em}(s) = \frac{\alpha_{\rm em}(0)}{1 - \Delta\alpha_{\rm lep}(s) - \Delta\alpha_{\rm had}(s)}. \tag{4.1}$$

The leptonic contribution $\Delta\alpha_{\rm lep}$ can be determined with high precision in perturbation theory, whilst the hadronic contribution is $\Delta\alpha_{\rm had}(s)$. As explained in the previous Section §3.4.6, the quantity $\Delta\alpha_{\rm had}(s)$ is a key input parameter for Standard Model fits to electroweak precision data, which have been used to determine the Higgs mass [162, 163], and is strongly negatively correlated[1] with the Higgs mass obtained in this way. The most recent of such fit [163] obtains $M_H = 94^{+25}_{-22}\,\text{GeV}$, which represents a $\sim 1.3\,\sigma$ discrepancy with the possible Higgs measured by the ATLAS Collaboration $M_H = 125.3(0.6)\,\text{GeV}$ [164] and the CMS Collaboration $M_H = 126(0.6)\,\text{GeV}$ [165].

The QED coupling at the scale M_Z is of particular interest, so we will consider this point from now on. We will also set $\alpha_{\rm em} \equiv \alpha_{\rm em}(0)$. Then the hadronic contribution $\Delta\alpha_{\rm had}(M_Z^2)$ is given by

$$\Delta\alpha_{\rm had}(M_Z^2) = 4\pi\alpha_{\rm em}\Big(\Pi(0) - \text{Re}[\Pi(M_Z^2)]\Big), \tag{4.2}$$

[1] The exact correlation between $\ln M_H$ and $\Delta_{\rm had}(M_Z)$ is -0.395 [162].

where the correlator $\Pi(s)$ is defined via (1.1) and the EM current $j_\mu^{\text{em}}(x) = \sum_f Q_f \bar{f}(x)\gamma_\mu f(x)$, with the sum going over all quark-flavours. It was shown by [173] that (4.2) can be written as a dispersion relation

$$\Delta\alpha_{\text{had}}(M_Z^2) = \frac{\alpha_{\text{em}} M_Z^2}{3\pi} P \int \frac{R(s)}{s(M_Z^2 - s)} ds. \tag{4.3}$$

The standard approach [103] to evaluating (4.3) is to make use of e^+e^- cross-section data for the flavour threshold regions, and pQCD for regions sufficiently far from the threshold. They obtain

$$\Delta\alpha_{\text{had}}(M_Z^2) = (275.0 \pm 1.0) \cdot 10^{-4} \tag{4.4}$$

We have two main goals in this thesis:

1. We will obtain the entire heavy-quark contribution to $\Delta\alpha_{\text{had}}(s)$ purely from pQCD. Avoiding the use of experimental cross-section data in the charm threshold region will reduce the current uncertainty of $\Delta\alpha_{\text{had}}(s)$ by around 30%.

2. We will develop a method that allows for existing LQCD calculations for the $g-2$ of the muon to be used to obtain the light-quark contribution to $\Delta\alpha_{\text{had}}(s)$. We will perform the first (to our knowledge) entirely theoretical (and model independent) calculation of $\Delta\alpha_{\text{had}}(s)$. Unfortunately, the LQCD results are not precise enough to provide competitive precision to using experimental cross-section data in the low-energy light-quark region.

We will follow our work [174].

4.2 Charm Quark Contribution

It might seem obvious how to obtain the charm-quark contribution: simply use

$$\Delta\alpha_{\text{had}}^{(c)}(M_Z^2) = 4\pi\alpha_{\text{em}}\Big(\Pi^{(c)}(0) - \text{Re}[\Pi^{(c)}(M_Z^2)]\Big), \tag{4.5}$$

where we have $\Pi^{(c)}(0)$ from the low-energy expansion (2.15) and $\Pi^{(c)}(M_Z^2)$ from the high-energy expansion (2.12). However, an issue arises as to which scale μ to choose,

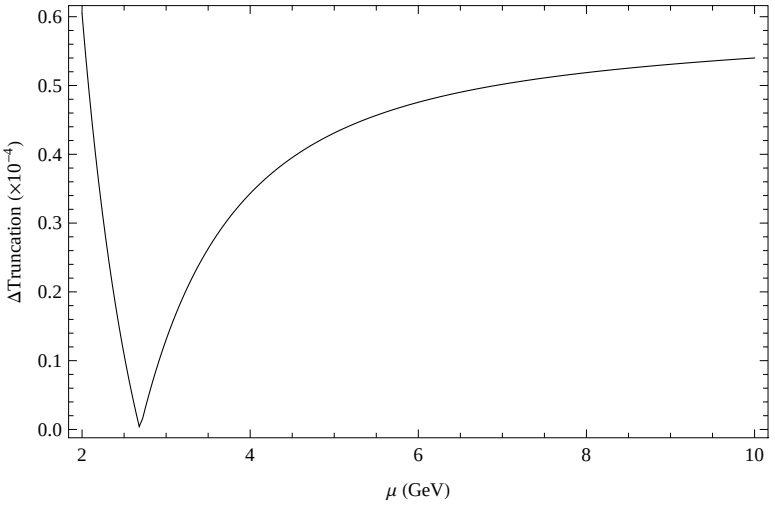

FIGURE 4.1: The difference between the $\mathcal{O}(\alpha_s^3)$ and $\mathcal{O}(\alpha_s^2)$ for the pQCD prediction of $4\pi\alpha_{\rm em}(\Pi^{(c)}(0) - {\rm Re}[\Pi^{(c)}(M_Z^2)])$ (ΔTruncation). We plot this as a function of the renormalization scale μ.

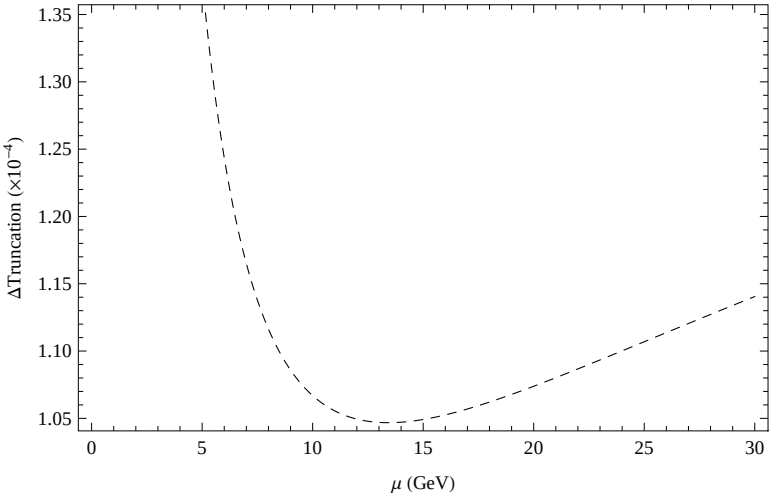

FIGURE 4.2: The difference between the $\mathcal{O}(\alpha_s^2)$ and $\mathcal{O}(\alpha_s^1)$ for the pQCD prediction of $4\pi\alpha_{\rm em}(\Pi^{(c)}(0) - {\rm Re}[\Pi^{(c)}(M_Z^2)])$ (ΔTruncation). We plot this as a function of the renormalization scale μ.

as we must use the same scale for both $\Pi_{(c)}(0)$ and $\Pi^{(c)}(M_Z^2)$, as neither individually is an observable (and hence both are scale-dependent). Now if μ is chosen too large, then the low-energy expansion fails to converge well, and if μ is too small, the high-energy expansion at $s = M_Z^2 \sim 8313\,{\rm GeV}^2$ fails to converge well. This is an issue, as if one varies μ in the range $2\,{\rm GeV} < \mu < M_Z$, then $\Delta\alpha_{\rm had}^{(c)}(M_Z^2)$ varies by 0.77×10^{-4}. This is unacceptable, in the context of the uncertainty in (4.4).

One approach is to fix μ by asking at which value the convergence of the pQCD series for (4.5) is optimal. For example, one can look at the difference between the $\mathcal{O}(\alpha_s^3)$ and $\mathcal{O}(\alpha_s^2)$ results, and chose μ where this point was minimized. This point is roughly

$\mu \sim 3\,\text{GeV}$, as can be seen in Fig. 4.1. Then using $n_f = 5$, we find

$$\begin{aligned}\Delta\alpha^{(c)}_{\text{had}}(M_Z^2) &= 4\pi\alpha_{\text{em}}\left(\Pi^{(c)}(0) - \text{Re}[\Pi^{(c)}(M_Z^2)]\right) \\ &= (79.19 \pm 0.13_{\Delta\text{trun}} \pm 0.03_{\Delta\alpha} \pm 0.01_{\Delta\langle G^2\rangle} \pm 0.11_{\Delta\bar{m}_c}) \cdot 10^{-4}\end{aligned} \tag{4.6}$$

The issue is that this is highly *ad hoc*, as can be appreciated from Fig. 4.2: choosing instead to minimize the difference $\mathcal{O}(\alpha_s^2)$ and $\mathcal{O}(\alpha_s)$ leads to $\mu \sim 14\,\text{GeV}$, which gives $\Delta\alpha^{(c)}_{\text{had}}(M_Z^2) = 79.58 \cdot 10^{-4}$. There is no clear way to control this uncertainty.

Therefore we need a new approach that allows us to seperate the different scales correctly.

4.2.1 Adler Function Approach

This approach is inspired by [175]. We first note that

$$\frac{d}{ds}\Delta\alpha^{(c)}_{\text{had}}(s) = 4\pi\alpha_{em}\frac{d}{ds}\Pi^{(c)}(s) = \frac{\alpha_{em}}{3\pi}\frac{D^{(c)}(s)}{s} \tag{4.7}$$

where $D^{(c)}(s)$ is the (charmed) Adler function. It is understood that we take the real part of the above. The idea is then that

$$\begin{aligned}\Delta\alpha^{(c)}_{\text{had}}(M_z^2) &= \left[\Delta\alpha^{(c)}_{\text{had}}(M_z^2) - \Delta\alpha^{(c)}_{\text{had}}(s_0)\right] + \Delta\alpha^{(c)}_{\text{had}}(s_0) \\ &= \frac{\alpha_{em}}{3\pi}\int_{s_0}^{M_Z^2}\frac{D^{(c)}(s)}{s}ds + 4\pi\alpha_{em}(\Pi^{(c)}(0) - \Pi^{(c)}(s_0))\end{aligned} \tag{4.8}$$

We can now choose $s_0 \ll M_Z^2$, but also large enough that pQCD is safe to use. We can then use one scale for the right hand side, whilst another for integrating over the Adler function (we can also use a running scale, like $\mu^2 = s$).

Using $n_f = 4$, $s_0 = 9.3^2\,\text{GeV}$ (which is below the bottom threshold) and $\mu = 5\,\text{GeV}$, we get

$$\begin{aligned}4\pi\alpha_{em}(\Pi^{(c)}(0) - \Pi^{(c)}(s_0)) &= (29.57 \pm 0.25_{\Delta\text{trun}} \\ &\pm 0.05_{\Delta\alpha} \pm 0.01_{\Delta\langle G^2\rangle} \pm 0.12_{\Delta\bar{m}_c}) \cdot 10^{-4}\end{aligned} \tag{4.9}$$

As a check, we vary μ in the above between $[2\,\text{GeV}, 9.3\,\text{GeV}]$, which varies the central value of (4.9) between $[29.31, 29.62] \cdot 10^{-4}$, which is within the truncation error we gave.

For the second piece, we use $n_f = 5$ and $\mu = \frac{1}{2}M_Z^2$ to obtain

$$\begin{aligned}&\frac{\alpha_{em}}{3\pi}\int_{s_0}^{M_Z^2}\frac{D^{(c)}(s)}{s}ds\\&= (49.91 \pm 0.05_{\Delta\text{trun}} \pm 0.04_{\Delta\alpha} \pm 0.01_{\Delta\bar{m}_c}) \cdot 10^{-4}\end{aligned} \tag{4.10}$$

Again, as a check, we vary μ in the range $[9.3\,\text{GeV}, M_z]$, which gives varies the result (4.10) in the interval $[49.82, 49.95] \cdot 10^{-4}$. The final result using this approach is

$$\begin{aligned}\Delta\alpha_{\text{had}}^{(c)}(M_Z^2) = (79.49 \pm 0.30_{\Delta\text{trun}} \pm 0.09_{\Delta\alpha} \pm 0.01_{\Delta\langle G^2\rangle}\\ \pm 0.11_{\Delta\bar{m}_c}) \cdot 10^{-4}\end{aligned} \tag{4.11}$$

4.2.2 Sum Rule Approach

This approach is a direct analogy of the method employed to compute the heavy-quark contributions to $a_\mu^{\text{had,LO}}$ in the threshold-regions (3.10), except that we require no fitting. We have from (1.7)

$$\begin{aligned}\Delta\alpha_{\text{had}}^{(c)}(M_z^2) = 4\alpha_{\text{em}}M_Z^2\Big[\frac{i}{2}\oint_{|s|=s_0} ds\,\frac{\Pi^{(c)}(s)}{s(M_Z^2-s)} + \frac{\pi}{M_Z^2}\Pi^{(c)}(0)\Big]\\ + \frac{\alpha_{\text{em}}M_Z^2}{3\pi}P\int_{s_0}^{\infty}\frac{R^{(c)}(s)}{s(M_Z^2-s)}ds\end{aligned} \tag{4.12}$$

The above is only valid for $s_0 < M_Z^2$. We choose s_0 to be large enough that pQCD is valid. We can see that we now have two sets of scales, rather than the single scale that caused us problems earlier.

For the contour integral piece, we again use $n_f = 4$, $s_0 = 9.3^2\,\text{GeV}$ and $\mu = 5\,\text{GeV}$. For the integral over $R^{(c)}(s)$, we use $n_f = 5$ (the contribution above the top threshold is negligible) obtaining

$$\begin{aligned}\Delta\alpha_{\text{had}}^{(c)}(M_Z^2) \quad &= (79.34 \pm 0.26_{\Delta\text{trun}} \pm 0.04_{\Delta\alpha}\\ &\pm 0.01_{\Delta\langle G^2\rangle} \pm 0.11_{\Delta\bar{m}_c}) \cdot 10^{-4}\end{aligned} \tag{4.13}$$

We again varied μ in the respective regions, and found that the error is within the truncation error we have quoted. We will use this result for our final charm contribution, as it has a lower total uncertainty compared to the Adler Function approach (4.11).

4.3 The Bottom and Top Quark Contributions

For the bottom quark contribution, all three methods give virtually the same result. We will therefore only quote the result using (4.5) with $\mu = 10\,\text{GeV}$ and $n_f = 5$, obtaining

$$\begin{aligned}\Delta\alpha^{(b)}_{\text{had}}(M_Z^2) &= 4\pi\alpha_{\text{em}}\left(\Pi^{(b)}(0) - \text{Re}[\Pi^{(b)}(M_Z^2)]\right)\\ &= (12.79 \pm 0.06_{\Delta\text{trunc}} \pm 0.09_{\Delta\alpha} \pm 0.03_{\Delta\bar{m}_b}) \cdot 10^{-4}\end{aligned}$$

Even if we vary μ in an incredibly large range $[10\,\text{GeV}, 10M_Z]$, the bottom contribution only varies by $0.04 \cdot 10^{-4}$. This is remarkable stability.

For the top quark, $\Pi^{(t)}(M_Z^2)$ is evaluated below the top threshold, meaning that the high-energy expansion of $\Pi^{(t)}(s)$ is not valid. However, one can use the low energy expansion to calculate both $\Pi^{(t)}(0)$ and $\Pi^{(t)}(M_Z^2)$. Up to $\mathcal{O}(\alpha_s)$, the full analytic correlator is known, and we have checked that there is no practical difference between using the low-energy expansion of the correlator and the full result up to this order to determine $\Pi^{(t)}(M_Z^2)$. We require the $\overline{\text{MS}}$-scheme top quark mass, which we take as [176] $\bar{m}_t(\bar{m}_t) = 160^{+4.8}_{-4.3}\,\text{GeV}$. Using $\mu = \bar{m}_t$ and $n_f = 6$, we find that

$$\begin{aligned}\Delta\alpha^{(t)}_{\text{had}}(M_Z^2) &= 4\pi\alpha_{\text{em}}\left(\Pi^{(t)}(0) - \text{Re}[\Pi^{(t)}(M_Z^2)]\right)\\ &= (-0.76 \pm 0.03_{\Delta\bar{m}_t}) \cdot 10^{-4}\end{aligned} \tag{4.14}$$

Only the the uncertainty in the top mass produces non-negligible uncertainty in $\Delta\alpha^{(t)}_{\text{had}}(M_Z^2)$.

4.4 The light-quark contribution

One cannot use pQCD to determine the low-energy contribution of the light-quarks. There are two approaches to this: either employ e^+e^- data, or use LQCD. We will look at both of these options here. But first we give the high-energy light-quark contribution obtained from pQCD.

	Contributions to $\Delta\alpha_{\text{had}}$ ($\times 10^{-4}$)					
	$[0-3.7\,\text{GeV}]$ (uds)	$[3.7-9.3\,\text{GeV}]$ $(udsc)$	$[9.3-40\,\text{GeV}]$ $(udscb)$	$[>40\,\text{GeV}]$ $(udscb)$	$[>40\,\text{GeV}]$ (t)	Total
Davier *et al.* [103]	79.29(69)	60.21(51)	93.50(16)	42.70(6)	−0.72(1)	275.0(1.0)
pQCD + e^+e^-	79.39(68)	60.46(33)	93.82(14)	42.76(6)	−0.76(3)	275.7(8)

TABLE 4.1: The contributions to $\Delta\alpha_{\text{had}}(M_Z)$ from different regions using either Eq. (4.3) (Davier *et al.* [103]) or Eq. (4.12) (this work), which requires data only below $\sqrt{s} < 1.8\,\text{GeV}$. The total error takes into account the correlations of the uncertainties from the different regions.

4.4.1 High Energy Light Quark Contribution

The final contribution that can be calculated using pQCD is the light-quark contribution at high-energy. It is often assumed [103] that pQCD starts already at $\sqrt{s} = 1.8\,\text{GeV}$. Thus Using (3.30) which includes the $\mathcal{O}(\alpha_s^4)$ massless pQCD result, we find

$$\frac{\alpha_{\text{em}} M_Z^2}{3\pi} \int_{1.8^2\,\text{GeV}^2}^{\infty} \frac{R^{(uds)}_{\text{pQCD}}(s)}{s(M_Z^2 - s)} ds' = (129.26 \pm 0.16_{\Delta\text{trunc}} \pm 0.29_{\Delta\alpha}) \cdot 10^{-4}$$

4.4.2 e^+e^- data

For the e^+e^- contribution below $\sqrt{s} = 1.8\,\text{GeV}$, we will make use of the results of Davier 2011 [103].[2] In this analysis, it was assumed that pQCD begins already at $\sqrt{s} = 1.8\,\text{GeV}$. The data contribution was found to be

$$\frac{\alpha_{\text{em}} M_Z^2}{3\pi} \int_{0}^{1.8^2\,\text{GeV}^2} \frac{R^{(uds)}_{\text{data}}(s)}{s(M_Z^2 - s)} ds' = (55.02 \pm 0.66) \cdot 10^{-4}$$

Therefore we finally obtain for the light-quark contribution

$$\Delta\alpha^{(uds)}_{\text{had}}(M_Z^2) = (184.28 \pm 0.66_{\text{data}} \pm 0.16_{\Delta\text{trunc}} \pm 0.29_{\Delta\alpha}) \cdot 10^{-4}. \tag{4.15}$$

We show a region-by-region comparison of the our calculation versus that of [103] in Table 4.1.

[2] We could use our own data collection, but we want to maximize the precision of our final result, which is why we use the result from [103]. Our uncertainties in our data collection are roughly twice the size of those of [103].

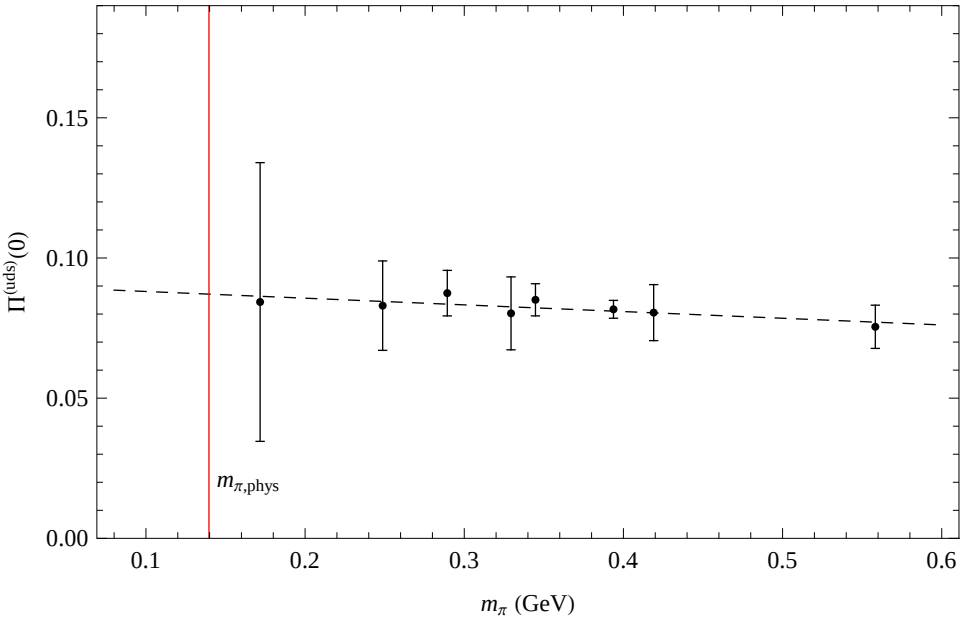

FIGURE 4.3: The value of $\Pi^{(\mathrm{uds})}(0)$ at different values of the pseudoscalar mass. The linear extrapolation to the physical pion mass is shown (dashed line). The errors from the fit parameters added in quadrature. These errors should not be taken too seriously, as there are likely to be correlations (and anti-correlations) between the fit parameters. However, these correlations were not given in [148]. $\Pi^{(\mathrm{uds})}(0)$ is given in the $\overline{\mathrm{MS}}$-bar scheme at $\mu = 2\,\mathrm{GeV}$.

4.4.3 LQCD Determination of the Light Contribution

A large effort is currently underway to calculate $\Pi^{(uds)}(s)$ in the space-like region using LQCD, with the aim of providing a first-principles determination the hadronic contribution to the $g-2$ of the muon [146–148]. The reason for calculating the correlator in the space-like region is the absence of resonances, which makes it easier to determine on the lattice. Then one has a dispersion relation [177]

$$a_\mu^{\mathrm{had,LO}} = \frac{8\alpha_{\mathrm{em}}^2}{3}\int_0^\infty dK^2 f(K^2)\hat{\Pi}(-K^2), \tag{4.16}$$

where $\hat{\Pi}(K^2) \equiv \Pi(K^2) - \Pi(0)$. The kernel $f(K^2)$ can be found in §3.1. The above dispersion relation is derived directly from Feynman diagrams by [177]. We are not aware of a direct mathematical proof of the equivalence of (4.16) and (3.7), so for interest we give the proof in §A.6.

One cannot make use of the space-like lattice data for $\Pi(s)$ directly in either (4.2) and (4.3). However, our sum rule and Adler function methods can easily be modified to incorporate the lattice data.

The more elegant approach is using the Adler function.[3] We have

$$\begin{aligned}\Delta\alpha^{(uds)}_{\rm had}(M_Z^2) &= \Delta\alpha^{(uds)}_{\rm had}(-s_0) + \left[\Delta\alpha^{(uds)}_{\rm had}(s_0) - \Delta\alpha^{(uds)}_{\rm had}(-s_0)\right] \\ &+ \left[\Delta\alpha^{(uds)}_{\rm had}(M_z) - \Delta\alpha^{(uds)}_{\rm had}(s_0)\right] \\ &= 4\pi\alpha_{\rm em}(\Pi^{(uds)}_{\rm LQCD}(0) - \Pi^{(uds)}_{\rm LQCD}(-s_0)) \\ &+ \frac{\alpha_{\rm em}}{3\pi}\int_{-s_0}^{s_0}\frac{D^{(uds)}_{\rm pQCD}(s)}{s}ds \\ &+ \frac{\alpha_{\rm em}}{3\pi}\int_{s_0}^{M_Z^2}\frac{D^{(uds)}_{\rm pQCD}(s)}{s}ds. \end{aligned} \tag{4.17}$$

To try out the method, we can use the LQCD data from [148], which supplies eight fits to LQCD data on the correlator for different values of the pion mass. We plot the values of $\Pi^{(uds)}(0)$ obtained from these fits in Fig. 4.3, converted to the $\overline{\rm MS}$-scheme for interest. These values must be extrapolated to the physical pion mass, and we choose a linear interpolation to do this.

LQCD cannot currently determine $\Pi^{(uds)}(0)$ directly. The approach used by [148] is to employ a phenomenologically inspired fit function

$$\Pi^{(uds)}(s) = A - \frac{F_1^2}{m_1^2 - s} - \frac{F_2^2}{m_2^2 - s} \tag{4.18}$$

which can then be extrapolated to $s = 0$. Although this approach is model-dependent, there exist model-independent parameterizations [178] that can in principle be used.

Using $s_0 = -3.5\,{\rm GeV}^2$, we find the LQCD contribution

$$4\pi\alpha_{\rm em}[\Pi^{(uds)}_{\rm LQCD}(0) - \Pi^{(uds)}_{\rm LQCD}(-s_0)] \sim 52.32 \times 10^{-4}. \tag{4.19}$$

The pQCD contribution is

$$\begin{aligned}&\frac{\alpha_{\rm em}}{3\pi}\int_{-s_0}^{s_0}\frac{D^{(uds)}_{\rm pQCD}(s)}{s}ds + \frac{\alpha_{\rm em}}{3\pi}\int_{s_0}^{M_Z^2}\frac{D^{(uds)}_{\rm pQCD}(s)}{s}ds \\ &= (128.5 \pm 0.2_{\Delta\rm tr} \pm 0.3_{\Delta\alpha_s}) \times 10^{-4}\end{aligned} \tag{4.20}$$

[3] For the FESR approach, one obtains $\Pi^{(uds)}(0)$ from LQCD, and performs the contour integral in pQCD. However, the LQCD determination of $\Pi^{(uds)}(0)$ is not in the $\overline{\rm MS}$-scheme. One must thus match the pQCD and LQCD results at some point where pQCD is valid to fix the scheme. This is avoided in the Adler function approach.

Authors	$\Delta\alpha^{(5)}_{\rm had}(M_Z^2)(\times 10^{-4})$	Method
Groote *et al* (1998) [179]	277.6(4.1)	pQCD driven
Kühn *et al* (1998) [180]	277.5(1.7)	pQCD driven
Burkhardt *et al* (2011) [181]	275.8(3.5)	Data driven
Trocóniz *et al* (2005) [182]	274.9(1.2)	Data driven
Jegerlehner (2008) [175]	275.15(1.49)	Adler function approach
Jegerlehner (2008) [183]	275.94(2.19)	Data driven
Hagiwara *et al* (2011) [105]	276.26(1.38)	Data driven
Davier *et al* (2011) [103]	275.7(1.0)	Data driven
This work	276.5(0.8)	pQCD
This work	~ 273	Lattice + pQCD

TABLE 4.2: The results of other analyses for $\Delta\alpha_{\rm had}(M_Z^2)$. We only give the latest available analysis from each collobaration.

This then leads to

$$\Delta\alpha^{(uds)}_{\rm had}(M_Z^2) \sim 181 \times 10^{-4}. \tag{4.21}$$

This is reasonably close to the result obtained using data (4.15).

Our results are compared with those in the literature in Table 4.2.

Appendix A

Appendix

A.1 Mass Definitions

A variety of mass definitions are employed for defining the quark masses. We explain here the ones used in the thesis, along with conversion formulas.

More detailed reviews can be found in [1] and [184].[1]

A.1.1 $\overline{\text{MS}}$-mass

The QCD Lagrangian is

$$\mathcal{L} = \sum_{k=1}^{n_f} \overline{q}_k (i\gamma^\mu D_\mu - m_k) q_k - \frac{1}{4} G_{\mu\nu} G^{\mu\nu} \tag{A.1}$$

for a n_f quark flavour theory, where m_k is the mass parameter of the k^{th} quark. Like any parameter of the Lagrangian related to some physical observable, the mass parameter m_k will depend on the renormalization scheme used to define the theory, and hence also depend on some scale parameter μ. The running of this quantity is given by the renormalization group equation (A.4). Most analytic perturbative calculations are done making use of dimensional regularization, and subtracting the divergences in the $\overline{\text{MS}}$-scheme. The mass obtained by this procedure is the $\overline{\text{MS}}$-scheme mass $\overline{m}(\mu)$, which is the primary mass definition we use in this thesis.

[1] This paper reviews various definitions relevant to the bottom quark, but they are mostly relevant to the charm quark as well.

A.1.2 Scale Invariant Mass

A closely related mass is the *scale invariant mass*, which is simply the $\overline{\text{MS}}$-mass $\overline{m}$ at the scale $\mu = \overline{m}$. This mass is denoted straightforwardly by $\overline{m}(\overline{m})$, and is calculated recursively from a given $\overline{m}(\mu)$. Given $\overline{m}(\mu_0)$, we use equation (A.7) to run the mass to a new scale $\mu_1 = \overline{m}(\mu_0)$. We run this again to a new scale $\mu_2 = \overline{m}(\mu_1)$, and so on. After an infinite number of recursions, we obtain $\overline{m}(\overline{m})$. In practice, only around 10 recursions are required for the precision we are working at.[2]

A.1.3 Pole Mass

The usual definition of the mass for some observable particle (such as the electron) is simply the position of the pole in the propagator. The position of the pole in the quark propagator is defined as the *pole mass* $M_{\text{pole}} \equiv M$. However, due to confinement, there is no pole in the full quark propagator beyond perturbation theory. Hence the pole mass is only defined in perturbation theory, and suffers from a variety of problems stemming from its sensitivity to long distance effects.[3] However, it can be useful in intermediate calculations.

In particular, we will need to convert results for the heavy quark correlator expressed in terms of the pole mass into the $\overline{\text{MS}}$-mass. The relation between these two has been calculated in perturbation theory up to $\mathcal{O}(\alpha_s^3)$ by [187]. The result here was quoted relating $\overline{m}(\overline{m})$ and $\overline{m}(M)$ to M. Although we can generalize this result to relate $\overline{m}(\mu)$ to M, we simply take the result from [42]:

[2] There exists a Mathematica package RunDec [42] that can calculate the scale invariant mass. However, it was noted in [20] that using this routine to calculate $\overline{m}(\overline{m})$ is not precise enough, giving a result off by a few MeV. The reason for this was developing the right-hand-side of equation (A.7) as a series in α_s, thus losing information. Our routine avoids this problem by performing the integral in (A.7) exactly, and using our exact numerical solution for α_s. Exact in this context means solving (A.3) and (A.4) exactly using all the available information on the β and γ functions. Alternatively, a new C++ version of RunDec has just recently been released [185], which could be used in place of our routine.

[3] Most notable was the demonstration by [186] that the pole mass suffers from so-called renormalon-singularity, and hence can't be determined with a greater accuracy than $\delta M \approx \Lambda_{\text{QCD}}$

$$
\begin{aligned}
M = \overline{m}(\mu)\Big(1 + \Big[\frac{4}{3} + L_m\Big]a_s + \Big[(14.4847 - 1.04136 n_f) + (7.208 - 0.3611 n_f)L_m \\
+ (1.875 - 0.0833 n_f)L_m^2\Big]a_s^2 + \Big[(217.90 - 27.96 n_f + 0.6526 n_f^2) \\
+ (104.94 - 14.122 n_f + 0.3201 n_f^2)L_m + (24.968 - 2.673 n_f + 0.06018 n_f^2)L_m^2 \\
+ (4.0625 - 0.3888 n_f + 0.009259 n_f^2)L_m^3\Big]a_s^3 + \mathcal{O}(a_s^4)\Big)
\end{aligned}
\tag{A.2}
$$

where $L_m \equiv \log(\mu^2/\overline{m}(\mu))$ and $a_s \equiv \alpha_s(\mu)/\pi$.

A.2 The Renormalization Group

The running of the mass m and the strong coupling $a_s \equiv \frac{\alpha_s}{\pi}$ is given by the differential renormalization group equations

$$\frac{d\, a_a}{d\, \ln s} = \beta(a_s) = -a_s^2(\beta_0 + a_s\beta_1 + a_s^2\beta_2 + \ldots) \tag{A.3}$$

$$\frac{1}{\bar{m}}\frac{d\, \bar{m}}{d\, \ln s} = \gamma(a_s) = -a_s(\gamma_0 + a_s\gamma_1 + a_s^2\gamma_2 + \ldots) \tag{A.4}$$

The known coefficients of the QCD β-function are:

$$
\begin{aligned}
\beta_0 &= \frac{1}{4}\left(11 - \frac{2}{3}n_f\right) \\
\beta_1 &= \frac{1}{16}\left(102 - \frac{38}{3}n_f\right) \\
\beta_2 &= \frac{1}{64}\left(\frac{2857}{2} - \frac{5033}{18}n_f + \frac{325}{54}n_f^2\right) \\
\beta_3 &= \frac{1}{256}\left(\frac{149753}{6} + 3564\zeta_3 - \left(\frac{1078361}{162} + \frac{6508}{27}\zeta_3\right)n_f + \left(\frac{50065}{162} + \frac{6472}{81}\zeta_3\right)n_f^2 + \frac{1093}{729}n_f^3\right)
\end{aligned}
$$

The known coefficients of the quark anomalous dimension γ are:

$$
\begin{aligned}
\gamma_0 &= 1 \\
\gamma_1 &= \frac{1}{16}\left(\frac{202}{3} - \frac{20}{9}n_f\right) \\
\gamma_2 &= \frac{1}{64}\left(1249 - \left(\frac{2216}{27} + \frac{160}{3}\zeta_3\right)n_f - \frac{140}{81}n_f^2\right) \\
\gamma_3 &= \frac{1}{256}\left[\frac{4603055}{162} + \frac{135680}{27}\zeta_3 - 8800\zeta_5 + \left(\frac{-91723}{27} - \frac{34192}{9}\zeta_3 + 880\zeta_4 + \frac{18400}{9}\zeta_5\right)n_f \right. \\
&\qquad \left. + \left(\frac{5242}{243} + \frac{800}{9}\zeta_3 - \frac{160}{3}\zeta_4\right)n_f^2 + \left(\frac{-332}{243} + \frac{64}{27}\zeta_3\right)n_f^3\right]
\end{aligned}
$$

A.2.1 Solving the α_s RGE

We solve the differential equation (A.3) in two different ways. For performing the contour integral in CIPT, we solve it numerically using the Mathematica built differential equation solver NDSolve. When solving (A.3), we use as initial condition $\alpha_s^{(4)}(5\,\text{GeV}) = 0.2231 \pm 0.0050$.

Equation (A.3) can also be solved by Taylor developing $a(s)$ about some reference scale $a_s(s_0) \equiv a_s$, The result of $\alpha_s(s)$ in terms of $\alpha_s(s_0)$ to $\mathcal{O}(a_s^5(s_0))$ is well known (see for example [188]), and is

$$\begin{aligned} a_s(s) = a_s &+ a_s^2(-\beta_0\eta) + a_s^3\left(-\beta_1\eta + \beta_0^2\eta^2\right) \\ &+ a_s^4\left(-\beta_2\eta + \frac{5}{2}\beta_0\beta_1\eta^2 - \beta_0^3\eta^3\right) \\ &+ a_s^5\left(-\beta_3\eta + \frac{3}{2}\beta_1^2\eta^2 + 3\beta_0\beta_2\eta^2 - \frac{13}{3}\beta_0^2\beta_1\eta^3 + \beta_0^4\eta^4\right) \\ &+ \mathcal{O}(a_s^6) \end{aligned} \tag{A.5}$$

with $\eta \equiv \ln(s/s_0)$.

A.2.2 Solving the $m(s)$ RGE

Integrating the renormalization group equation (A.4), we would obtain, with $\bar{m}(s_0)$ as the initial condition, [188]

$$\ln\frac{\bar{m}(s)}{\bar{m}(s_0)} = \int_{a_s(s_0)}^{a_s(s)} da_s' \frac{\gamma(a_s')}{\beta(a_s')} \tag{A.6}$$

$$\implies \quad \bar{m}(s) = \bar{m}(s_0)\text{Exp}\left[\int_{a_s(s_0)}^{a_s(s)} da_s' \frac{\gamma(a_s')}{\beta(a_s')}\right] \tag{A.7}$$

Now the coefficients of expansions of β and γ are known up to γ_3 and β_3. Thus we have

$$\frac{\gamma(a_s)}{\beta(a_s)} = \frac{\gamma_0 + a_s\gamma_1 + a_s^2\gamma_2 + a_s^3\gamma_3}{a_s\beta_0 + a_s^2\beta_1 + a_s^3\beta_2 + a_s^4\beta_3} \tag{A.8}$$

Although the integral (A.7) does not have an analytic solution in terms of algebraic functions, Mathematica has a built in non-algebraic function RootSum which allows one to integrate any rational function. This, together with our solution for $\alpha_s(s)$ in the previous subsection allows us to run the mass to any scale.

We will also need the result (A.7) developed as a series in α_s. We use (A.5) to express $\alpha_s(s)$ in terms of $\alpha_s(s_0)$, and after expanding get

$$\begin{aligned}\bar{m}(s) =&\bar{m}(s_0)\Big(1-\eta a_s+\Big[-\frac{101\eta}{24}+\frac{5n_f\eta}{36}+\frac{15\eta^2}{8}-\frac{n_f\eta^2}{12}\Big]a_s^2\\&+\Big[(-\frac{1249}{64}+\frac{201n_f}{88}+\frac{n_f^2}{37})\eta+(\frac{607}{32}-\frac{233n_f}{144}+\frac{3n_f^2}{130})\eta^2\\&+(-\frac{65}{16}+\frac{7n_f}{18}-\frac{n_f^2}{108})\eta^3\Big]a_s^3\\&+\Big[(-\frac{5244}{53}+\frac{1777\mathrm{nf}}{93}-\frac{29\mathrm{nf}^2}{105}-\frac{\mathrm{nf}^3}{172})\eta+(\frac{16889}{115}-\frac{6812\mathrm{nf}}{289}+\frac{142\mathrm{nf}^2}{237}+\frac{\mathrm{nf}^3}{148})\eta^2\\&+(-\frac{8843}{128}+\frac{931\mathrm{nf}}{96}-\frac{7\mathrm{nf}^2\eta^3}{18}+\frac{\mathrm{nf}^3\eta^3}{259})\eta^3+(\frac{1024}{109}-\frac{159\mathrm{nf}}{113}+\frac{7\mathrm{nf}^2}{100}-\frac{\mathrm{nf}^3}{864})\eta^4\Big]a_s^4\Big)\end{aligned} \tag{A.9}$$

where $\eta \equiv \log(s/s_0)$ and as usual $a_s \equiv \alpha_s/\pi$.

A.3 Contour Improved Perturbation Theory

Although we know the correlator $\Pi(s)$ effectively only up to $\mathcal{O}(\alpha_s^3)$, we know the coupling α_s much better, with equation (A.5) known up to $\mathcal{O}(\alpha_s^5)$. The idea of Contour Improved Perturbation Theory (CIPT) is to be able to make use of this extra information. The first step is to relate the correlator to some observable, in this case the Adler function $D(s)$,

$$D(s) \equiv -s\frac{d\Pi(s)}{ds} \tag{A.10}$$

Letting $P(s) = \int_0^s ds'\, p(s')$ and using integration by parts,

$$\oint_{C(|s_0|)} ds\, \Pi(s)p(s) = \big[\Pi(s)\big(P(s)-P(s_0)\big)\big]_{C(|s_0|)} \tag{A.11}$$

$$- \oint_{C(|s_0|)} ds\, \big(P(s)-P(s_0)\big)\frac{d\Pi(s)}{ds} \tag{A.12}$$

$$= 0 + \oint \frac{ds}{s}\,\big(P(s)-P(s_0)\big)D(s) \tag{A.13}$$

Setting $\big[\Pi(s)\big(P(s)-P(s_0)\big)\big]_{C(|s_0|)} = 0$ is only valid if $P(s)$ has no branch cut. This is the case for all $p(s) = s^n$ where $n \neq -1$. We won't be using CIPT when considering inverse moments, so we won't consider here the case $p(s) = s^{-1}$.

After calculating $D(s,\mu)$, we set $\mu = i\sqrt{s}$ to eliminate any logarithms of the form $\log(-s/\mu^2)$. The mass and coupling are now functions of s, $\alpha_s(-s)$ and $\bar{m}(-s)$. We make a substitution of $s' = -s$, so that the branch cuts of the Adler function, coupling and mass are now on the negative real axis. The coupling $\alpha_s(s)$ is obtained by numerical

integration of (A.3), as explained in §A.2.1. For $\bar{m}(s)$, one can use equation (A.7). We will not however use CIPT when integrating massive correlators.

A.4 $\bar{C}_0$ and $\bar{C}_1$ at arbitrary scale μ

The moments $\bar{C}_0$ and $\bar{C}_1$ are calculated in [38]. However, they are given at a scale $\mu = \bar{m}$, and we require these expressions for an arbitrary scale. The scale dependence can be obtain via renormalization group methods.[4] $\bar{C}_0$ is

$$\begin{aligned}
\bar{C}_0^{(0)} &= \frac{4}{3} l_m \; ; \; \bar{C}_0^{(10)} = \frac{13}{9} \; ; \; \bar{C}_0^{(11)} = -\frac{4}{3} \; ; \; \bar{C}_0^{(20)} = \frac{722 n_f + 11790\zeta(3) - 11541}{1944} \\
\bar{C}_0^{(21)} &= -\frac{2}{27}(n_f + 15) \; ; \; \bar{C}_0^{(22)} = \frac{n_f}{9} - \frac{11}{6} \\
\bar{C}_0^{(30)} &= -1.95491 - 1.18601(n_f - 1) + 0.0257066(n_f - 1)^2 \\
\bar{C}_0^{(31)} &= \frac{-152 n_f^2 - 2250 n_f \zeta(3) + 9690 n_f + 72765\zeta(3) - 104877}{1944} \\
\bar{C}_0^{(32)} &= \frac{1}{324}\left(4 n_f^2 + 93 n_f - 1179\right) ; \; \bar{C}_0^{(33)} = -\frac{1}{324}(33 - 2n_f)^2
\end{aligned}$$

Next we give $\bar{C}_1$,

$$\begin{aligned}
\bar{C}_1^{(0)} &= \frac{16}{15} \; ; \; \bar{C}_1^{(10)} = \frac{3104}{1215} \; ; \; \bar{C}_1^{(11)} = -\frac{32}{15} \\
\bar{C}_1^{(20)} &= \frac{231744 n_f + 13833711\zeta(3) - 16682234}{349920} \\
\bar{C}_1^{(21)} &= -\frac{4(118 n_f + 2547)}{3645} \; ; \; \bar{C}_1^{(22)} = \frac{4}{45}(2n_f - 9) \\
\bar{C}_1^{(30)} &= 1.87882 - 2.79472(-1. + n_f) + 0.0961014(-1. + n_f)^2 \\
\bar{C}_1^{(31)} &= \frac{-342528 n_f^2 + n_f(40518196 - 23934942\zeta(3)) + 290507931\zeta(3) - 399253218}{2099520} \\
\bar{C}_1^{(32)} &= \frac{236 n_f^2 + 4722 n_f - 12177}{10935} \; ; \; \bar{C}_1^{(33)} = -\frac{2}{405}\left(4 n_f^2 - 60 n_f + 189\right)
\end{aligned}$$

A.5 Gluon Condensate contribution to Correlator

The full analytical expression for the two-loop massive Wilson Coefficient of the gluon condensate can be found in [44], given in terms of the pole mass. We will use the $\overline{\text{MS}}$-scheme expression.

[4] We thank J.H. Kuhn for making these coefficients available to us.

The low-energy limit is given in [44], but the we will make use of equation (24) in [58], which is already in the $\overline{\text{MS}}$-scheme.[5]

$$\text{Res}[\frac{\Pi_{\text{np}}(s)}{s^{n+1}}, s=0] = \frac{e_c^2}{(4\bar{m}_c^2)^{(n+2)}} \left\langle (\alpha_s/\pi) G^2 \right\rangle a_n \Big(1 + \frac{\alpha_s}{\pi} \bar{b}_n\Big) \tag{A.14}$$

for $n \geq 0$, and with

$$a_n = -\frac{2n+2}{15} \frac{\Gamma(4+n)\Gamma(\frac{7}{2})}{\Gamma(4)\Gamma\big(\frac{7}{2}+n\big)} \tag{A.15}$$

$$\bar{b}_n = b_n - (2n+4)\big(\frac{4}{3} + L_{\mu m}\big) \tag{A.16}$$

where $L_{\mu m} \equiv \log(\mu^2/\bar{m}^2(\mu))$. The constants b_n are taken from Table 2 of Ref. [44], and are

$$b_0 = \frac{1469}{162},\ b_1 = \frac{135779}{12960},\ b_2 = \frac{1969}{168},\ b_3 = \frac{546421}{42525},\ b_4 = \frac{661687433}{47628000} \tag{A.17}$$

In the high-energy limit, $\Pi_{\text{np}}(s)$ with mass-corrections is not given. We will thus derive it ourselves from the general result, and converting the masses to the $\overline{\text{MS}}$-scheme. We find

$$\Pi_{\text{np}}(s) = -\frac{\langle \frac{\alpha_s}{\pi} G^2 \rangle}{s^2} \Big[\Big\{ \frac{1}{12} + \frac{1}{3}\frac{\bar{m}^2}{s} + \left(\frac{\bar{m}^2}{s}\right)^2 \Big(\frac{7}{3} - l_s\Big) + \ldots \Big\} \tag{A.18}$$

$$+ \frac{\alpha_s(\mu)}{\pi} \Big\{ \frac{5}{12} + \frac{\bar{m}^2}{s} \Big(\frac{299}{108} - \frac{17}{36} l_m + \frac{2}{3} l_s \Big) + \ldots \Big\} + \mathcal{O}(\alpha_s^2) \Big] \tag{A.19}$$

where $l_s \equiv \log(-s/\bar{m}^2)$ and $l_m \equiv \log(-\mu^2/\bar{m}^2)$. Given how badly the gluon condensate is known, these terms are easily sufficient for all practical purposes.

A.6 A Proof of a $g-2$ Identity

We have from [177]

$$a_\mu^{\text{had,LO}} = \frac{8\alpha_{\text{em}}^2}{3} \int_0^\infty dK^2 f(K^2) \hat{\Pi}(-K^2), \tag{A.20}$$

[5] We convert ourselves the result for $n=0$, which is not given in [58].

where $\hat{\Pi}(K^2) \equiv \Pi(K^2) - \Pi(0)$, and

$$f(K^2) = \frac{m_\mu^2 K^2 Z^3 (1 - K^2 Z)}{1 + m_\mu^2 K^2 Z^2} \tag{A.21}$$

$$Z = -\frac{K^2 - \sqrt{K^4 + 4m_\mu^2 K^2}}{2m_\mu^2 K^2} \tag{A.22}$$

We want to prove that (A.20) is equivalent to the dispersion relation we used previously, (3.7),

$$a_\mu^{\text{had,LO}} = \frac{8\alpha_{\text{em}}^2}{3} \int_0^\infty \frac{ds}{s} K(s) \frac{1}{\pi} \text{Im}\Pi(s) \tag{A.23}$$

$$K(s) = \int_0^1 dy \frac{y^2(1-y)}{y^2 + \frac{s}{m_\mu^2}(1-y)} \equiv \int_0^1 dy G(y,s)$$

Let us show that (A.23) implies (A.20):

$$a_\mu^{\text{had,LO}} = \frac{8\alpha_{\text{em}}^2}{3} \int_0^\infty \frac{ds}{s} K(s) \frac{1}{\pi} \text{Im}\Pi(s) \tag{A.24}$$

$$= \frac{8\alpha_{\text{em}}^2}{3} \int_0^\infty \frac{ds}{s} \Big[\int_0^1 dy G(y,s) \Big] \frac{1}{\pi} \text{Im}\Pi(s) \tag{A.25}$$

$$= \frac{8\alpha_{\text{em}}^2}{3} \int_0^1 dy \Big[\int_0^\infty \frac{ds}{s} G(y,s) \frac{1}{\pi} \text{Im}\Pi(s) \Big] \tag{A.26}$$

$$= \frac{8\alpha_{\text{em}}^2}{3} \int_0^1 dy \lim_{s_0 \to \infty} \Big[\int_0^{s_0} \frac{ds}{s} G(y,s) \frac{1}{\pi} \text{Im}\Pi(s) \Big] \tag{A.27}$$

$$= \frac{8\alpha_{\text{em}}^2}{3} \int_0^1 dy \lim_{s_0 \to \infty} \Big[\sum_{\text{poles}} \text{Res}[\Pi(s) \frac{G(y,s)}{s}, s = \text{poles}] - \frac{1}{2\pi i} \int_{|s|=s_0} \frac{ds}{s} G(y,s) \Pi(s) \Big] \tag{A.28}$$

$$= \frac{8\alpha_{\text{em}}^2}{3} \int_0^1 dy \Big[\sum_{\text{poles}} \text{Res}[\Pi(s) \frac{G(y,s)}{s}, s = \text{poles}] \Big] \tag{A.29}$$

$$= \frac{8\alpha_{\text{em}}^2}{3} \int_0^1 dy \Big[\text{Res}[\Pi(s) \frac{G(y,s)}{s}, s = 0] + \text{Res}[\Pi(s) \frac{G(y,s)}{s}, s = -\frac{y^2 m_\mu^2}{1-y}] \Big] \tag{A.30}$$

$$= \frac{8\alpha_{\text{em}}^2}{3} \int_0^1 dy \Big[(1-y)\Pi(-\frac{y^2 m_\mu^2}{1-y}) - (1-y)\Pi(0) \Big] \tag{A.31}$$

$$= \frac{8\alpha_{\text{em}}^2}{3} \int_0^1 dy (1-y) \hat{\Pi}(-\frac{y^2 m_\mu^2}{1-y}) \tag{A.32}$$

$$= \frac{8\alpha_{\text{em}}^2}{3} \int_0^\infty dy \frac{(1 - K^2 Z)^3}{K^2 m_\mu^2 Z (K^2 Z - 2)} \hat{\Pi}(-K^2) \tag{A.33}$$

$$= \frac{8\alpha_{\text{em}}^2}{3} \int_0^\infty dK^2 f(K^2) \hat{\Pi}(-K^2) \tag{A.34}$$

Some remarks for non-trivial steps:

(A.26) We interchanged integrals. That one can do this should ideally be proven rigorously, but it is not trivial to do so (one needs some generalization of Fubini's theorem for infinite ranges.).

(A.27) The introduction of the limit is in preparation for the next step where the Residue Theorem will be applied, and it requires closed contours.

(A.28) The key step. Using the integration contour Fig. 1.1, along with Schwarz's symmetry principle and the Residue Theorem, gets us this result.

(A.29) Now we take the limit $s_0 \to \infty$. The contour integral will vanish as for the vector correlator $\lim_{s\to\infty} \Pi(s) \propto \log(s)$ and $\lim_{s\to\infty} s^{-1}G(y,s) \propto s^{-2}$, and hence $\oint_{|s|=s_0} s^{-1}G(y,s)\Pi(s) \propto \oint_{|s|=s_0} s^{-2}\log(s) \propto 1/s_0$ which vanishes in the limit.

(A.32) Using the previous definition of $\hat{\Pi}(s) \equiv \Pi(s) - \Pi(0)$. This is a remarkably simple expression for a_μ, not requiring any fancy kernel that needs to be written down seperately!

(A.33) Make a change of variables, let $K^2 = (y^2m^2/(1-y)$. Then solving for y,

$$y = -\frac{K^2 - \sqrt{K^4 + 4m_\mu^2 K^2}}{2m_\mu^2} \equiv ZK^2 \tag{A.35}$$

This is almost identical to (A.22), and we use this definition of Z. A note: there obviously two solutions for y, but the other solution leads to a sign error and can be discarded.

(A.34) We have to show that

$$f(K^2) = \frac{(1-K^2Z)^3}{K^2m_\mu^2 Z(K^2Z-2)} \tag{A.36}$$

I couldn't find a particularly easy way to do this without resorting to lots of algebraic crunching. In the end, I got Mathematica to check this identity symbolically. As a final check, I also checked it numerically.

A.7 Condensate Determinations from e^+e^- Data

For completeness, we give a brief summary of condensate determinations based on the e^+e^- data collection presented in §3.3. This work was published in [113].

In this work, the OPE (1.8) expansion of the light vector correlator was parameterized as

$$\Pi^{(uds)}_{\rm OPE}(s) = (Q_u^2 + Q_d^2 + Q_s^2)\Pi_{VV} \tag{A.37}$$

$$= (Q_u^2 + Q_d^2 + Q_s^2)\frac{1}{8\pi}\sum_{n=0}^{\infty}(-s)^{-n}C_{2n}(s,\mu^2)\langle 0|\hat{O}_{2n}(\mu^2)|0\rangle. \tag{A.38}$$

The normalization for the pQCD part of Π_{VV} was chosen differently from the rest of this thesis,

$$8\pi {\rm Im}\Pi^{\rm pQCD}_{VV} = 1 + \alpha_s/\pi + \ldots \tag{A.39}$$

The condensates $C_{2n}(s,\mu^2)$ have logarithmic energy dependence, which can be approximated as being constant.[6] With this approximation, the sum-rule (1.7) with $p(s) = s^n$ implies that

$$(-1)^n C_{2n+2}\langle 0|\hat{O}_{2n+2}|0\rangle = 8\pi^2\int_0^{s_0} ds\,\frac{1}{\pi}{\rm Im}\Pi^{(uds)}_{\rm OPE}(s) - s_0^{n+1}M_{2n+2}(s_0), \tag{A.40}$$

where the dimensionless pQCD moments are given by

$$M_{2n+2}(s_0) = -8\pi^2\frac{1}{2\pi i}\oint_{|s|=s_0}\frac{ds}{s_0}\left(\frac{s}{s_0}\right)^n\Pi^{\rm pQCD}_{VV}(s). \tag{A.41}$$

Given how large the uncertainties will be on the condensates, we neglect small corrections such as QED and mass corrections. We use the $\mathcal{O}(\alpha_s^4)$ pQCD correlator from (3.31), and our data collection in §3.3 to integrate over ${\rm Im}\Pi^{(uds)}_{\rm OPE}$. We also use both FOPT ($\mu^2 = -s_0^2$) and CIPT when performing the contour integration in (A.41), and choose a value of the strong coupling of $\alpha_s(m_\tau) = 0.321 \pm 0.015$. Using $s_0 = 4.5\,{\rm GeV}^2$, we found

[6] It was checked that the energy corrections produce a negligible change in the condensate value compared to the very large uncertainties on the condensates stemming from the e^+e^- data.

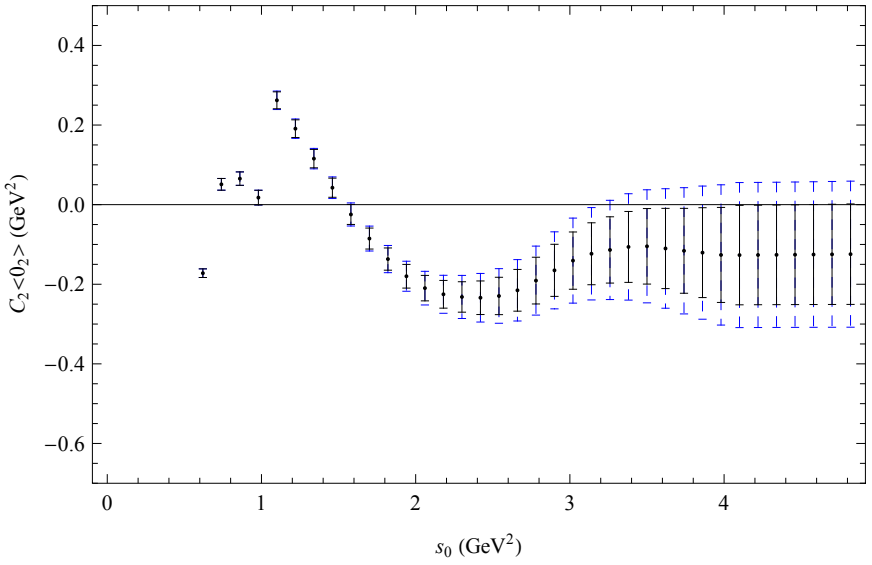

FIGURE A.1: $C_2 \langle \mathcal{O}_2 \rangle$ calculated in FOPT using a strong coupling of $\alpha_s(M_\tau^2) = 0.321 \pm 0.015$. The smaller uncertainties are obtained assuming no correlations between experiments, whilst the higher ones assume 100% correlations for data obtained at the same experimental facility.

for the first three condensates

$$C_2\langle 0|\hat{O}_2|0\rangle = \begin{cases} (-0.13 \pm_{\Delta\text{exp}} 0.13 \pm_{\Delta\alpha_s} 0.03)\,\text{GeV}^2 & \text{(FOPT)} \\ (-0.14 \pm_{\Delta\text{exp}} 0.13 \pm_{\Delta\alpha_s} 0.03)\,\text{GeV}^2 & \text{(CIP)} \end{cases} \tag{A.42}$$

$$C_4\langle 0|\hat{O}_4|0\rangle = \begin{cases} (+0.16 \pm_{\Delta\text{exp}} 0.38 \pm_{\Delta\alpha_s} 0.04)\,\text{GeV}^4 & \text{(FOPT)} \\ (+0.10 \pm_{\Delta\text{exp}} 0.38 \pm_{\Delta\alpha_s} 0.04)\,\text{GeV}^4 & \text{(CIP)} \end{cases} \tag{A.43}$$

$$C_6\langle 0|\hat{O}_6|0\rangle = \begin{cases} (-0.40 \pm_{\Delta\text{exp}} 1.30 \pm_{\Delta\alpha_s} 0.10)\,\text{GeV}^6 & \text{(FOPT)} \\ (-0.40 \pm_{\Delta\text{exp}} 1.30 \pm_{\Delta\alpha_s} 0.10)\,\text{GeV}^6 & \text{(CIP)} \end{cases} \tag{A.44}$$

The uncertainties in the condensates arise from experimental uncertainties (Δexp) and the strong coupling ($\Delta\alpha_s$). We assumed that the uncertainties between results obtained at the same experimental facility were uncorrelated. The FOPT results are plotted for varying s_0 in Figures A.1, A.2, A.3. Two important features of these results stand out. First, the e^+e^- data is not precise enough to rule out a dimension-2 condensate. Second, the dimension-4 term (dominated by the gluon condensate) is consistent with both negative and positive signs, again due to the low precision of the condensate determination employing the e^+e^- data.

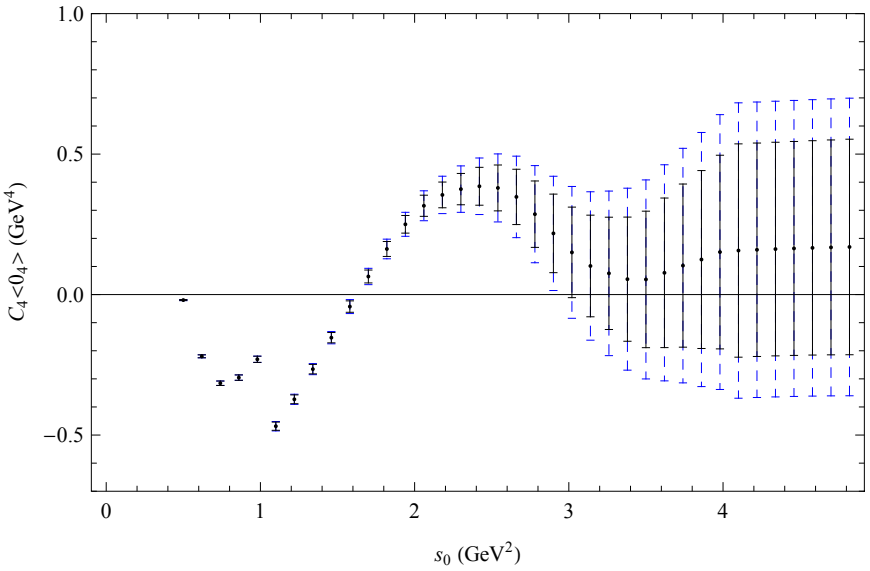

FIGURE A.2: $C_4 \langle \mathcal{O}_4 \rangle$ calculated in FOPT using a strong coupling of $\alpha_s(M_\tau^2) = 0.321 \pm 0.015$. The smaller uncertainties are obtained assuming no correlations between experiments, whilst the higher ones assume 100% correlations for data obtained at the same experimental facility.

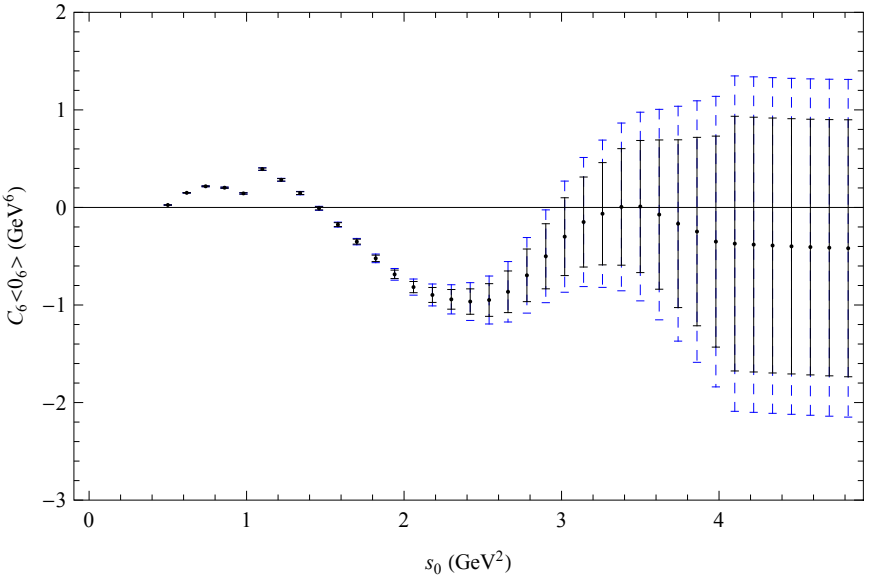

FIGURE A.3: $C_6 \langle \mathcal{O}_6 \rangle$ calculated in FOPT using a strong coupling of $\alpha_s(M_\tau^2) = 0.321 \pm 0.015$. The smaller uncertainties are obtained assuming no correlations between experiments, whilst the higher ones assume 100% correlations for data obtained at the same experimental facility.

Bibliography

[1] **Particle Data Group** Collaboration, J. Beringer *et al.*, "Review of Particle Physics (RPP)," *Physical Review D* **86** (2012) 010001.

[2] M. A. Shifman, A. Vainshtein, and V. I. Zakharov, "QCD and Resonance Physics. Sum Rules," *Nuclear Physics B* **147** (1979) 385–447.

[3] L. Reinders, H. Rubinstein, and S. Yazaki, "Hadron Properties from QCD Sum Rules," *Phys.Rept.* **127** (1985) 1.

[4] M. Shifman, ed., *Vacuum Structure and QCD Sum Rules*. North Holland, 1992.

[5] E. de Rafael, "An Introduction to sum rules in QCD: Course," arXiv:hep-ph/9802448 [hep-ph].

[6] A. Radyushkin, "Introduction into QCD sum rule approach," arXiv:hep-ph/0101227 [hep-ph].

[7] P. Colangelo and A. Khodjamirian, "QCD sum rules, a modern perspective," arXiv:hep-ph/0010175 [hep-ph].

[8] K. Wilson and W. Zimmermann, "Operator product expansions and composite field operators in the general framework of quantum field theory," *Communications in Mathematical Physics* **24** (1972) 87–106.

[9] K. G. Wilson, "Nonlagrangian models of current algebra," *Physical Review* **179** (1969) 1499–1512.

[10] D. Gross and F. Wilczek, "Asymptotically Free Gauge Theories. 1," *Physical Review D* **8** (1973) 3633–3652.

[11] H. Georgi and H. D. Politzer, "Electroproduction scaling in an asymptotically free theory of strong interactions," *Physical Review D* **9** (1974) 416–420.

[12] N. Bogoliubov and D. Shirkov, *Introduction to the Theory of Quantum Fields*. John Wiley & Sons, 3rd ed., 1980.

[13] R. Oehme, "Dispersion relations in quantum chromodynamics," *πN Newsletter* **7** (1992) 1–32, arXiv:hep-ph/9205236 [hep-ph].

[14] R. Oehme, "Analytic structure of amplitudes in gauge theories with confinement," *International Journal of Modern Physics A* **10** (1995) 1995–2014, arXiv:hep-th/9412040 [hep-th].

[15] R. Oehme, "Dispersion relations in gauge theories with confinement," arXiv:hep-th/9511007 [hep-th].

[16] A. White, "The Past and future of S matrix theory," *Scattering: Scattering and inverse scattering in Pure and Applied Science* **2** (2000) , arXiv:hep-ph/0002303 [hep-ph].

[17] M. Peskin and D. Schroeder, *An Introduction To Quantum Field Theory*. Westview Press, 1995.

[18] I. I. Bigi, Y. L. Dokshitzer, V. A. Khoze, J. H. Kuhn, and P. M. Zerwas, "Production and Decay Properties of Ultraheavy Quarks," *Phys.Lett.* **B181** (1986) 157.

[19] E. Eichten, K. Gottfried, T. Kinoshita, K. Lane, and T.-M. Yan, "Charmonium: Comparison with Experiment," *Physical Review D* **21** (1980) 203.

[20] K. Chetyrkin, J. Kuhn, A. Maier, P. Maierhofer, P. Marquard, *et al.*, "Charm and Bottom Quark Masses: An Update," *Physical Review D* **80** (2009) 074010, arXiv:0907.2110 [hep-ph].

[21] A. Signer, "The Charm quark mass from non-relativistic sum rules," *Physics Letters B* **672** (2009) 333–338, arXiv:0810.1152 [hep-ph].

[22] J. Penarrocha and K. Schilcher, "QCD duality and the mass of the charm quark," *Physics Letters B* **515** (2001) 291–296, arXiv:hep-ph/0105222 [hep-ph].

[23] J. Bordes, J. Penarrocha, and K. Schilcher, "Bottom quark mass and QCD duality," *Physics Letters B* **562** (2003) 81–86, arXiv:hep-ph/0212083 [hep-ph].

[24] S. Bodenstein, J. Bordes, C. Dominguez, J. Penarrocha, and K. Schilcher, "Charm-quark mass from weighted finite energy QCD sum rules," *Physical Review D* **82** (2010) 114013, arXiv:1009.4325 [hep-ph].

[25] S. Bodenstein, J. Bordes, C. Dominguez, J. Penarrocha, and K. Schilcher, "Bottom-quark mass from finite energy QCD sum rules," *Physical Review D* **85** (2012) 034003, arXiv:1111.5742 [hep-ph].

[26] S. Bodenstein, J. Bordes, C. Dominguez, J. Penarrocha, and K. Schilcher, "QCD sum rule determination of the charm-quark mass," *Physical Review D* **83** (2011) 074014, arXiv:1102.3835 [hep-ph].

[27] S. Bodenstein, "Precise determinations of the charm and bottom quark masses," *Modern Physics Letters A* **28** no. 26, (2013) 1360020.

[28] C. McNeile, C. Davies, E. Follana, K. Hornbostel, and G. Lepage, "High-Precision c and b Masses, and QCD Coupling from Current-Current Correlators in Lattice and Continuum QCD," *Physical Review D* **82** (2010) 034512, arXiv:1004.4285 [hep-lat].

[29] K. Chetyrkin, R. Harlander, J. H. Kuhn, and M. Steinhauser, "Mass corrections to the vector current correlator," *Nuclear Physics B* **503** (1997) 339–353, arXiv:hep-ph/9704222 [hep-ph].

[30] P. Baikov, K. Chetyrkin, and J. Kuhn, "$R(s)$ and hadronic τ-Decays in $\mathcal{O}(\alpha_s^4)$: Technical aspects," *Nuclear Physics B (Proceedings Supplements)* **189** (2009) 49–53, arXiv:0906.2987 [hep-ph].

[31] K. Chetyrkin, R. Harlander, and J. H. Kuhn, "Quartic mass corrections to R_{had} at $\mathcal{O}(\alpha_s^3)$," *Nuclear Physics B* **586** (2000) 56–72, arXiv:hep-ph/0005139 [hep-ph].

[32] Y. Kiyo, A. Maier, P. Maierhofer, and P. Marquard, "Reconstruction of heavy quark current correlators at $\mathcal{O}(\alpha_s^3)$," *Nuclear Physics B* **823** (2009) 269–287, arXiv:0907.2120 [hep-ph].

[33] P. Baikov, K. Chetyrkin, and J. H. Kuhn, "Order $\mathcal{O}(\alpha_s^4)$ QCD Corrections to Z and τ Decays," *Physical Review Letters* **101** (2008) 012002, arXiv:0801.1821 [hep-ph].

[34] P. Baikov, K. Chetyrkin, and J. H. Kuhn, "Vacuum polarization in pQCD: First complete $\mathcal{O}(\alpha_s^4)$ result," *Nuclear Physics B (Proceedings Supplements)* **135** (2004) 243–246.

[35] R. Boughezal, M. Czakon, and T. Schutzmeier, "Charm and bottom quark masses from perturbative QCD," *Physical Review D* **74** (2006) 074006, arXiv:hep-ph/0605023 [hep-ph].

[36] A. Maier, P. Maierhofer, and P. Marquard, "Higher Moments of Heavy Quark Correlators in the Low Energy Limit at $\mathcal{O}(\alpha_s^2)$," *Nuclear Physics B* **797** (2008) 218–242, arXiv:0711.2636 [hep-ph].

[37] A. Maier, P. Maierhofer, and P. Marqaurd, "The Second physical moment of the heavy quark vector correlator at $\mathcal{O}(\alpha_s^3)$," *Physics Letters B* **669** (2008) 88–91, arXiv:0806.3405 [hep-ph].

[38] K. Chetyrkin, J. H. Kuhn, and C. Sturm, "Four-loop moments of the heavy quark vacuum polarization function in perturbative QCD," *The European Physical Journal C* **48** (2006) 107–110, arXiv:hep-ph/0604234 [hep-ph].

[39] A. Maier, P. Maierhofer, P. Marquard, and A. Smirnov, "Low energy moments of heavy quark current correlators at four loops," *Nuclear Physics B* **824** (2010) 1–18, arXiv:0907.2117 [hep-ph].

[40] G. Corcella and A. Hoang, "Uncertainties in the MS-bar bottom quark mass from relativistic sum rules," *Physics Letters B* **554** (2003) 133–140, arXiv:hep-ph/0212297 [hep-ph].

[41] S. Bethke, "The 2009 World Average of α_s," *The European Physical Journal C* **64** (2009) 689–703, arXiv:0908.1135 [hep-ph].

[42] K. Chetyrkin, J. H. Kuhn, and M. Steinhauser, "RunDec: A Mathematica package for running and decoupling of the strong coupling and quark masses," *Computer Physics Communications* **133** (2000) 43–65, arXiv:hep-ph/0004189 [hep-ph].

[43] T. Appelquist and J. Carazzone, "Infrared Singularities and Massive Fields," *Physical Review D* **11** (1975) 2856.

[44] D. J. Broadhurst, P. Baikov, V. Ilyin, J. Fleischer, O. Tarasov, *et al.*, "Two loop gluon condensate contributions to heavy quark current correlators: Exact results and approximations," *Physics Letters B* **329** (1994) 103–110, arXiv:hep-ph/9403274 [hep-ph].

[45] F. Yndurain, "Gluon condensate from superconvergent QCD sum rule," *Physics Reports* **320** (1999) 287–293, arXiv:hep-ph/9903457 [hep-ph].

[46] R. Horsley, P. E. Rakow, and G. Schierholz, "Separating perturbative and nonperturbative contributions to the plaquette," *Nucl.Phys.Proc.Suppl.* **106** (2002) 870–872, arXiv:hep-lat/0110210 [hep-lat].

[47] B. Ioffe, "Condensates in quantum chromodynamics," *Phys.Atom.Nucl.* **66** (2003) 30–43, arXiv:hep-ph/0207191 [hep-ph].

[48] A. Samsonov, "Gluon condensate in charmonium sum rules for the axial-vector current," arXiv:hep-ph/0407199 [hep-ph].

[49] P. E. Rakow, "Stochastic perturbation theory and the gluon condensate," *PoS* **LAT2005** (2006) 284, arXiv:hep-lat/0510046 [hep-lat].

[50] **ALEPH Collaboration** Collaboration, S. Schael *et al.*, "Branching ratios and spectral functions of tau decays: Final ALEPH measurements and physics implications," *Physics Reports* **421** (2005) 191–284, arXiv:hep-ex/0506072 [hep-ex].

[51] C. A. Dominguez and K. Schilcher, "QCD vacuum condensates from tau-lepton decay data," *JHEP* **0701** (2007) 093, arXiv:hep-ph/0611347 [hep-ph].

[52] M. Davier, S. Descotes-Genon, A. Hocker, B. Malaescu, and Z. Zhang, "The Determination of α_s from τ decays revisited," *European Physical Journal C* **56** (2008) 305–322, arXiv:0803.0979 [hep-ph].

[53] S. Narison, "Gluon Condensates and $\bar{m}_{c,b}$ from QCD-Moments and their ratios to Order α_s^3 and $\langle G^4 \rangle$," *Physics Letters B* **706** (2012) 412–422, arXiv:1105.2922 [hep-ph].

[54] **BES Collaboration** Collaboration, J. Bai *et al.*, "Measurement of the total cross-section for hadronic production by e^+e^- annihilation at energies between

2.6-5 GeV," *Physical Review Letters* **84** (2000) 594–597, arXiv:hep-ex/9908046 [hep-ex].

[55] **BES Collaboration** Collaboration, J. Bai *et al.*, "Measurements of the cross-section for $e^+e^- \to$ hadrons at center-of-mass energies from 2 to 5 GeV," *Physical Review Letters* **88** (2002) 101802, arXiv:hep-ex/0102003 [hep-ex].

[56] M. Ablikim, J. Bai, Y. Ban, J. Bian, X. Cai, *et al.*, "Measurements of the continuum $R_{\rm uds}$ and R values in e^+e^- annihilation in the energy region between 3.650 and 3.872 GeV," *Physical Review Letters* **97** (2006) 262001, arXiv:hep-ex/0612054 [hep-ex].

[57] **CLEO Collaboration** Collaboration, D. Cronin-Hennessy *et al.*, "Measurement of Charm Production Cross Sections in e^+e^- Annihilation at Energies between 3.97 and 4.26 GeV," *Physical Review D* **80** (2009) 072001, arXiv:0801.3418 [hep-ex].

[58] J. H. Kuhn, M. Steinhauser, and C. Sturm, "Heavy Quark Masses from Sum Rules in Four-Loop Approximation," *Nuclear Physics B* **778** (2007) 192–215, arXiv:hep-ph/0702103 [HEP-PH].

[59] **CLEO Collaboration** Collaboration, J. Libby, "The Measurement of R at CLEO," *Nuclear Physics B - Proceedings Supplements* **181-182** (2008) 127–131, arXiv:0807.1220 [hep-ex].

[60] A. Hoang and M. Jamin, "$\overline{\rm MS}$ charm mass from charmonium sum rules with contour improvement," *Physics Letters B* **594** (2004) 127–134, arXiv:hep-ph/0403083 [hep-ph].

[61] **BaBar Collaboration** Collaboration, B. Aubert *et al.*, "Measurement and interpretation of moments in inclusive semileptonic decays $\overline{B} \to X_c l^- \overline{\nu}$," *Physical Review D* **81** (2010) 032003, arXiv:0908.0415 [hep-ex].

[62] A. Laschka, N. Kaiser, and W. Weise, "Quark-antiquark potential to order $1/m$ and heavy quark masses," *Physical Review D* **83** (2011) 094002, arXiv:1102.0945 [hep-ph].

[63] S. Alekhin, J. Blümlein, K. Daum, K. Lipka, and S. Moch, "Precise charm-quark mass from deep-inelastic scattering," *Physics Letters B* **720** (2013) 172–176, arXiv:1212.2355 [hep-ph].

[64] **ETM Collaboration** Collaboration, B. Blossier *et al.*, "Average up/down, strange and charm quark masses with Nf=2 twisted mass lattice QCD," *Physical Review D* **82** (2010) 114513, arXiv:1010.3659 [hep-lat].

[65] B. Dehnadi, A. H. Hoang, V. Mateu, and S. M. Zebarjad, "Charm Mass Determination from QCD Charmonium Sum Rules at Order α_s^3," arXiv:1102.2264 [hep-ph].

[66] S. Narison, "Summary on $m_{c,b}(m_{c,b})$ and precise $f_{D_{(s)},B_{(s)}}$ from heavy-light QCD spectral sum rules," *Nuclear Physics B - Proceedings Supplements* **234** (2013) 187–190, arXiv:1209.2925 [hep-ph].

[67] **BaBar Collaboration** Collaboration, B. Aubert *et al.*, "Measurement of the $e^+e^- \to b\bar{b}$ cross section between $\sqrt{s} = 10.54\,\text{GeV}$ and $11.20\,\text{GeV}$," *Physical Review Letters* **102** (2009) 012001, arXiv:0809.4120 [hep-ex].

[68] R. V. Harlander and M. Steinhauser, "rhad: A Program for the evaluation of the hadronic R-ratio in the perturbative regime of QCD," *Computer Physics Communications* **153** (2003) 244–274, arXiv:hep-ph/0212294 [hep-ph].

[69] **CLEO Collaboration** Collaboration, D. Besson *et al.*, "Observation of New Structure in the e^+e^- Annihilation Cross-Section Above the $\Upsilon(4S)$," *Physical Review Letters* **54** (1985) 381.

[70] **CLEO Collaboration** Collaboration, R. Ammar *et al.*, "A Measurement of the total cross-section for $e^+e^- \to$ hadrons at $\sqrt{s} = 10.52\,\text{GeV}$," *Physical Review D* **57** (1998) 1350–1358, arXiv:hep-ex/9707018 [hep-ex].

[71] K. Chetyrkin, J. Kuhn, A. Maier, P. Maierhofer, P. Marquard, *et al.*, "Precise Charm- and Bottom-Quark Masses: Theoretical and Experimental Uncertainties," *Theoretical and Mathematical Physics* **170** (2012) 217–228, arXiv:1010.6157 [hep-ph].

[72] **Belle Collaboration** Collaboration, C. Schwanda *et al.*, "Measurement of the Moments of the Photon Energy Spectrum in $B \to X_S\gamma$ Decays and

Determination of $|V_{cb}|$ and m_b at Belle," *Physical Review D* **78** (2008) 032016, arXiv:0803.2158 [hep-ex].

[73] P. Gambino and C. Schwanda, "Inclusive semileptonic fits, heavy quark masses, and V_{cb}," arXiv:1307.4551 [hep-ph].

[74] **HPQCD Collaboration** Collaboration, A. Lee *et al.*, "The mass of the b-quark from lattice NRQCD and lattice perturbation theory," *Physical Review D* **87** (2013) 074018, arXiv:1302.3739 [hep-lat].

[75] A. Hoang, P. Ruiz-Femenia, and M. Stahlhofen, "Renormalization Group Improved Bottom Mass from Upsilon Sum Rules at NNLL Order," *Journal of High Energy Physics* **1210** (2012) 188, arXiv:1209.0450 [hep-ph].

[76] S. Narison, "Revisiting f_B and $m_b(m_b)$ from HQET spectral sum rules," *Physics Letters B* **721** (2013) 269–276, arXiv:1212.5544 [hep-ph].

[77] W. Lucha, D. Melikhov, and S. Simula, "Accurate bottom-quark mass from Borel QCD sum rules for f_B and f_{B_s}," *Physical Review D* **88** (2013) 056011, arXiv:1305.7099 [hep-ph].

[78] S. Bodenstein, C. A. Dominguez, and K. Schilcher, "Strange quark mass from sum rules with improved perturbative QCD convergence," *Journal of High Energy Physics* **1307** (2013) 138, arXiv:1305.3796 [hep-ph].

[79] C. A. Dominguez, N. F. Nasrallah, R. Rontsch, and K. Schilcher, "Strange quark mass from finite energy QCD sum rules to five loops," *Journal of High Energy Physics* **0805** (2008) 020, arXiv:0712.0768 [hep-ph].

[80] E. Caliceti, M. Meyer-Hermann, P. Ribeca, A. Surzhykov, and U. Jentschura, "From useful algorithms for slowly convergent series to physical predictions based on divergent perturbative expansions," *Physics Reports* **446** (2007) 1–96, arXiv:0707.1596 [physics.comp-ph].

[81] J. R. Ellis, E. Gardi, M. Karliner, and M. A. Samuel, "Pade approximants, Borel transforms and renormalons: The Bjorken sum rule as a case study," *Physics Letters B* **366** (1996) 268–275, arXiv:hep-ph/9509312 [hep-ph].

[82] J. R. Ellis, E. Gardi, M. Karliner, and M. A. Samuel, "Renormalization scheme dependence of Pade summation in QCD," *Physical Review D* **54** (1996) 6986–6996, arXiv:hep-ph/9607404 [hep-ph].

[83] E. Gardi, "Why Pade approximants reduce the renormalization scale dependence in QFT?," *Physical Review D* **56** (1997) 68–79, arXiv:hep-ph/9611453 [hep-ph].

[84] H. Kleinert, *Path Integrals in Quantum Mechanics, Statistics, Polymer Physics, and Financial Markets*. World Scientific, 4th ed., 2006.

[85] K. Chetyrkin and A. Khodjamirian, "Strange quark mass from pseudoscalar sum rule with $\mathcal{O}(\alpha_s^4)$ accuracy," *European Physical Journal C* **46** (2006) 721–728, arXiv:hep-ph/0512295 [hep-ph].

[86] A. Gomez Nicola, J. Pelaez, and J. Ruiz de Elvira, "Non-factorization of four-quark condensates at low energies within Chiral Perturbation Theory," *Physical Review D* **82** (2010) 074012, arXiv:1005.4370 [hep-ph].

[87] J. Bordes, C. A. Dominguez, J. Penarrocha, and K. Schilcher, "Chiral condensates from tau decay: A Critical reappraisal," *Journal of High Energy Physics* **0602** (2006) 037, arXiv:hep-ph/0511293 [hep-ph].

[88] C. A. Dominguez, N. F. Nasrallah, and K. Schilcher, "Strange quark condensate from QCD sum rules to five loops," *Journal of High Energy Physics* **0802** (2008) 072, arXiv:0711.3962 [hep-ph].

[89] J. Bordes, C. Dominguez, P. Moodley, J. Penarrocha, and K. Schilcher, "Chiral corrections to the $SU(2) \times SU(2)$ Gell-Mann-Oakes-Renner relation," *Journal of High Energy Physics* **1005** (2010) 064, arXiv:1003.3358 [hep-ph].

[90] J. Bordes, C. Dominguez, P. Moodley, J. Penarrocha, and K. Schilcher, "Corrections to the $\mathbf{SU(3)} \times \mathbf{SU(3)}$ Gell-Mann-Oakes-Renner relation and chiral couplings L_8^r and H_2^r," *Journal of High Energy Physics* **1210** (2012) 102, arXiv:1208.1159 [hep-ph].

[91] C. Dominguez, "Hadronic corrections to QCD sum rules and light quark masses," *Zeitschrift für Physik C* **26** (1984) 269.

[92] C. Dominguez and K. Schilcher, "Chiral sum rules and duality in QCD," *Physics Letters B* **448** (1999) 93–98, arXiv:hep-ph/9811261 [hep-ph].

[93] M. Jamin and M. Munz, "The Strange quark mass from QCD sum rules," *Zeitschrift für Physik C* **66** (1995) 633–646, arXiv:hep-ph/9409335 [hep-ph].

[94] P. Fritzsch, F. Knechtli, B. Leder, M. Marinkovic, S. Schaefer, *et al.*, "The strange quark mass and Lambda parameter of two flavor QCD," *Nuclear Physics B* **865** (2012) 397–429, arXiv:1205.5380 [hep-lat].

[95] **RBC Collaboration, UKQCD Collaboration** Collaboration, Y. Aoki *et al.*, "Continuum Limit Physics from 2+1 Flavor Domain Wall QCD," *Physical Review D* **83** (2011) 074508, arXiv:1011.0892 [hep-lat].

[96] S. Durr, Z. Fodor, C. Hoelbling, S. Katz, S. Krieg, *et al.*, "Lattice QCD at the physical point: light quark masses," *Physical Letters B* **701** (2011) 265–268, arXiv:1011.2403 [hep-lat].

[97] T. Blum, R. Zhou, T. Doi, M. Hayakawa, T. Izubuchi, *et al.*, "Electromagnetic mass splittings of the low lying hadrons and quark masses from $2+1$ flavor lattice QCD+QED," *Physical Review D* **82** (2010) 094508, arXiv:1006.1311 [hep-lat].

[98] P. A. Dirac, "The Quantum theory of electron," *Proceedings of the Royal Society London* **A117** (1928) 610–624.

[99] P. Dirac, "The Quantum theory of electron. 2.," *Proceedings of the Royal Society London* **A118** (1928) 351.

[100] P. Kusch and H. M. Foley, "The magnetic moment of the electron," *Physical Review* **74** (Aug, 1948) 250–263. http://link.aps.org/doi/10.1103/PhysRev.74.250.

[101] H. Foley and P. Kusch, "On the Intrinsic Moment of the Electron," *Physical Review* **73** (1948) 412–412.

[102] J. S. Schwinger, "On Quantum electrodynamics and the magnetic moment of the electron," *Physical Review* **73** (1948) 416–417.

[103] M. Davier, A. Hoecker, B. Malaescu, and Z. Zhang, "Reevaluation of the Hadronic Contributions to the Muon $g-2$ and to $\alpha(M_Z)$," *The European Physical Journal C* **71** (2011) 1515, arXiv:1010.4180 [hep-ph].

[104] **Muon G-2 Collaboration** Collaboration, G. Bennett *et al.*, "Final Report of the Muon E821 Anomalous Magnetic Moment Measurement at BNL," *Physical Review D* **73** (2006) 072003, arXiv:hep-ex/0602035 [hep-ex].

[105] K. Hagiwara, R. Liao, A. D. Martin, D. Nomura, and T. Teubner, "$(g-2)_\mu$ and $\alpha(M_Z^2)$ re-evaluated using new precise data," *Journal of Physics G* **38** (2011) 085003, arXiv:1105.3149 [hep-ph].

[106] F. Jegerlehner and A. Nyffeler, "The Muon g-2," *Physics Reports* **477** (2009) 1–110, arXiv:0902.3360 [hep-ph].

[107] J. P. Miller, E. d. Rafael, B. L. Roberts, and D. Stöckinger, "Muon (g-2): Experiment and Theory," *Annual Review of Nuclear and Particle Science* **62** (2012) 237–264.

[108] M. Passera, "The Standard model prediction of the muon anomalous magnetic moment," *Journal of Physics G* **31** (2005) R75–R94, arXiv:hep-ph/0411168 [hep-ph].

[109] D. Stockinger, "The Muon Magnetic Moment and Supersymmetry," *Journal Physics G* **34** (2007) R45–R92, arXiv:hep-ph/0609168 [hep-ph].

[110] E. D. Commins, "Electron spin and its history," *Annual Review of Nuclear and Particle Science* **62** (2012) 133–157.

[111] S. J. Brodsky and E. De Rafael, "Suggested Boson-Lepton Pair Couplings and the Anomalous Magnetic Moment of the Muon," *Physical Review* **168** (1968) 1620–1622.

[112] S. Bodenstein, C. Dominguez, and K. Schilcher, "Hadronic contribution to the muon $g-2$: A Theoretical determination," *Physical Review D* **85** (2012) 014029, arXiv:1106.0427 [hep-ph].

[113] S. Bodenstein, C. Dominguez, S. Eidelman, H. Spiesberger, and K. Schilcher, "Confronting electron-positron annihilation into hadrons with QCD: An

Operator product expansion analysis," *Journal of High Energy Physics* **1201** (2012) 039, arXiv:1110.2026 [hep-ph].

[114] S. Bodenstein, C. Dominguez, K. Schilcher, and H. Spiesberger, "Hadronic Contribution to the muon $g-2$ factor," *Physical Review D* **88** (2013) 014005, arXiv:1302.1735 [hep-ph].

[115] S. Bodenstein, "The hadronic contribution to the muon magnetic anomalous moment," *Modern Physics Letters A* **28** no. 26, (2013) 1360021.

[116] **BES Bollaboration** Collaboration, M. Ablikim *et al.*, "R value measurements for e^+e^- annihilation at 2.60, 3.07 and 3.65 GeV," *Physics Letters* **677** (2009) 239–245, arXiv:0903.0900 [hep-ex].

[117] **CMD2 Collaboration** Collaboration, R. Akhmetshin *et al.*, "Study of the processes $e^+e^- \to \eta\gamma$, $\pi^0\gamma \to 3\gamma$ in the c.m. energy range $600-1380$ MeV at CMD-2," *Physics Letters B.* **605** (2005) 26–36, arXiv:hep-ex/0409030 [hep-ex].

[118] **BaBar Collaboration** Collaboration, B. Aubert *et al.*, "Precise measurement of the $e^+e^- \to \pi^+\pi^-(\gamma)$ cross section with the Initial State Radiation method at BABAR," *Physical Review Letters* **103** (2009) 231801, arXiv:0908.3589 [hep-ex].

[119] **BaBar Collaboration** Collaboration, J. Lees *et al.*, "Precise Measurement of the $e^+e^- \to \pi^+\pi^-(\gamma)$ Cross Section with the Initial-State Radiation Method at BABAR," *Physical Review D* **86** (2012) 032013, arXiv:1205.2228 [hep-ex].

[120] **BaBar Collaboration** Collaboration, B. Aubert *et al.*, "Study of $e^+e^- \to \pi^+\pi^-\pi^0$ process using initial state radiation with BaBar," *Physical Review D* **70** (2004) 072004, arXiv:hep-ex/0408078 [hep-ex].

[121] R. Akhmetshin, V. Aulchenko, V. S. Banzarov, L. Barkov, N. Bashtovoy, *et al.*, "Study of $\phi \to \pi^+\pi^-\pi^0$ with CMD-2 detector," *Physics Letters B* **642** (2006) 203–209.

[122] M. Achasov, V. Aulchenko, K. Beloborodov, A. Berdyugin, A. Bogdanchikov, *et al.*, "Study of the process $e^+e^- \to \pi^+\pi^-\pi^0$ in the energy region $\sqrt{s}$ from 0.98

to 1.38 GeV," *Physical Review D* **66** (2002) 032001, arXiv:hep-ex/0201040 [hep-ex].

[123] M. Achasov, K. Beloborodov, A. Berdyugin, A. Bogdanchikov, A. Bozhenok, *et al.*, "Study of the process $e^+e^- \to \pi^+\pi^-\pi^0$ in the energy region $\sqrt{s}$ below 0.98 GeV," *Physical Review D* **68** (2003) 052006, arXiv:hep-ex/0305049 [hep-ex].

[124] **BaBar Collaboration** Collaboration, B. Aubert *et al.*, "The $e^+e^- \to \pi^+\pi^-\pi^+\pi^-$, $K^+K^-\pi^+\pi^-$, and $K^+K^-K^+K^-$ cross sections at center-of-mass energies $0.5, \text{GeV} - 4.5\,\text{GeV}$ measured with initial-state radiation," *Physical Review D* **71** (2005) 052001, arXiv:hep-ex/0502025 [hep-ex].

[125] V. Druzhinin, "Study of e^+e^- annihilation at low energies," arXiv:0710.3455 [hep-ex].

[126] M. Achasov, K. Beloborodov, A. Berdyugin, A. Botov, A. Vasilev, *et al.*, "Study of process $e^+e^- \to \pi^+\pi^-\pi^0\pi^0$ at energies $\sqrt{s} < 1\,\text{GeV}$ with the spherical neutral detector," *Journal of Experimental and Theoretical Physics* **109** (2009) 379–392.

[127] **BaBar Collaboration** Collaboration, B. Aubert *et al.*, "The $e^+e^- \to 2(\pi^+\pi^-)\pi^0$, $2(\pi^+\pi^-)\eta$, $K^+K^-\pi^+\pi^-\pi^0$ and $K^+K^-\pi^+\pi^-\eta$ Cross Sections Measured with Initial-State Radiation," *Physical Review D* **76** (2007) 092005, arXiv:0708.2461 [hep-ex].

[128] **BaBar Collaboration** Collaboration, B. Aubert *et al.*, "The $e^+e^- \to 3(\pi^+\pi^-), 2(\pi^+\pi^-\pi^0)$ and $K^+K^-2(\pi^+\pi^-)$ cross sections at center-of-mass energies from production threshold to 4.5 GeV measured with initial-state radiation," *Physical Review D* **73** (2006) 052003, arXiv:hep-ex/0602006 [hep-ex].

[129] **CMD-2 Collaboration** Collaboration, R. Akhmetshin *et al.*, "Study of the process $e^+e^- \to \omega\pi^0 \to \pi^0\pi^0\gamma$ in c.m. energy range $920 - 1380\,\text{MeV}$ at CMD-2," *Physical Letters B* **562** (2003) 173–181, arXiv:hep-ex/0304009 [hep-ex].

[130] **CMD-2 Collaboration** Collaboration, R. Akhmetshin *et al.*, "Measurement of $e^+e^- \to \phi \to K^+K^-$ cross section with the CMD-2 detector at VEPP-2M Collider," *Physics Letters B* **669** (2008) 217–222, arXiv:0804.0178 [hep-ex].

[131] M. Achasov, K. Beloborodov, A. Berdyugin, A. Bogdanchikov, A. Bukin, *et al.*, "Measurement of the $e^+e^- \to K^+K^-$ process cross-section in the energy range $\sqrt{s} = 1.04 - 1.38\,\text{GeV}$ with the SND detector in the experiment at VEPP-2M e^+e^- collider," *Physical Review D* **76** (2007) 072012, arXiv:0707.2279 [hep-ex].

[132] **DM2 Collaboration** Collaboration, D. Bisello *et al.*, "Study of the Reaction $e^+e^- \to K^+K^-$ in the Energy Range $1350 \leq \sqrt{s} \leq 2400$-MeV," *Zeitschrift für Physik C Particles and Fields* **C39** (1988) 13.

[133] M. Achasov, K. Beloborodov, A. Berdyugin, A. Bogdanchikov, A. Bozhenok, *et al.*, "Measurements of the parameters of the $\phi(1020)$ resonance through studies of the processes $e^+e^- \to K^+K^-$, K_SK_L, and $\pi^+\pi^-\pi^0$," *Physical Review D* **63** (2001) 072002, arXiv:hep-ex/0009036 [hep-ex].

[134] M. Achasov, K. Beloborodov, A. Berdyugin, A. Bozhenok, D. Bukin, *et al.*, "Experimental study of the reaction $e^+e^- \to K_SK_L$ in the energy range $\sqrt{s} = 1.04 - 1.38\,\text{GeV}$," *Journal of Experimental and Theoretical Physics* **103** (2006) 720–727, arXiv:hep-ex/0606057 [hep-ex].

[135] F. Mane, D. Bisello, J. Bizot, J. Buon, A. Cordier, *et al.*, "Study of the Reaction $e^+e^- \to K^0_SK^0_L$ in the Total Energy Range 1.4, GeV to 2.18 GeV and Interpretation of the K^+ and K^0 Form-factors," *Physics Letters B* **99** (1981) 261.

[136] **BaBar Collaboration** Collaboration, B. Aubert *et al.*, "Measurements of $e^+e^- \to K^+K^-\eta$, $K^+K^-\pi^0$ and $K^0_sK^\pm\pi^\mp$ cross- sections using initial state radiation events," *Physical Review D* **77** (2008) 092002, arXiv:0710.4451 [hep-ex].

[137] **BaBar Collaboration** Collaboration, B. Aubert *et al.*, "A Study of $e^+e^- \to p\bar{p}$ using initial state radiation with BABAR," *Physical Review D* **73** (2006) 012005, arXiv:hep-ex/0512023 [hep-ex].

[138] A. Antonelli, R. Baldini, P. Benasi, M. Bertani, M. Biagini, *et al.*, "The first measurement of the neutron electromagnetic form-factors in the timelike region," *Nuclear Physics B* **517** (1998) 3–35.

[139] M. Davier, S. Eidelman, A. Hocker, and Z. Zhang, "Confronting spectral functions from e^+e^- annihilation and tau decays: Consequences for the muon

magnetic moment," *The European Physical Journal C* **27** (2003) 497–521, arXiv:hep-ph/0208177 [hep-ph].

[140] K. Hagiwara, A. Martin, D. Nomura, and T. Teubner, "Predictions for $g-2$ of the muon and $\alpha_{\rm QED}(M_Z^2)$," *Physical Review D* **69** (2004) 093003, arXiv:hep-ph/0312250 [hep-ph].

[141] A. Hoefer, J. Gluza, and F. Jegerlehner, "Pion pair production with higher order radiative corrections in low energy e^+e^- collisions," *The European Physical Journal C* **24** (2002) 51–69, arXiv:hep-ph/0107154 [hep-ph].

[142] **CMD-2 Collaboration** Collaboration, R. Akhmetshin *et al.*, "Reanalysis of hadronic cross-section measurements at CMD-2," *Physics Letters B* **578** (2004) 285–289, arXiv:hep-ex/0308008 [hep-ex].

[143] **BaBar Collaboration** Collaboration, B. Aubert *et al.*, "The $e^+e^- \to K^+K^-\pi^+\pi^-$, $K^+K^-\pi^0\pi^0$ and $K^+K^-K^+K^-$ cross-sections measured with initial-state radiation," *Physical Review D* **76** (2007) 012008, arXiv:0704.0630 [hep-ex].

[144] **KLOE Collaboration** Collaboration, F. Ambrosino *et al.*, "Measurement of $\sigma(e^+e^- \to \pi^+\pi^-)$ from threshold to 0.85 GeV^2 using Initial State Radiation with the KLOE detector," *Physics Letters B* **700** (2011) 102–110, arXiv:1006.5313 [hep-ex].

[145] **BaBar Collaboration** Collaboration, J. Lees *et al.*, "Precision Measurement of the $e^+e^- \to K^+K^-(\gamma)$ Cross Section with the Initial-State Radiation Method at BaBar," *Physical Review D* **88** (2013) 032013, arXiv:1306.3600 [hep-ex].

[146] B. Brandt, M. Della Morte, B. Jager, A. Juttner, and H. Wittig, "Hadronic contribution to the lepton anomalous magnetic moment and pion form factor in lattice QCD," *Progress in Particle and Nuclear Physics* **67** (2012) 223–227.

[147] X. Feng, K. Jansen, M. Petschlies, and D. B. Renner, "Two-flavor QCD correction to lepton magnetic moments at leading-order in the electromagnetic coupling," *Physical Review Letters* **107** (2011) 081802, arXiv:1103.4818 [hep-lat].

[148] P. Boyle, L. Del Debbio, E. Kerrane, and J. Zanotti, "Lattice Determination of the Hadronic Contribution to the Muon $g-2$ using Dynamical Domain Wall Fermions," *Physical Review D* **85** (2012) 074504, arXiv:1107.1497 [hep-lat].

[149] S. Groote, J. Korner, and J. Maul, "QCD improved determination of the hadronic contribution to the anomalous magnetic moment of the muon," arXiv:hep-ph/0309226 [hep-ph].

[150] K. Chetyrkin and A. Maier, "Massless correlators of vector, scalar and tensor currents in position space at orders α_s^3 and α_s^4: Explicit analytical results," *Nuclear Physics B* **844** (2011) 266–288, arXiv:1010.1145 [hep-ph].

[151] M. Beneke and M. Jamin, "α_s and the τ hadronic width: fixed-order, contour-improved and higher-order perturbation theory," *Journal of High Energy Physics* **0809** (2008) 044, arXiv:0806.3156 [hep-ph].

[152] S. Gorishnii, A. Kataev, and S. Larin, "Three Loop Corrections of Order $\mathcal{O}(m^2)$ to the Correlator of Electromagnetic Quark Currents," *Il Nuovo Cimento A* **A92** (1986) 119–131.

[153] K. Chetyrkin and J. H. Kuhn, "Quadratic mass corrections of order $\mathcal{O}(\alpha_s^3)m_q^2/s)$ to the decay rate of Z and W-bosons," *Physics Letters B* **406** (1997) 102–109, arXiv:hep-ph/9609202 [hep-ph].

[154] K. Chetyrkin, V. Spiridonov, and S. Gorishnii, "Wilson expansion for correlators of vector currents at the two-loop level: Dimension-four operators," *Physics Letters B* **160** (1985) 149–153.

[155] E. Braaten, S. Narison, and A. Pich, "QCD analysis of the tau hadronic width," *Nuclear Physics B* **373** (1992) 581–612.

[156] B. Krause, "Higher order hadronic contributions to the anomalous magnetic moment of leptons," *Physics Letters B* **390** (1997) 392–400, arXiv:hep-ph/9607259 [hep-ph].

[157] K. Chetyrkin, S. Narison, and V. I. Zakharov, "Short distance tachyonic gluon mass and $1/Q^2$ corrections," *Nuclear Physics B* **550** (1999) 353–374, arXiv:hep-ph/9811275 [hep-ph].

[158] M. Gockeler, R. Horsley, W. Kurzinger, V. Linke, D. Pleiter, *et al.*, "The Vacuum polarization: power corrections beyond OPE?," *Nuclear Physics B - Proceedings Supplements* **94** (2001) 571–574, arXiv:hep-lat/0012010 [hep-lat].

[159] C. Dominguez and K. Schilcher, "Is there evidence for dimension two corrections in QCD two point functions?," *Physical Review D* **61** (2000) 114020, arXiv:hep-ph/9903483 [hep-ph].

[160] O. Cata, M. Golterman, and S. Peris, "Possible duality violations in τ-decay and their impact on the determination of α_s," *Physical Review D* **79** (2009) 053002, arXiv:0812.2285 [hep-ph].

[161] M. Passera, W. Marciano, and A. Sirlin, "The Muon $g-2$ and the bounds on the Higgs boson mass," *Physical Review D* **78** (2008) 013009, arXiv:0804.1142 [hep-ph].

[162] H. Flacher, M. Goebel, J. Haller, A. Hocker, K. Monig, *et al.*, "Revisiting the Global Electroweak Fit of the Standard Model and Beyond with Gfitter," *European Physical Journal C* **60** (2009) 543–583, arXiv:0811.0009 [hep-ph].

[163] M. Baak, M. Goebel, J. Haller, A. Hoecker, D. Kennedy, *et al.*, "The Electroweak Fit of the Standard Model after the Discovery of a New Boson at the LHC," *European Physical Journal C* **72** (2012) 2205, arXiv:1209.2716 [hep-ph].

[164] **ATLAS Collaboration** Collaboration, G. Aad *et al.*, "Observation of a new particle in the search for the Standard Model Higgs boson with the ATLAS detector at the LHC," *Physics Letters B* **716** (2012) 1–29, arXiv:1207.7214 [hep-ex].

[165] **CMS Collaboration** Collaboration, S. Chatrchyan *et al.*, "Observation of a new boson at a mass of 125 GeV with the CMS experiment at the LHC," *Physics Letters B* **716** (2012) 30–61, arXiv:1207.7235 [hep-ex].

[166] J. Prades, E. de Rafael, and A. Vainshtein, "Hadronic Light-by-Light Scattering Contribution to the Muon Anomalous Magnetic Moment," arXiv:0901.0306 [hep-ph].

[167] **CDF Collaboration, D0 Collaboration** Collaboration, T. Aaltonen *et al.*, "Combination of the top-quark mass measurements from the Tevatron collider," *Physical Review D* **86** (2012) 092003, arXiv:1207.1069 [hep-ex].

[168] A. Buckley, J. Butterworth, S. Gieseke, D. Grellscheid, S. Hoche, *et al.*, "General-purpose event generators for LHC physics," *Physics Reports.* **504** (2011) 145–233, arXiv:1101.2599 [hep-ph].

[169] P. Z. Skands and D. Wicke, "Non-perturbative QCD effects and the top mass at the Tevatron," *European Physical Journal C* **52** (2007) 133–140, arXiv:hep-ph/0703081 [HEP-PH].

[170] D. Wicke and P. Z. Skands, "Non-perturbative QCD Effects and the Top Mass at the Tevatron," *Nuovo Cimento B* **123** (2008) S1, arXiv:0807.3248 [hep-ph].

[171] A. H. Hoang, A. Jain, I. Scimemi, and I. W. Stewart, "Infrared Renormalization Group Flow for Heavy Quark Masses," *Physics Review Letters* **101** (2008) 151602, arXiv:0803.4214 [hep-ph].

[172] A. H. Hoang and I. W. Stewart, "Top Mass Measurements from Jets and the Tevatron Top-Quark Mass," *Nuclear Physics - Proceedings Supplement* **185** (2008) 220–226, arXiv:0808.0222 [hep-ph].

[173] N. Cabibbo and R. Gatto, "Electron Positron Colliding Beam Experiments," *Physical Review* **124** (1961) 1577–1595.

[174] S. Bodenstein, C. Dominguez, K. Schilcher, and H. Spiesberger, "Hadronic contribution to the QED running coupling $\alpha(M_Z^2)$," *Physical Review D* **86** (2012) 093013, arXiv:1209.4802 [hep-ph].

[175] F. Jegerlehner, "The Running fine structure constant alpha(E) via the Adler function," *Nuclear Physics B - Proceedings Supplements* **181-182** (2008) 135–140, arXiv:0807.4206 [hep-ph].

[176] **D0 Collaboration** Collaboration, V. M. Abazov *et al.*, "Determination of the pole and MSbar masses of the top quark from the $t\bar{t}$ cross section," *Physical Letters B* **703** (2011) 422–427, arXiv:1104.2887 [hep-ex].

[177] T. Blum, "Lattice calculation of the lowest order hadronic contribution to the muon anomalous magnetic moment," *Physical Review Letters* **91** (2003) 052001, arXiv:hep-lat/0212018 [hep-lat].

[178] C. Aubin, T. Blum, M. Golterman, and S. Peris, "Model-independent parametrization of the hadronic vacuum polarization and g-2 for the muon on the lattice," *Physical Review D* **86** (2012) 054509, arXiv:1205.3695 [hep-lat].

[179] S. Groote, J. Korner, K. Schilcher, and N. Nasrallah, "QCD sum rule determination of alpha (M(Z)) with minimal data input," *Physics Letters B* **440** (1998) 375–385, arXiv:hep-ph/9802374 [hep-ph].

[180] J. H. Kuhn and M. Steinhauser, "A Theory driven analysis of the effective QED coupling at M_Z," *Physics Letters B* **437** (1998) 425–431, arXiv:hep-ph/9802241 [hep-ph].

[181] H. Burkhardt and B. Pietrzyk, "Recent BES measurements and the hadronic contribution to the QED vacuum polarization," *Physical Review D* **84** (2011) 037502, arXiv:1106.2991 [hep-ex].

[182] J. de Troconiz and F. Yndurain, "The Hadronic contributions to the anomalous magnetic moment of the muon," *Physical Review D* **71** (2005) 073008, arXiv:hep-ph/0402285 [hep-ph].

[183] F. Jegerlehner, "Electroweak effective couplings for future precision experiments," *Nuovo Cimento C* **034S1** (2011) 31–40, arXiv:1107.4683 [hep-ph].

[184] A. X. El-Khadra and M. Luke, "The Mass of the b quark," *Annual Review of Nuclear and Particle Science* **52** (2002) 201–251, arXiv:hep-ph/0208114 [hep-ph].

[185] B. Schmidt and M. Steinhauser, "CRunDec: a C++ package for running and decoupling of the strong coupling and quark masses," *Computer Physics Communications* **183** (2012) 1845–1848, arXiv:1201.6149 [hep-ph].

[186] M. Beneke and V. M. Braun, "Heavy quark effective theory beyond perturbation theory: Renormalons, the pole mass and the residual mass term," *Nuclear Physics B* **426** (1994) 301–343, arXiv:hep-ph/9402364 [hep-ph].

[187] K. Melnikov and T. v. Ritbergen, "The Three loop relation between the MS-bar and the pole quark masses," *Physics Letters B* **482** (2000) 99–108, arXiv:hep-ph/9912391 [hep-ph].

[188] M. Davier, A. Hocker, and Z. Zhang, "The Physics of hadronic tau decays," *Reviews of Modern Physics* **78** (2006) 1043–1109, arXiv:hep-ph/0507078 [hep-ph].